Memorandum of Understanding
ECT/FG/CB/95.205

Contract ESA-ESTEC PRF 151739

Modelling of the Nitrifying compartment of MELiSSA

Description of the nitrifying column model and first simulations

- Parameters of the model
- RTD analysis of the nitrifying column using the developed model
- Definition of a standart configuration for simulations
- First simulations for various initial functionning conditions

TECHNICAL NOTE 27.2

Version 1 Issue 0

L. Poughon
Laboratoire de Génie Chimique Biologique, 63177 AUBIERE Cedex, FRANCE

May 1996

Contents

T.N. 27.2: Modelling the nitrifying compartment
Numerical treatment and simulations

L. Poughon.
Laboratoire de Génie Chimique Biologique
63177 AUBIERE Cedex. France.

Introduction

This technical note is the continuation of the TN 27.1. Its purpose is the numerical treatment of the previous developped model for the autotrophic nitrification in a fixed bed column, and the analysis of the first simulations performed with this model.

The first part concerns to the evaluation of the variables and of the parameters of the model, using literature data and UAB Laboratory data (TN 25.330). In order to have a reference for comparing the first simulations, a standart configuration for the model and for the working conditions of the nitrifying column is defined.

In the second part, the numerical treatment of the model is presented, and the results of the simulations of the model for several column configurations are discussed. The results of the simulations are reported into 2 forms:

- 2 dimension curves for the outlet flows composition
- 3 dimension curves for the compounds concentrations profiles for gas and liquid inside the column (appendix).

I. Nitrifying model: variables, parameters and definition of a standard simulation configuration

The nitrifying model has been described (hydrodynamic equations, mass transfer equations and physico-chemical relations) in TN 27.1. The purpose of this section is to set the values of the parameters and of the variables involved in this model, by using literature data (TN27.1), ESTEC Laboratory results (Forler, 1994) and UAB Laboratory results (TN 25.330).

This section is the continuation of the fourth section of TN 27.1. The variable names defined in the previous model are conserved here.

1.1 Compounds involved and their physico-chemical constants.

The list of the compounds involved in autotrophic nitrification are reported in table 1.

Table 1: compounds involved in the model and their physico-chemical constants.

Compound: non ionic form	Compound: first dissociated form	Compound: second dissociated form	Compound: third dissociated form	K_A (25°C)	k_i (25°C)
NH_3	NH_4^+			1.762 10^{-5} [TN 23.1.][c]	1.173 10^{-2} [TN 23.1.][c]
HNO_2	NO_2^-			Complete dissociation	
HNO_3	NO_3^-			Complete dissociation	
CO_2	HCO_3^-	CO_3^{2-}		4.320 10^{-7} [TN 17.1.]c 4.557 10^{-11} [TN 17.1.][c]	1635 [TN 17.1][c]
O_2					4.272 10^4 [TN 17.1][c]
H_3PO_4	$H_2PO_4^-$	HPO_4^{2-}	PO_4^{3-}	6.918 10^{-3} [TN 27.1.] 6.166 10^{-8} [TN 27.1.] 4.780 10^{-13} [TN 27.1.]	
H_2SO_4	HSO_4^-	SO_4^{2-}		Complete dissociation 1.047 10^{-2} [TN 27.1.]	
H_2O	OH^-			10^{-14}	Po=0.031 atm [c]
Biomass *Nitrosomonas*					
Biomass *Nitrobacter*					

[c]: calculated from a temperature dependent relation

Some of them are in aqueous solutions both in ionic and non ionic forms. The fraction of ionic versus non ionic forms mainly depends on the pH value and can be calculated by using the acid base equilibrium constant K_A (TN 27.1). For several compounds, a relation of K_A as a function of temperature ($K_A(T)$) exists (TN 17.1, TN 23.1, TN 27.1). Nevertheless, the values of K_A used are defined for a temperature of 25°C (optimal temperature of the process 28°C) and are not recalculated with the $K_A(T)$ relations. The difference between $K_A(25°C)$ and $K_A(28°C)$ can be neglected as a first approximation.

Non ionic compounds can be found both in the gas and liquid phases. The gas-liquid equilibrium for a compound i depends of two coefficients, K_La and k_i. k_i is a physico-chemical constant and K_La characterize the dynamics of the exchanges between the gas and the liquid phases. The k_i values used in the model are calculated for a temperature of 25°C (for consistency with K_A values), by using the relations detailed in TN 17.1 and in TN 23.1. The problem of the K_La value, which depends both on the column design and on the working conditions, will be further discussed in sections 1.3.1.

1.2. Kinetic parameters

In order to take into account the pH effect on the biological kinetics, the stoichiometries established in TN 23.3 and 27.1 have been rewritten into a ionic form.

Nitrosomonas
Biosynthesis

$$HCO_3^- + 0.0089\ HPO_4^{2-} + 0.0035\ SO_4^{2-} + 5.4269\ O_2 + 4.5341\ NH_3$$
$$\Downarrow$$
$$CH_{1.6147}O_{0.3906}N_{0.1994}S_{0.0035}P_{0.0089} + 4.3347\ NO_2^- + 4.3099\ H^+ + 3.8433\ H_2O + OH^-$$

Maintenance

$$NH_3 + 1.5\ O_2 \rightarrow NO_2^- + H^+ + H_2O$$

Nitrobacter
Biosynthesis

$$HCO_3^- + 0.0089\ HPO_4^{2-} + 0.0035\ SO_4^{2-} + 6.5106\ O_2$$
$$+ 15.1714\ NO_2^- + 0.1994\ NH_3 + 0.4914\ H_2O + 0.0248\ H^+$$
$$\Downarrow$$
$$CH_{1.6147}O_{0.3906}N_{0.1994}S_{0.0035}P_{0.0089} + 15.1714\ NO_3^- + OH^-$$

Maintenance

$$NO_2^- + 0.5\ O_2 \rightarrow NO_3^-$$

Table 2: kinetic parameters

			Reference	Remarks
μ_{max}^{Ns}	$5.7\ 10^{-2}\ h^{-1}$		Hunik et al (1994)	mean values calculated
μ_{max}^{Nb}	$3.6\ 10^{-2}\ h^{-1}$		Hunik et al (1994)	from several
m^{Ns}	$3.38\ 10^{-3}$		Hunik et al (1994)	continuous cultures
m^{Nb}	$7.92\ 10^{-3}$		Hunik et al (1994)	
Limiting substrate	K^{Ns}	K^{Nb}		
NH_3	$6.625\ 10^{-5}$ mol/l	-	Hunik et al (1994)	Model parameter
NO_2^-	-	$3.6\ 10^{-4}$ mol/l	Hunik et al (1994)	values for a fixed bed
O_2	$5.05\ 10^{-6}$ mol/l	$1.7\ 10^{-5}$ mol/l	Hunik et al (1994)	of carragenan beads
HCO_3^-	10^{-10} mol/l	10^{-10} mol /l		no carbon limitation
Inhibitory substrate	I^{Ns}	I^{Nb}		
None	-	-		no inhition
Substrate	$Y_{X/Si}^{Ns}$	$Y_{X/Si}^{Nb}$		g biomass / mol substrate Si Agebraic value
NH_3	-5.082	-115.566		
NO_2^-	5.316	-1.519		
NO_3^-		1.342		
O_2	-4.246	-3.539		
HCO_3^-	-23.0438	-23.0438		
HPO_4^{2-}	-2589.191	-2589.191		
SO_4^{2-}	-6583.943	-6583.943		
H^+	5.347	929.1854		
OH^-	23.044	23.0438		
	5.996	-46.894		
	$Y_{Smt/Si}^{Ns}$	$Y_{Smt/Si}^{Nb}$		mol maintenance substrate / mol Si Agebraic value
NH_3	-1			
NO_2^-	1	-1		
NO_3^-		1		
H_2O	1			
H+	1			
O_2	-0.5	-1.5		

The growth kinetics associated to the stoichiometries have been discussed in TN 27.1. The kinetic parameter values used in the model are reported in table 2. The maximum growth rates, the maintenance coefficients, the half saturation constants and the inhibitory constants are taken from literature data while the growth yields, $Y_{X/Si}$, are calculated from the previous stoichiometries.

$$r_X^{Ns} = \mu^{Ns}.C_{X-Ns}\big|_B + Y_{X/Smt}^{Ns}.m^{Ns}.\left(\frac{\mu^{Ns}}{\mu_{max}^{Ns}} - 1\right).C_{X-Ns}\big|_B$$

$$r_X^{Nb} = \mu^{Nb}.C_{X-Nb}\big|_B + Y_{X/Smt}^{Nb}.m^{Nb}.\left(\frac{\mu^{Nb}}{\mu_{max}^{Nb}} - 1\right).C_{X-Nb}\big|_B$$

and

$$r_X^{Ns-free} = K_{wo}.r_X^{Ns}$$
$$r_X^{Nb-free} = K_{wo}.r_X^{Nb}$$

$$r_{Si}^{Ns} = \frac{1}{Y_{X/Si}^{Ns}}.r_X^{Ns} + \frac{1}{Y_{Smt/Si}^{Ns}}r_m^{Ns}$$

$$r_{Si}^{Ns} = \frac{1}{Y_{X/Si}^{Ns}}.r_X^{Ns} + \frac{1}{Y_{Smt/Si}^{Ns}}r_m^{Ns}$$

with

$$\mu = \mu_{max}.\prod_{\text{Limiting substrates j}} \frac{C_j\big|_B}{(Ks_{sj} + C_j\big|_B).Ki} \quad \text{where} \quad Ki = \prod_{\text{Inhibitory Substrate k}} \left(1 + \frac{C_k\big|_B}{I_k}\right)$$

1.3 The nitrifying column: hydrodynamic model and hydrodynamic behaviour analysis

A N-stirred tank model, including back-mixing between the tanks and a gas and liquid recycling between the output and the input of the column has been chosen (TN 27.1). The model can be represented by the following scheme:

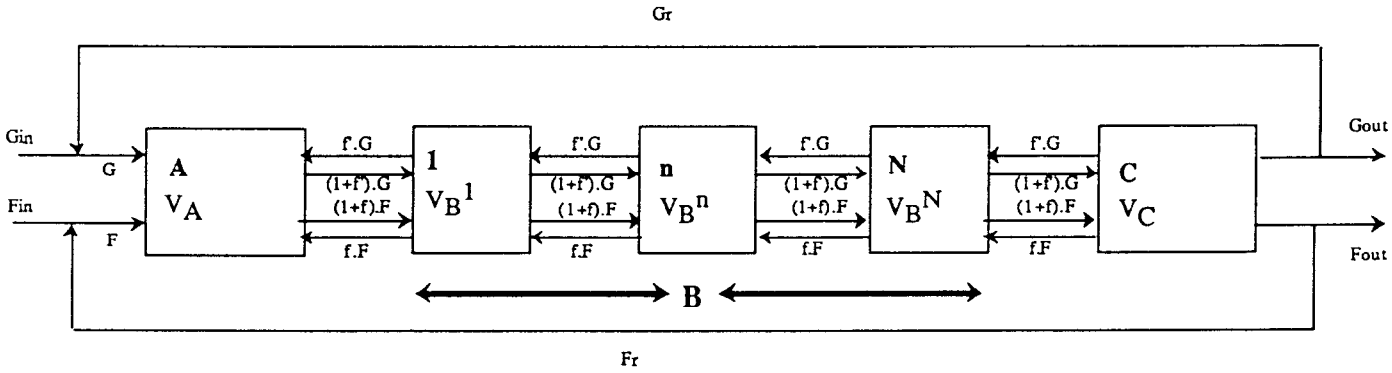

1.3.1 The nitrifying column model

The balance equations modelling the column are defined for each part of the column for the liquid and the gas phase.

Part A

$$\frac{\varepsilon_L}{\varepsilon} V_A \frac{dC_{Si}^A|_L}{dt} = F_{in}.C_{Si}^{in}|_L + F_r.C_{Si}^{out}|_L - (f+1).F.C_{Si}^A|_L + f.F.C_{Si}^1|_L + \frac{\varepsilon_L}{\varepsilon} V_A.\phi_{Si}^A|_{GL}$$

$$\frac{\varepsilon_G}{\varepsilon} V_A \frac{dC_{Si}^A|_G}{dt} = G_{in}.C_{Si}^{in}|_G + G_r.C_{Si}^{out}|_G - (f'+1).G.C_{Si}^A|_G + f'.G.C_{Si}^1|_G - \frac{\varepsilon_L}{\varepsilon} V_A.\phi_{Si}^A|_{GL}$$

Part B (fixed bed)

$$\varepsilon_L.V_B^n.\frac{dC_{Si}^n|_L}{dt} = (1+f).F.C_{Si}^{n-1}|_L + f.F.C_{Si}^{n+1}|_L - (f+1).F.C_{Si}^n|_L - f.F.C_{Si}^n|_L + \varepsilon_L.V_B^n.\phi_{Si}^n|_{GL} + \varepsilon_L.V_B^n.\phi_{Si}^n|_{LF}$$

$$\varepsilon_G.V_B^n.\frac{dC_{Si}^n|_G}{dt} = (1+f').G.C_{Si}^{n-1}|_G + f'.G.C_{Si}^{n+1}|_G - (f'+1).G.C_{Si}^n|_G - f'.G.C_{Si}^n|_G - \varepsilon_L.V_B^n.\phi_{Si}^n|_{GL}$$

Part C

$$\frac{\varepsilon_L}{\varepsilon} V_C \frac{dC_{Si}^C|_L}{dt} = (f+1).F.C_{Si}^N|_L - f.F.C_{Si}^C|_L - F_r.C_{Si}^C|_L - F_{out}.C_{Si}^C|_L + \frac{\varepsilon_L}{\varepsilon} V_C.\phi_{Si}^C|_{GL}$$

$$\frac{\varepsilon_G}{\varepsilon} V_C \frac{dC_{Si}^C|_G}{dt} = (f'+1).G.C_{Si}^N|_G - f'.G.C_{Si}^C|_G - G_r.C_{Si}^C|_G - G_{out}.C_{Si}^C|_G - \frac{\varepsilon_G}{\varepsilon} V_C.\phi_{Si}^C|_{GL}$$

with: n the number of the tank, 1<n<N

$\phi_{Si}^n|_{GL}$ the gas-liquid transfer term (mol/unit volume. unit time)

$\phi_{Si}^n|_{LB}$ the liquid-biofilm transfer term (mol/unit volume. unit time)

The parameters involved in these equations can be classified in a first approach in three types: flow rates variables, column design variables and transfer rate terms

☐ Flow rates variables

Three types of flow rate can be defined in the model:

- the input flow rates: F_{in} (liquid) and G_{in} (gas)
- the recycling flow rates represented by the recycling ratio ($\frac{\text{Inlet flow rate}}{\text{Recycling flow rate}}$): R_L (liquid) and R_G (gas)
- the back-mix flow fractions: f (liquid) and f' (gas) (see the previous scheme)

The two first types can be manipulated while the back-mix flow fractions depend on the column design and on the flow rate inside the column. A relation exist between f for N-stirred tank model and the axial dispersion term E_X in the plug flow model (TN 27.1), but even if E_X can be approximated in two phases fluidized and fixed beds (TN 27.1), there is no evidence

that these relations can be used for the nitrifying column. In fact the best way to estimate the back-mix fractions f and f' is RTD experiments (see section 1.3.2).

In experiments performed at UAB Laboratory, the liquid input flow rate is 2.8 ml/min with a recycling flow rate varying from 18 ml/min (ratio 6.4) to 45 ml/min (ratio 16). The standard total flow rate of gas inside the column is 3 l/min and the gas circuit is closed. In the model an open gas circuit has been chosen, but in order to mimic a closed circuit behaviour, a low input (0.03 l/min) and a high recycling flow (2.97 l/min, ratio of 99) are used.

☐ Column design

The column design parameters are set on the dimension and characteristics of the fixed bed reactor of UAB Laboratory (TN 25.330). The diameter of the real column is 120 mm execpted at the bottom and at the top of the column (112 mm). A diameter of 120 mm was chosen for the totality of the column. According to the volume of the real column (8.53 l), the total height of column is 755 mm instead of the 796 mm of the real column.

Column:

Diameter: 120 mm.

Height: 716.2 mm occupied by beads + liquid + gas (calculated from the occupied volume of 8,1 l).

755 mm total (calculated from the total volume of 8.53 l)

Volume: 8.1 l (experimental occupied volume measured at UAB Laboratory).

8.53 l (total volume calculated from the dimensions of the UAB column)

Void fraction ε^{col}: 0.52

Liquid void fraction $\varepsilon_L{}^{col}$: 0.475

Gas void fraction $\varepsilon_G{}^{col}$: 0.045

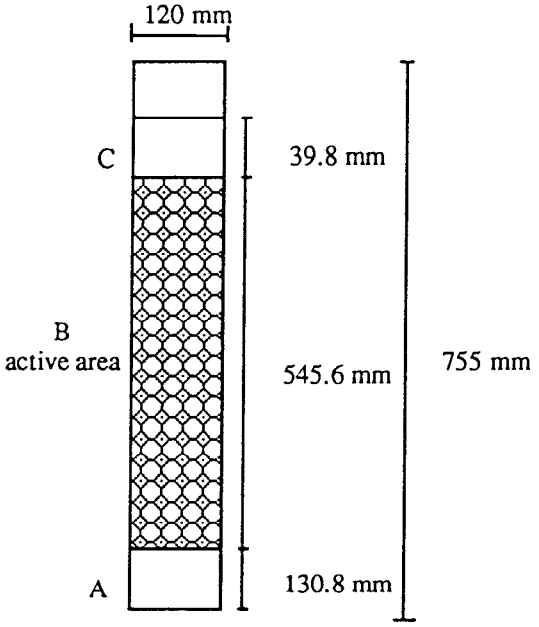

Part A

Volume: 1.48 l

Part B (active fixed bed area)

Volume: 6.17 l

ε: 0.37

ε_L: 0.33

ε_G:0.04

Part C

Volume: 0.45 l

☐ Transfer rates

The transfer rates terms involved in the model are:

- the gas-liquid transfer rate
- the liquid biofilm transfer rate

The coefficients governing the gas-liquid transfer rate are the $K_La|_{Si}$ and C^*_{Si} (gases) or P^o (liquids). For gases, the gas-liquid transfer term can be written:

$$\phi^n_{Si}|_{GL} = K_La|_{Si}.(C^*_{Si}|_L - C_{Si}|_L)$$

$K_La|_{Si}$ depends on the column design and on the working condition (stirring, air flow rate, recycling ratio) of the process. UAB Laboratory (TN 25.330) gives $K_La|_{O2}$ values from 0.013 s^{-1} to 0.024 s^{-1}, depending on the section of the column (top, bottom), on the inlet air flow rate and the stirring in the bottom of the column.

C^*_{Si} can be calculated from the k_{Si} by:

$$C^*_{Si}|_L \approx 55.55 \frac{y_{Si}}{k_{Si}}$$

For liquids (H_2O), the gas liquid transfer term is written:

$$\phi^n_{Si}|_{GL} = -K_La|_{Si}.(C^*_{Si}|_G - C_{Si}|_G)$$

with

$$C^*_{Si}|_G \approx \frac{x_{Si} \,.\, P \,.\, k_{Si}}{8.314 \,.\, T}$$

The liquid-biofilm transfer rate expressions have been studied in TN 27.1. In the present model, it was assumed that there is no biofilm limitation, thus the liquid-biofilm transfer rate expression is given by the production/consumption rates of the micro-organisms:

$$\phi^n_{Si}|_{LB} = r^{Ns}_{Si} + r^{Nb}_{Si}.$$

This assumption is valid until the thickness of the biofilm is less than 8.8 µm (TN27.1). The value of 8.8 µm has been defined has the thickness of a biofilm for wich the O_2 tranfer limitation occurs with a dissolved gas fraction of 45 % of the air saturation (Cox et al., 1980).

1.3.2 Analysis of the liquid RTD: model and experimental

Using the previous hydrodynamic equations, simulations of the liquid Residence Time Distribution were made for a pulse input.

The column design coefficients are set to the UAB Laboratory column as previously detailed.

The inlet gas flow rate is set to 0.03 l/min with a recycling ratio of 99.

The inlet liquid flow rate is set to 2.8 ml/min with a recycling flow of 18 ml/min and 45 ml/min, in order to compare simulations to UAB Laboratory experimental RTD measurements.

The pulse input (1g of tracer) was injected in the part A (bottom) of the column, and it is assumed that at t=0, there is a well-mixed solution of the tracer in the part A of the column:

$$C^A_{tracer}(t=0) = \frac{1}{V_A \,.\, \frac{\varepsilon_L}{\varepsilon}}$$

a)

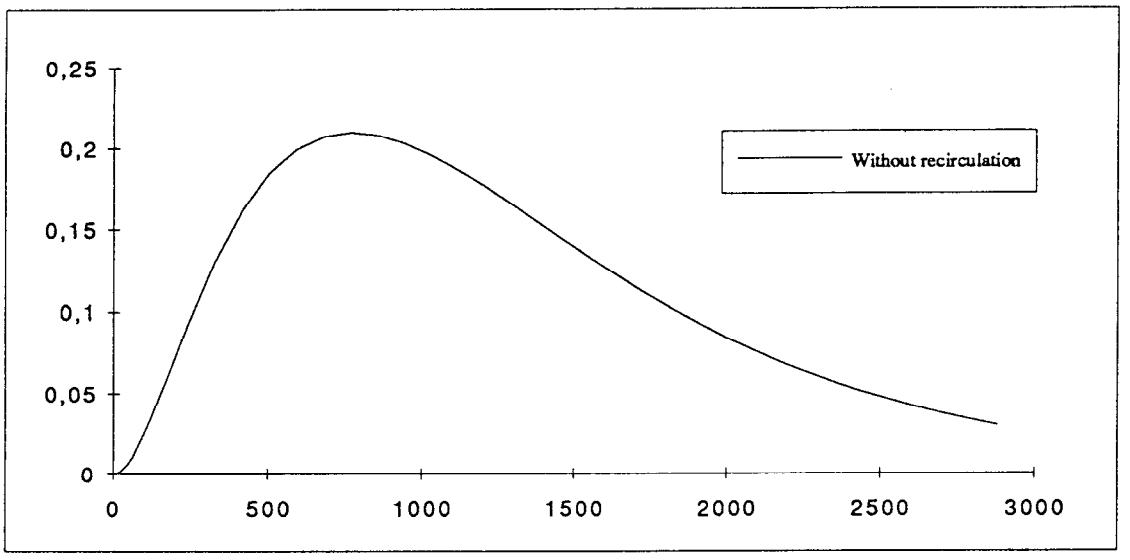

b)

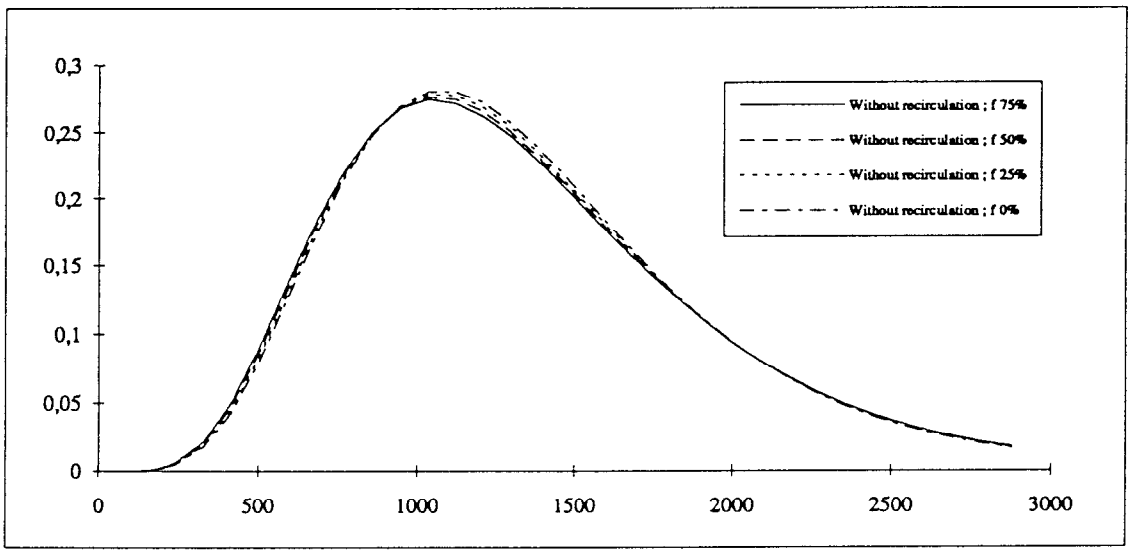

c)

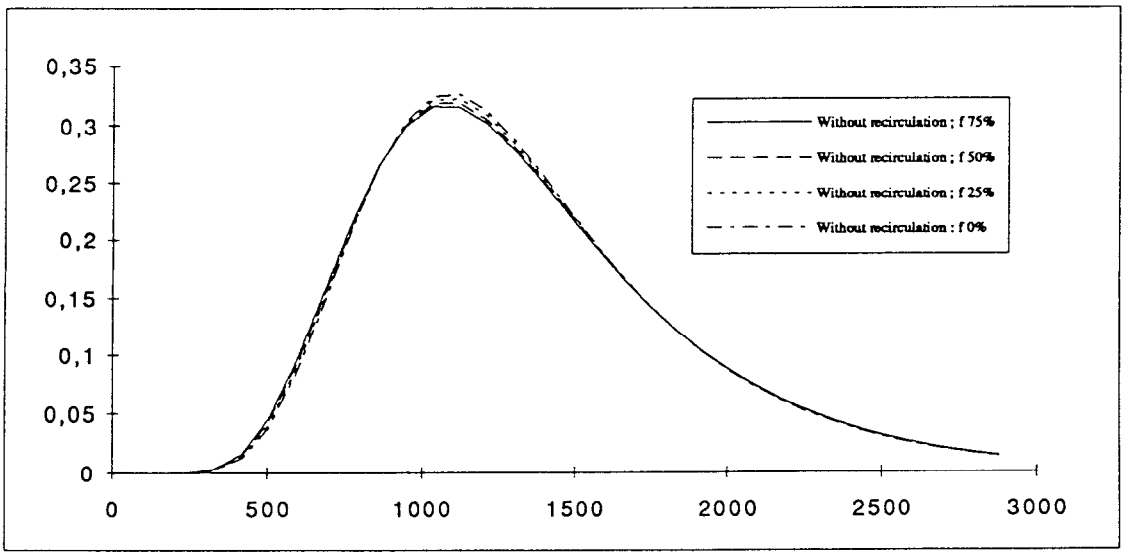

Figures 1a-b-c: RTD curves for no liquid recirculation
(a: fixed bed= 1 tank ; b: fixed bed= 5 tanks ; c: fixed bed= 10 tanks)

a)

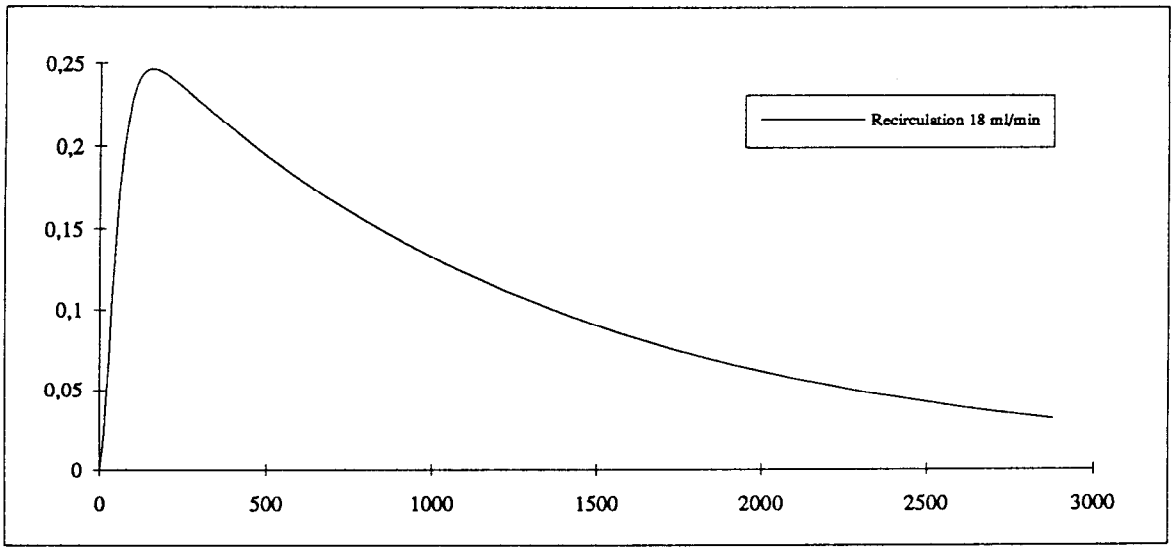

b)

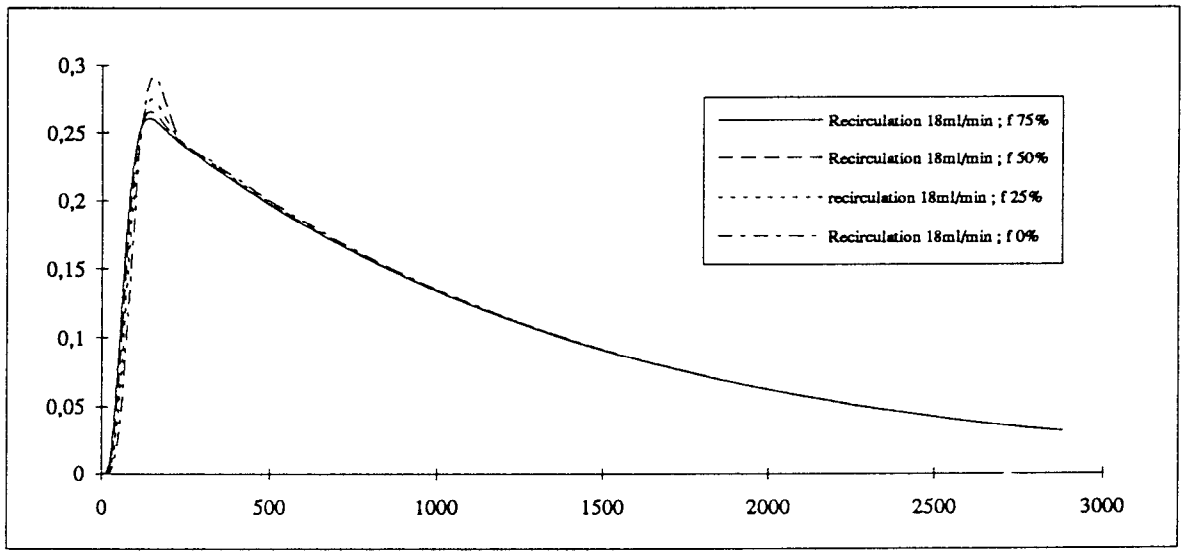

c)

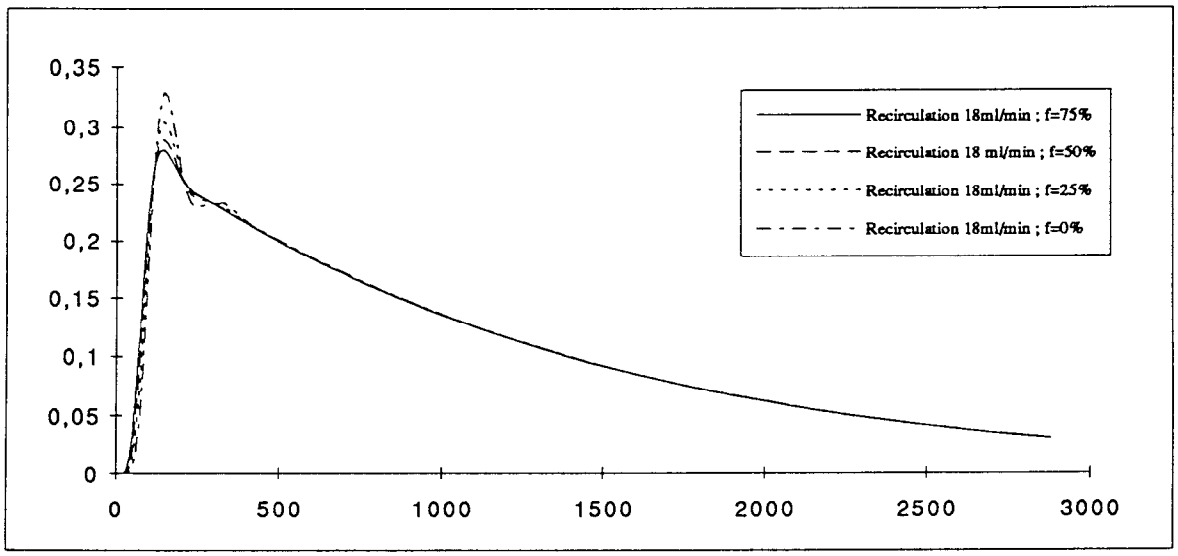

Figures 2a-b-c: RTD curves for a liquid recirculation of 18 ml/min
(a: fixed bed= 1 tank ; b: fixed bed= 5 tanks ; c: fixed bed= 10 tanks)

a)

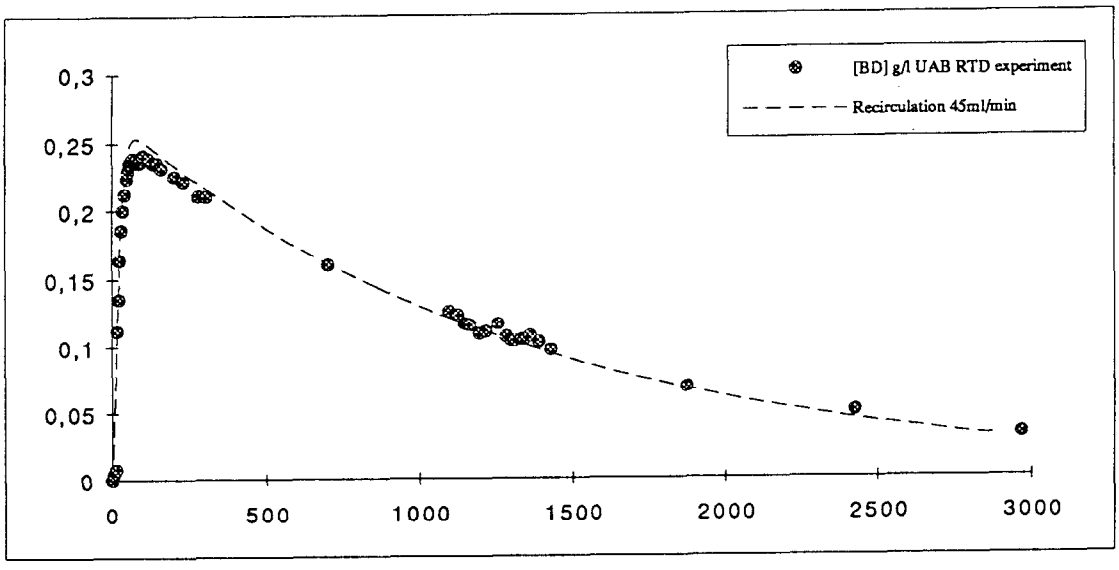

b)

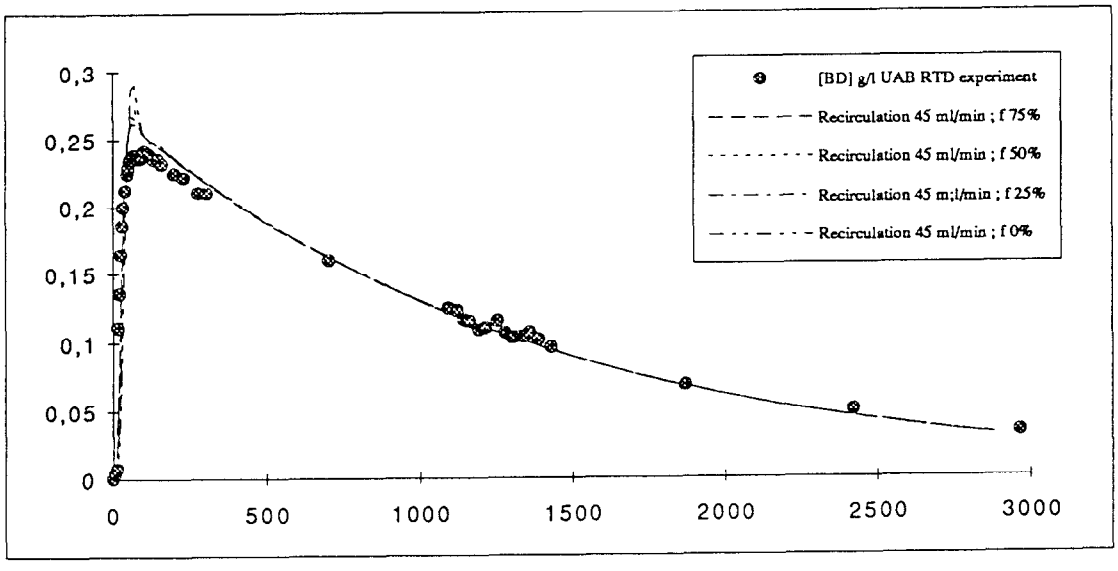

c)

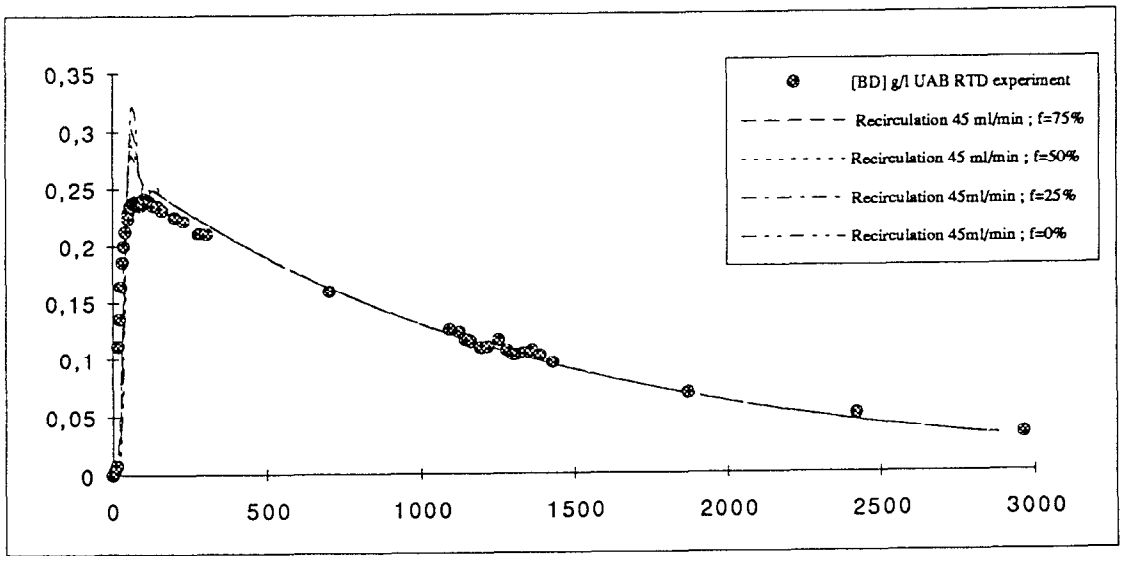

Figures 3a-b-c: RTD curves for a liquid recirculation of 45 ml/min.
Dots are for experimental data. Lines are for simulated RTD
(a: fixed bed= 1 tank ; b: fixed bed= 5 tanks ; c: fixed bed= 10 tanks)

Three liquid recirculations were tested: 0 ml/min, 18 ml/min and 45 ml/min. For each of them, different models were simulated: fixed bed (part B) equivalent to 1 tank, to 5 tanks and to 10 tanks. For the 5-stirred tank and 10-stirred tank configurations different back-mix liquid fractions (f) were considered: 0%, 25%, 50% and 75%.

These two parameters (f and N) govern the observed hydrodynamic behaviour of the column.

The output concentration of the tracer for the different simulation are reported in figures 1,2 and 3.

The RTD curves simulated for 18 and 45 ml/min recycling flow rates (figures 2 and 3) have a profile in agreement with the experimental ones measured at UAB fixed bed reactor.

The 1-stirred tank configuration for the fixed bed seems to be in better agreement with the experimental curves than the 5 or 10-stirred tank configuration. Nevertheless, it can be noted that by increasing the back-mix fraction (f), the RTD profile of the 5 and 10-stirred tank, tends towards the RTD profile of the 1-stirred tank configuration. In figures 3, the experimental values of RTD measured at UAB laboratory (TN 25.330), compared to the the simulated RTD for different N and f conditions, show that f would be greater than 75%, and that this value would increased with the number of tanks chosen to model the bed

For high liquid recycling ratio, the effect of the number of stirred tanks is limited, and the heigh of the output peak of tracer (figure 3) depends on the back-mix fraction. At the opposite, when no liquid recycling occurs, the RTD profile depends mainly on the number of stirred tank adopted to describe the fixed bed (figure 1).

In order to calibrate the model, two parameters need thus to be identified:

- N, the number of equivalent stirred tank for the fixed bed. The identification can be made for non recycling condition, in order to reduce the effect of back-mixing inside the column.
- the liquid back-mix fraction (f). This parameter must be identified for a defined N-stirred tank configuration. Moreover, the value of f can depend on the flow rate inside the column (this could explain the different heigh of the output tracer peak in experimental measurements, for the different recycling conditions).

The determination of f and N is important for the study of short dynamics (less than 30 hours). But for long dynamics, the influence of f and N is less important than the effect of the recycling ratio and of the boundary conditions.

1.3.3 Choice of a standard simulation configuration for the nitrifying column

In order to compare the response of the column to different working conditions, a standard simulation configuration must be first defined as a reference.

The column design,, standard working conditions (input and recycling flow rates), and the boundary conditions (liquid and gas composition; biomass fixed at t_0) are reported in table 3.

The 5-stirred tanks configuration with no back-mixing (f-f'=0) has been chosen for the fixed bed because:

- it allows to have a concentration profile inside the column, as reported by Cox et al (1980) for the fixed biomass;
- the back-mixing parameters f and f' are not yet identified, and as previously remarked in RTD analysis, these parameters are important for short dynamics. Taking f and f' equal to 0 does not affect the behaviour of the column for long dynamics.

The 4000 ppm value for CO_2 in the gas phase is the maximal fraction of CO_2 allowed in the cabin for the crew.

A concentration of 100 mg N-NH_3/l in the liquid inlet represents a load of 0.11 kg / m^3 liquid in the column and per day.

Table 3: standard configuration of the column for the first simulations.

Column	Height: 716.2 mm diameter:120 mm Volume part A:1.48 l Volume part B:0.45 l Pressure: 1 atm Temperature: 25°C
Fixed bed (active area)	Particle diameter: 4.1 mm N: 5 f: 0% f': 0%
Input flow rate	Fin: 2.8 ml/min Gin: 0.03 l/min
Recycling ratio	R_L: 6.42 R_G: 99
Gas composition	CO_2: 0.004% O_2: 21% H_2O: 0%
Liquid composition	NH_3: 7.14 mmol/l (100 mg N-NH_3/l) H_3PO_4: 0.1 mmol/l (no limiting) H2SO3: 0.1 mmol/l (no limiting)
Gas-Liquid transfer parameters	$K_La\|_{O2}$: 51 h^{-1} (0.014 s^{-1}) $K_La\|_{CO2}$: 51 h^{-1} (0.014 s^{-1}) $K_La\|_{H2O}$: 500 h^{-1} $K_La\|_{NH3}$: 0 h^{-1} (no gas-liquid transfer) [other parameters are defined in table 1]
Kinetics parameters	Kwo: 0% [other parameters are defined in table 2]
Physico-chemical parameters	[parameters are defined in table 1]
Biofilm	No biofilm limitation

II Simulation for various conditions

For each simulation, the results are expressed into 2 forms:
- the concentrations in the outlet flows of the column, and the total biomass inside the bed;
- the concentrations profiles inside the column and the biomass distribution inside the bed (all these profiles are reported in appendix).

2.1 Numerical treatment of the model

The system of differential equations is solved using a Runge-Kutta-Merson algorithm of the 4th order, with a variable integration step. The program is running on a Pentium 75 IBM PC compatible computer. The running time depends on the number of stirred tank considered for the fixed bed and on the pseudo-steady state assumptions for the numerical treatment of equations.

Considering all compounds (ionic and non ionic), for the two phases (gas and liquid), the column is described by a set of 46 differential equations. The system can be reduce to 24 equations if all the forms of a compound are added and represented by a single differential equation, assuming:

$$\frac{dC_{Si-ionic}}{dt} + \frac{dC_{Si-non\ ionic}}{dt} = \frac{dC_{Si-Tot.forms}}{dt}$$

The solution of the system gives the time evolution of the sum of all the forms of a compound. To obtain the dissociated and non dissociated forms time evolution, the pH equilibrium relations must be used:

$$\begin{cases} C_{Si-ionic} + C_{Si-non\ ionic} = C_{Si-Tot.forms} \\ C_{Si-ionic} = f(K_A, C_{Si-Tot.forms}) \end{cases}$$

Such an approximation is justified by the fact that the dissociation equilibria can be assumed to be instantaneous compared to the either dynamics of the process.

A pseudo-steady state assumption can be made for a compound S_i in one phase if the integration of $\frac{dC_{Si}}{dt}$ by the Runge-Kutta-Merson algorithm require an integration step much lower that the other variables. This generally means that the S_i dynamics is much faster than that the other dynamics, leading to consider that the average value of its time derivative can be neglected. In other words, that its dynamic is sufficiently rapid for S_i instantaneously reach its steady state value. Then it can be assumed that:

$$\frac{dC_{Si}}{dt} = 0$$

and C_{Si} can be numerically solved by using the expression of the differential equation. In the case of a compound in the gas phase in the part A, that lead to:

$$C_{Si}^{A}\Big|_G = \frac{G_{in}.C_{Si}^{in}\Big|_G + G_r.C_{Si}^{out}\Big|_G - (f'+1).G.C_{Si}^{A}\Big|_G + f'.G.C_{Si}^{1}\Big|_G - \frac{\varepsilon_L}{\varepsilon} V_A.\phi_{Si}^{A}\Big|_{GL}}{(f'+1).G}$$

Running times for various N-tanks configurations were studied for the simulation of a nitrification process of 100 hours. This time is 9'30" for the 1-stirred tank, 47'30 for the 5-stirred tanks and 95' for the 10-stirred tanks. Simulations with pseudo-steady state assumption on O_2 gas or/and CO_2 gas or/and H_2O gas failed. It seems that for transient periods (as it is at the beginning of a simulation) pseudo-steady state assumption can not be made on O_2 and CO_2. Perhaps after the short transient period of "adaptation" to the initial conditions, this assumption could be made for the two compounds, that should reduced the computing time for long dynamics.

2.2 Steady state [figures 4 - Appendix A]

In order to observe the steady state behaviour of the column with the model developped, a simulation of 750 h (31 days) was performed.

In the outlet flows, the steady state is not reached at the same time for all the compounds.

For O_2, (figures 4-c; 4-d), the steady state seems never really reached. But from 150 h, there is only a short variation for the gas fraction (figure 4-c) from a mean value of 0.1788 with a standard deviation of 0.4%, thus a steady state can be assumed at 150h. The minimun observed for the dissolved oxygen corresponds to the nitrite peak.

The liquid O_2 is in equilibrium with the gas phase (mean C_{O2} 2.32 10^{-4} mol/l), thus the curves are similar.

For CO_2, steady state is reached at 300 h (figures 4-a; 4-b). The mean gas fraction is 920 ppm (gas inlet of 4000 ppm) and the mean total liquid CO_2 concentration is 1.36 10^{-3} mol/l.

For mineral N-compounds, (figures 4-e; 4-g), the maximun conversion yield (97.5 % conversion of NH_3 into HNO_3) is reached at 150 h. This yield is constant until 225-275 h and slowly decrease to reach 95% at 750 h. This decrease seems to be the result of small changes in the biomass distribution in the bed. In the transient period (0h - 100h) the nitrite concentration reachs a maximun of 8 10^{-4} mol/l (11 mg N-NO_2/l). The decrease in the conversion yield leads to an increase in the outlet concentration of nitrite: 6 10^{-5} mol/l (0.84 mg N-NO_2/l) at 97.5 % of conversion to 9.6 10^{-5} (1.3 mg N-NO_2 /l) at 750 h. The residual N-NH_3 at 750 h is 3.17 10^{-4} mol/l (4.4 mg N-NH3 /l).

It can be noted than with 1.3 mg N-N02 /l, the nitrite concentration is 10 time higher than the potable water limit of 0.1 mg NO2 /l.

The H_2O gas fraction has a steady value of 3.08 10^{-2} (99.3 % of saturation).

The concentrations profiles inside the column (appendix A) give additionnal informations on the behaviour of the column.

First, excepted for O_2 and HNO_2, the compounds in the liquid phase have a remarkably steady concentration through the column. Only at the bottom of the column (part A) a difference can be noticed, due to the mixing of recycling and input flows. This step does not exist for gaseous compounds because of the high recycling flow compared to the inlet flow.

After the transient period, the nitrite concentration is higher in the first section of the column (1.5 10^{-4} mol/l) than in the others. This value must be compared with the half saturation constant of *Nitrobacter* (3.6 10^{-4} mol/l). The nitrite limitation can be another reason of the decrease in the ammonia conversion.

In a similar way, the O_2 concentration is the lowest in the first section of the bed ($1.4\ 10^{-4}$ mol/l). This represents 51 % of the air saturation (far of the limiting value of oxygen transfer in the biofilm), and more than 10 times higher than the half saturations constants. It can then be assumed that there is no oxygen limitation.

It appears that the nitrification is concentrated in the the first section of the fixed bed (first tank equivalent of the bed). That is confirmed by the biomass profiles. the distribution of the biomass inside the bed is in accordance with the experimental observations of Cox et al. (1980). There are a few differences between the distribution of the 2 organisms, but there growth reflect the higher growth rate of *Nitrosomonas*, and the delay in the transient period to eliminate the nitrite. The distribution of *Nitrosomonas* and *Nitrobacter* at the end of the simulation (750 h) is reported in table 4. The thickness of the biofilm stay over the limit of 8.8 µm for O_2 limitation.

Table 4: biomass distribution in the column at the end of the simulation

tank equivalent	1	2	3	4	5
Nitrosomonas (g/l)	0.745	0.052	0.014	0.006	0.003
Nitrobacter (g/l)	0.289	0.040	0.011	0.005	0.003
Ns+Nb (g/l) (mean: 0.2334 g/l)	1.034	0.091	0.025	0.011	0.006
% *Nitrosomonas* (tot: 70.5%)	72	57	56	54.5	50
Biofilm thickness (µm)	1.37	0.121	0.033	0.014	0.008

Simulations of 350 hours functionning seem sufficient to study and compare the behaviour of the column for various working conditions and parameters values. The next simulations are then performed for a nitrification process of 350 hours.

2.3 Simulations for different N-tank configuration [figures 5; 6; 7 - Appendix B; C; D]

The 3 N-stirred tank configurations (1 tank; 5 tanks; 10 tanks) tested in RTD analysis were used to simulated the same nitrification. There is no relevant difference for the outlet flows (figures 5; 6; 7) between the 3 configurations, excepted for the N-compounds curves. The nitrification efficiency and the outlet concentrations of N-compounds are reported in the table 5.

Table 5: results after 350 hours

Configuration of the fixed bed	N-NH_3 (mol/l)	N-NO_3 (mol/l)	N-NO_2 (mol/l)	Conversion yield	Mean biomass (g/l)
1	$3.85\ 10^{-4}$	$6.62\ 10^{-3}$	$1.36\ 10^{-4}$	92.7 %	0.229
5	$2.38\ 10^{-4}$	$6.84\ 10^{-3}$	$6\ 10^{-5}$	95.8 %	0.235
10	$2.09\ 10^{-4}$	$6.88\ 10^{-3}$	$5\ 10^{-5}$	96.3 %	0.237

Considering the previous experimental conversion yield of 98% reported by Forler (1994), the behaviour of the column is better represented by the high 10-stirred tank configuration than by the 1-stirred tank.

The profiles inside the column (appendix B; C; D) present great differences for O_2, HNO_2 and biomass distribution.

The 10-stirred tank biomass profiles confirm that the nitrification is concentrated at the bottom of the bed. In this configuration the difference in the distribution of the two organisms is most important and *Nitrobacter* colonizes the bed in the upper regions of the column. But it must be noted that the dissolved O_2 concentration ($1.01\ 10^{-4}$ mol/l) represents, in the first section of the bed, 36% of the air saturation, and even if the mean thickness of the biofilm in this section is 1.82 µm, there is no evidence that the "no biofilm limitation assumption" can be maintained.

The concentration in the bottom of the column indicates that the residence time of compounds (NH_3 and NO_2^-) in the first segment of the column is sufficient for the oxidation of these compounds by *Nitrosomonas* or *Nitrobacter*.

2.4 Simulations for different fixed biomass at t=0 [figures 5; 8; 9 - Appendix B; E; F]

The boundary conditions for the biomass is an important parameter for the simulation of the nitrifiying process. In the first simulations it appeared that the biomass distribution is not homogeneous in the column when the steady state is reached. This distribution, as the quantity of the biomass catalyzing the nitrification is important to know for the transient periods.

It is impossible to know how the biomass is distributed at the beginning of the simulation. That the reason why a concentration of 20 mg dry biomass/l is guessed both for *Nitrosomonas* and *Nitrobacter* in the standard configuration.

The purpose of the simulation with different biomass initial concentration profiles is then to have a first idea of the transient behaviour of the model and to view if for the same inputs on the column, the biomass distribution in steady state condition (assumed to be reached after 350 hours), is the same in the bed.

The transient behaviour is greatly affected by the biomass boundary conditions (figures 5; 8; 9). The outlet concentrations, and biomass distribution in the column are reported in table 6 for the three boundary biomass conditions tested: 2 mg/l, 20 mg/l and 200 mg/l

By initializing the standard configuration model with 2 mg biomass/l, the transient period up to 200 hours with a long and an important nitrite production (figure 8-e).

On the other hand, by initializing the model with 200 mg biomass /l, the transient period is less than 20 hours with low nitrite production (figure 9-e), but the oxygen fraction falls to 13% in the first hours of the simulation (oxygen limitation) (figure 9-d).

The biomass profiles in the column (appendix B; E; F) suggest that, at least for *Nitrobacter*, there is no more growth, at 350 hour in the first section of the bed, with the initialisation at 200 mg/l (appendix F), it is the end of the growth with the initialisation at 20 mg/l (appendix F), the growth is not ending with the initialisation at 2 mg/l (appendix F). This observation is confirmed by the results presented in table 6.

The results of table 6 show that even if the average biomass concentration in the column seems independant of the initial biomass concentration, the distribution of the biomass is different inside the bed. The distribution in the bed reachs a steady state far after the liquid and

gas compounds. If we assumed that the biomass distribution reported in table 4 is a steady state distribution, an initialisation with 2 mg biomass/l seems reachs this steady state faster than the other. The slow decrease in the conversion yield observed in figure 4-g can be the result of the changes in the biomass distribution inside the column.

Table 6: biomass distribution and outlet concentration at 350h for different biomass boundary conditions.

	Initial biomass (Ns or Nb)	Liquid (mol/l)					Gas fraction	
	g/l	O_2	CO_2 tot	$N\text{-}NH_3$	$N\text{-}HNO_3$	$N\text{-}HNO_2$	O_2	CO_2
	0.002	2.3 10-4	1.4 10-3	2.5 10-4	6.8 10-3	6.2 10-5	0.179	934 ppm
outlet flows	0.020	2.3 10-4	1.4 10-3	2.4 10-4	6.8 10-3	6.3 10-5	0.179	914 ppm
	0.200	2.3 10-4	1.4 10-3	2.2 10-4	6.9 10-3	5.8 10-5	0.179	900 ppm

			Section of the column					
		Initial biomass	1	2	3	4	5	average biomass in the column
	Ns	0.002	0.658	0.103	0.038	0.020	0.013	0.239
Biomass	*Nb*	0.002	0.230	0.072	0.031	0.018	0.013	
in the bed	*Ns*	0.020	0.621	0.122	0.047	0.025	0.015	0.235
	Nb	0.020	0.194	0.083	0.037	0.02	0.013	
g/l	*Ns*	0.200	0.576	0.141	0.059	0.032	0.021	0.233
	Nb	0.200	0.154	0.089	0.047	0.028	0.018	

2.5 Simulations for different liquid recirculations conditions [Figures 5; 10; 11 - Appendix A; G ; H]

The increase in the recycling flow rate, with a constant input liquid flow rate of 2.8 ml/min, leads to an increase in the liquid flow rate inside the column.

The comparison of the outlet flows for different recycling rate (0 ml/min; 18 ml/min and 45 ml/min) indicates that the less is the recycling rate the shorter is the transient period (figures 5-e; 10-e; 11-e), and the more rapid is the elimination of nitrite (table 7). This remark is in favour of using low recycling flow rate.

Table 7: Conversion yield and nitrite concentration in outlet flow for different recycling flow rates.

	0 ml/min	18 ml/min	45 ml/min
Nitrite at 50 h (mol/l)	9 10-6	1.2 10-4	1.8 10-4
Conversion yield at 50 h	98.1%	93.5%	91.1%
Nitrite at 350 h (mol/l)	4 10-6	6 10-5	9 10-5
Conversion yield at 350 h	96.5%	95.8%	94.9 %

The comparison of the profiles inside the column for the different recycling rate shows an important change in the biomass distribution inside the bed. For no recycling, the biomass, and by the way all biological reactions are fully concentrated in the the first section of the bed. By increasing the recycling rate, the biomass is more distributed inside the bed. As a consequense, the O_2 concentration and HNO_2 concentration are, respectively lower and higher in the first section of the column for low liquid recycling flow rates than for high liquid recycling flow rates.

With no recycling, the nitrite concentration in the first section of the column is 1.9 10^{-3} mol/l. It must be noted that this value perhaps inhibits the nitrification which is not taken into accounts because the inhibitory constants are not introduced in this first simulations (the same remark can be made with the previous figure 8-e, with a nitrite concentration up to 4 10^{-3} mol/l). At the end of the simulation 350 h) the dissolved oxygen is of 46% of air saturation. With a biofilm thickness of 1.5 µm in the first section of the bed, there is no biofilm limitation.

If we define the liquid residence time inside the column as $\frac{\text{column liquid volume}}{\text{inlet liquid flow rate}}$, with a constant input flow rate of 2.8 ml/min, the residence time distribution is constant (22.9 h).

But if we define the residence time distribution inside the bed as $\frac{\text{column liquid volume}}{\text{liquid flow rate in the column}}$, the changes in the recycling ratio lead to change the residence time distribution. Respectively, for 0 ml/min recycling, 18 ml/min and 45 ml/min, the residence time calculated are, 22.9 h, 3.08 h and 1.34 h.

2.6 Simulations for different gas recirculations conditions

With the standard gaz recycling ratio (recycling ratio of 99 and total gas flow rate of 3l/min), two other gas flow configuration were simulated:

- recycling ratio of 99 and total gas flow rate of 5l/min (figures 12 - Appendix I)
- recycling ratio of 199 and total gas flow rate of 3l/min (figures 13 - Appendix J)

The nitrifying conversion yield and the biomass distribution are not affected by the different gas flow conditions. This indicates that there was no gas (O_2 or CO_2) limitation.

The O_2 and CO_2 concentrations and the gas fractions are affected by the gas flows rates. The steady state values observed after 350 h are reported in table 8. The aspect of the profiles inside the column are not affected.

For a gas circuit very closed (recycling ratio of 199) approching the functionning conditions of the MELiSSA column, the steady state value of dissolved O_2 stays over the lowest value calculated in the first section of the bed (1.15 10^{-4} mol/l *i.e.* 42% of air saturation).

Table 8: outlet gas compostion for different gas flow rate conditions

	O_2 mol/l	CO_2 tot mol/l	O_2 gas fraction	CO_2 gas fraction
3l/min - recycling ratio: 99	2.3 10^{-4}	1.4 10^{-3}	0.179	914 ppm
5l/min - recycling ratio: 99	2.5 10^{-4}	2.0 10^{-3}	0.191	1326 ppm
3l/min - recycling ratio: 199	1.9 10^{-4}	7.7 10^{-4}	0.148	513 ppm

2.7 Simulation for a different f and f' values [figures 14 - Appendix K]

The liquid and gas back-mixing fractions (f and f'), set to 0% in the standard configuration are set to 75%. There is no relevant effect both on outlet flow composition (figures 14)and on the flows composition inside the column (appendix K).

This is compatible with the observation made on the RTD analysis (section1.3.2): the back-mixing fractions terms affect the behaviour of the column only for short dynamics, on small time observation scale (less than 8 hours).

Figures 4 a-f: Results of a simulation for the standard configuration (process of 750 h.) The curves (a-e) represent the composition in the gas or in the liquid outlet flows.

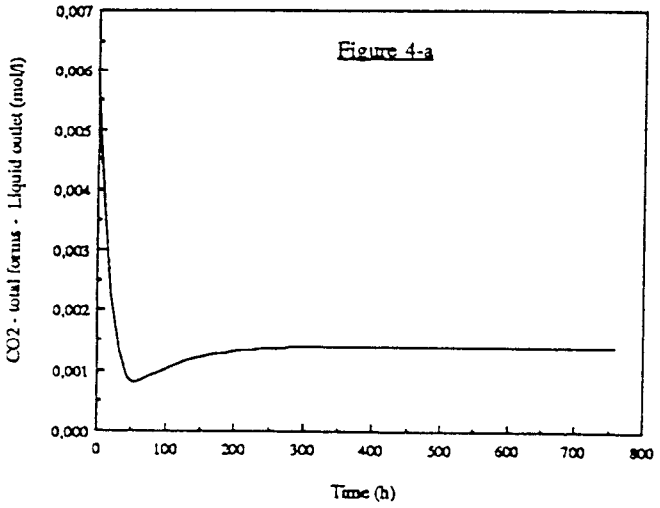

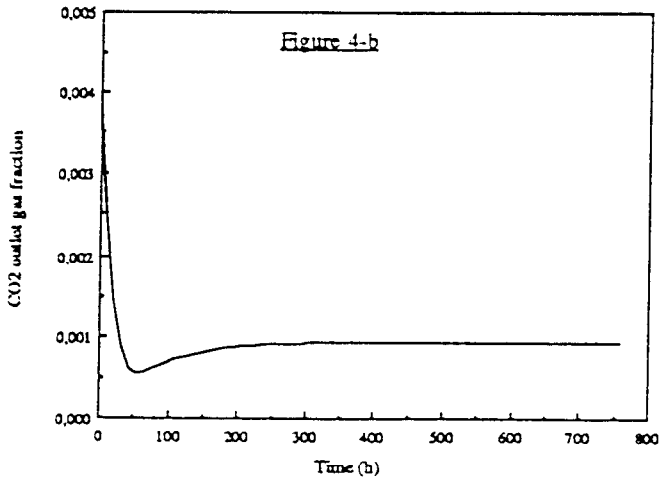

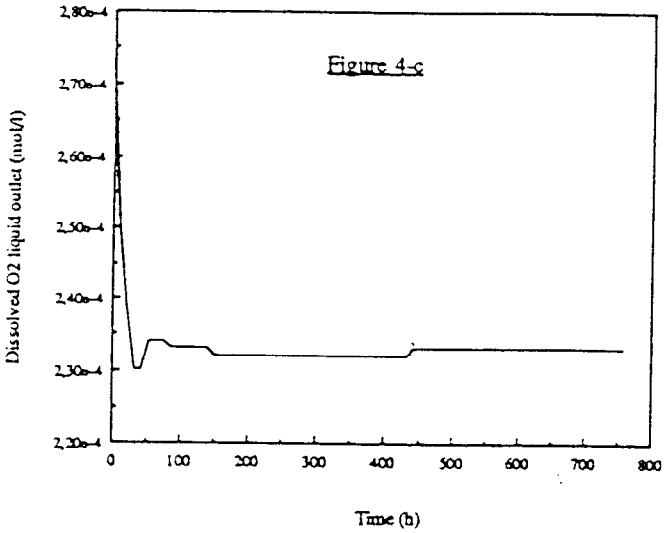

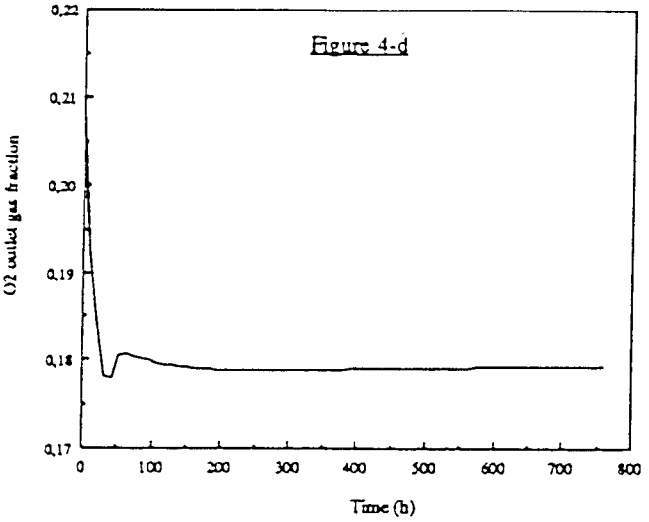

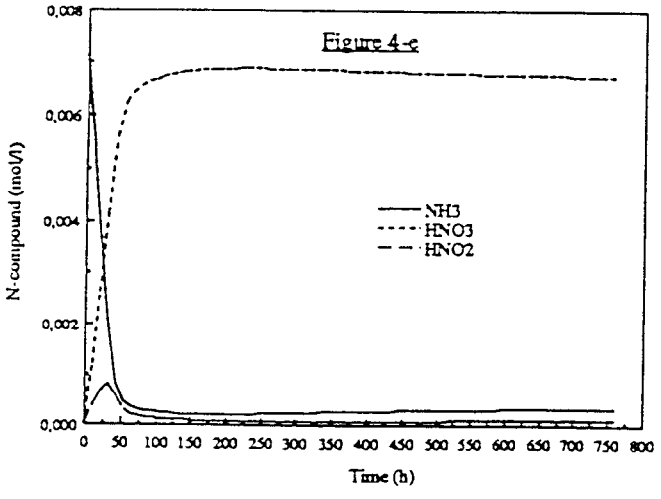

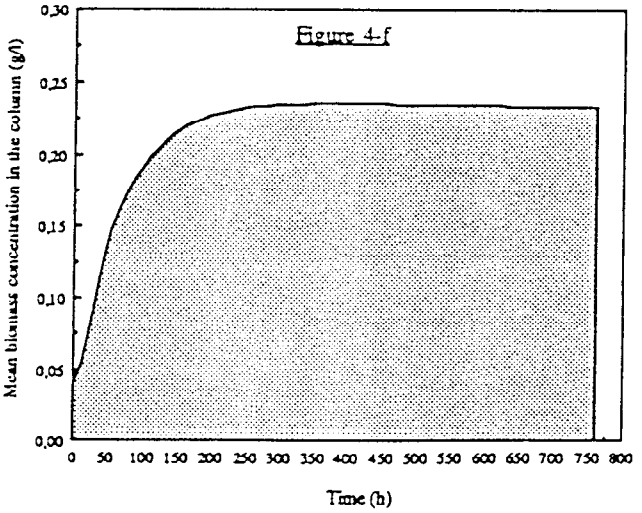

Figure 4 g: Results of a simulation for the standard configuration (process of 750 h.) The efficiency of the conversion of NH_3 is defined as : $\frac{[NH_3]_{in} - [NH_3]_{out}}{[NH_3]_{in}}$

Figure 4-g: efficiency of the nitrification

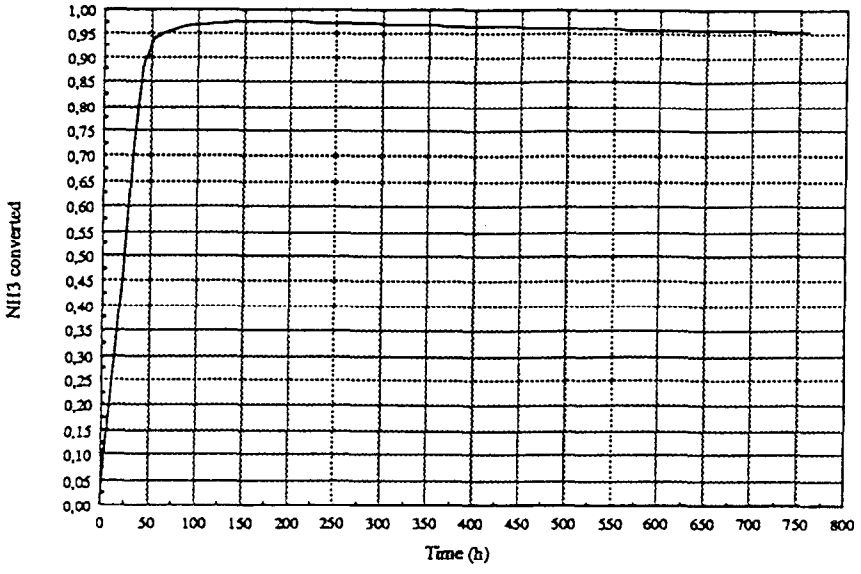

Figures 5 a-f: Results of a simulation for the standard configuration (process of 350 h.) The curves (a-e) represent the composition in the gas or in the liquid outlet flows.

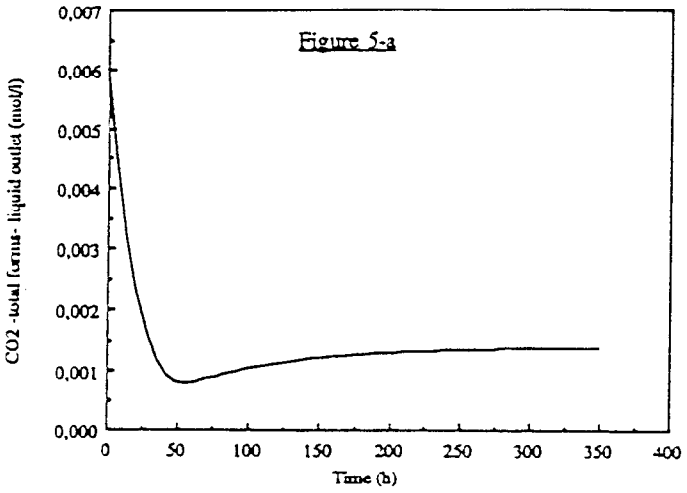

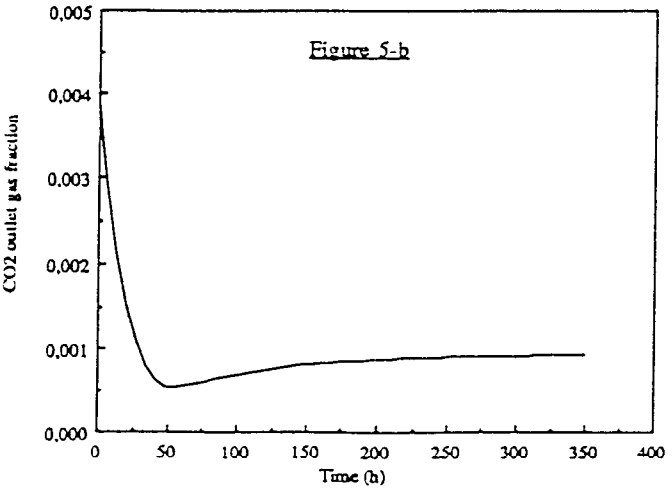

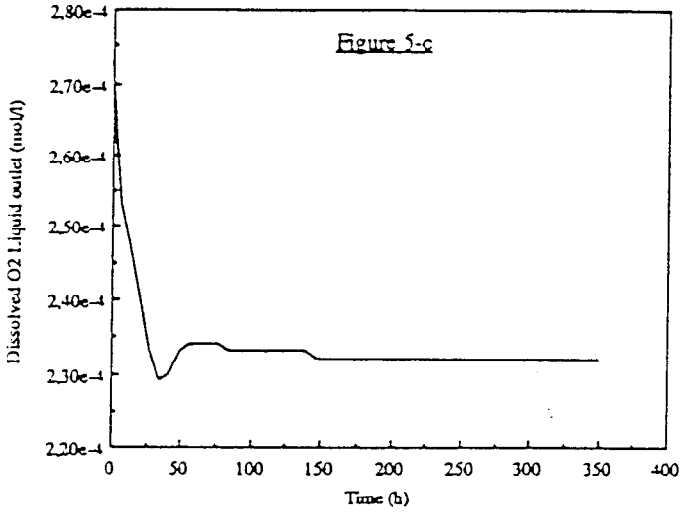

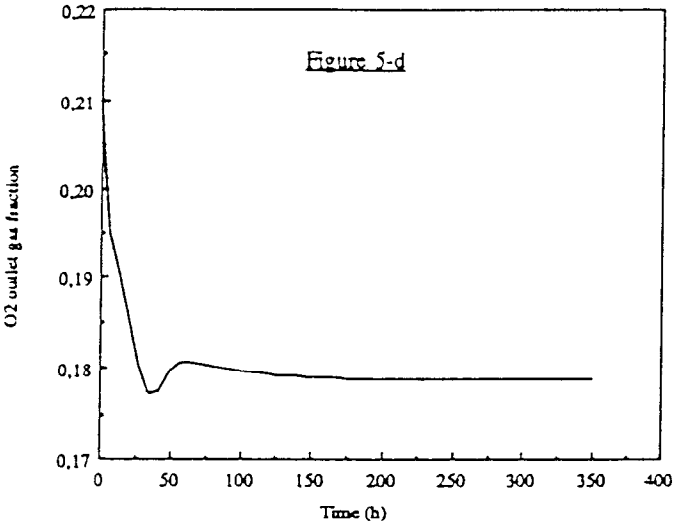

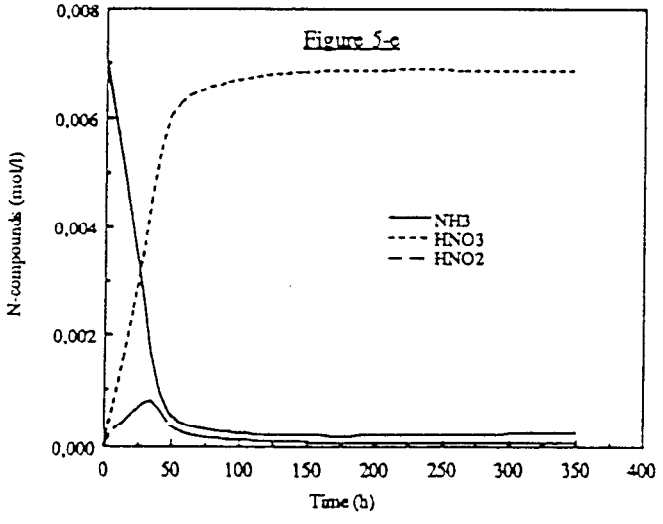

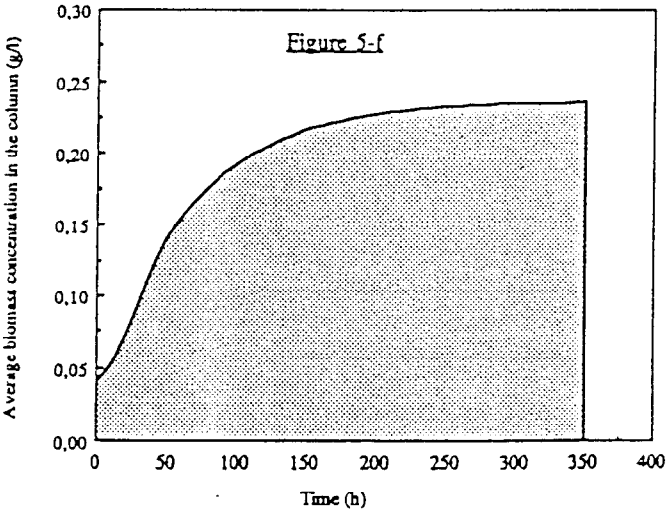

Figures 6 a-f: Results of a simulation for a standard configuration modified with a 1 stirred-tank configuration for the bed (process of 350 h.) The curves (a-e) represent the composition in the gas or in the liquid outlet flows.

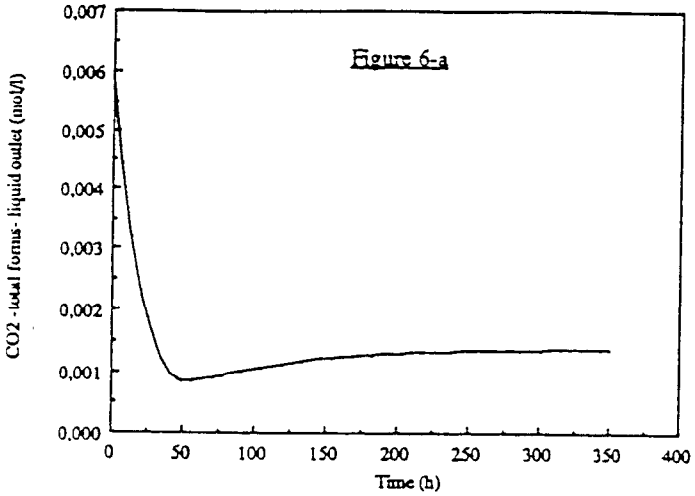

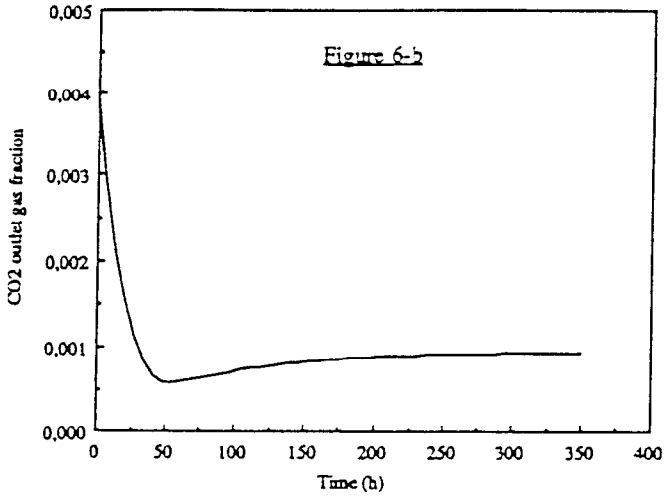

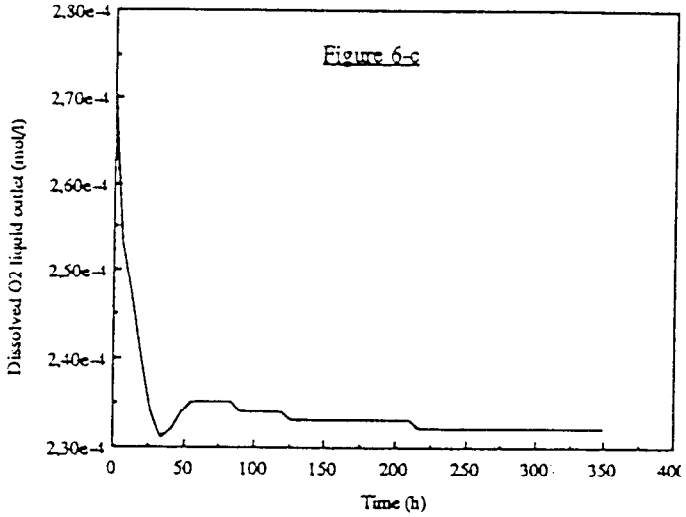

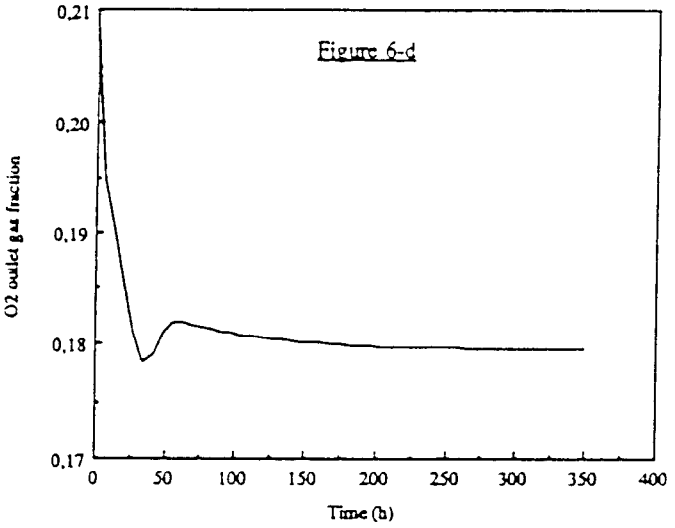

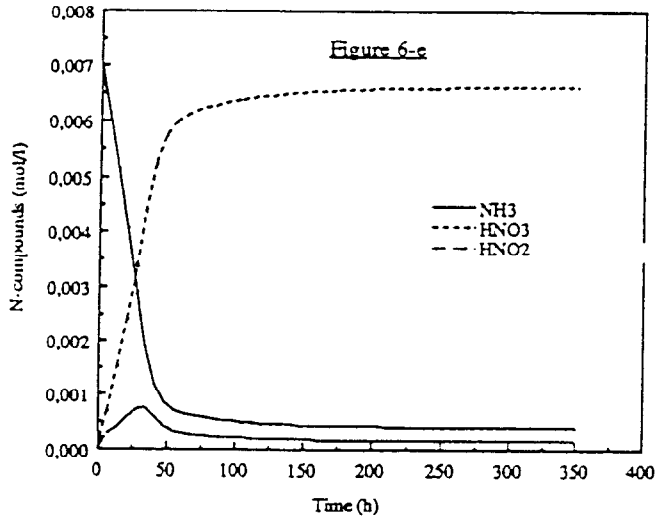

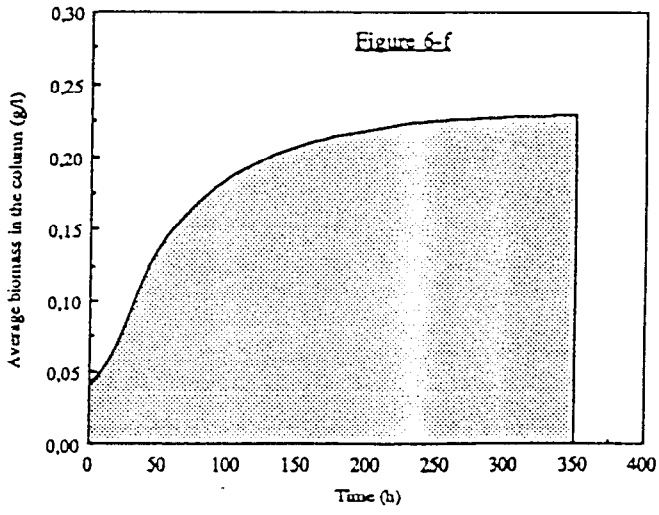

Figures 7 a-f: Results of a simulation for a standard configuration modified with a 10 stirred-tanks configuration for the bed (process of 350 h.) The curves (a-e) represent the composition in the gas or in the liquid outlet flows.

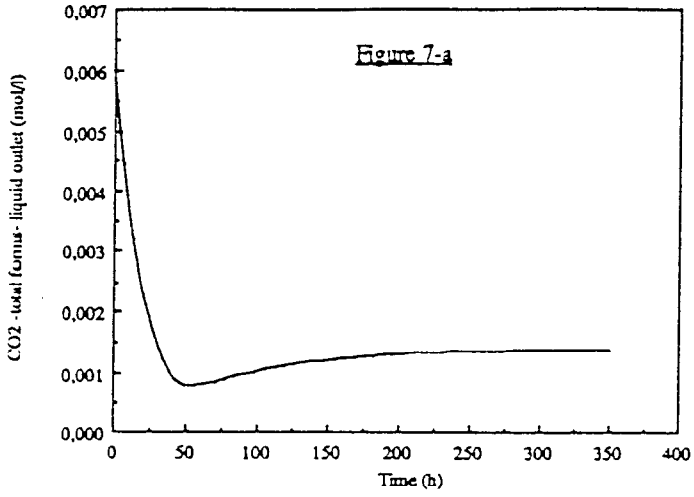

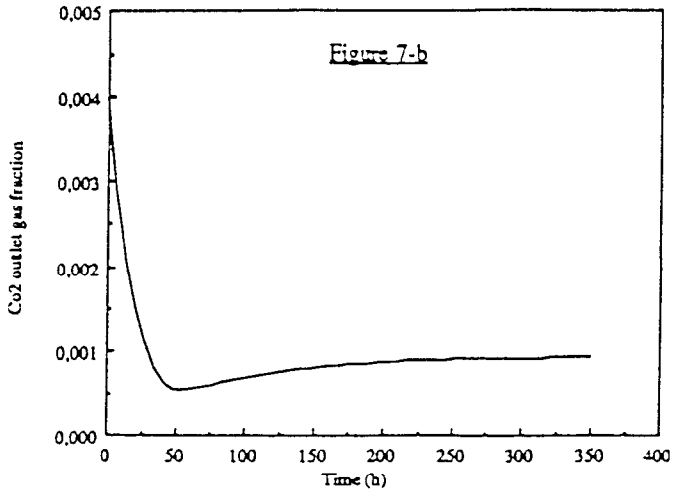

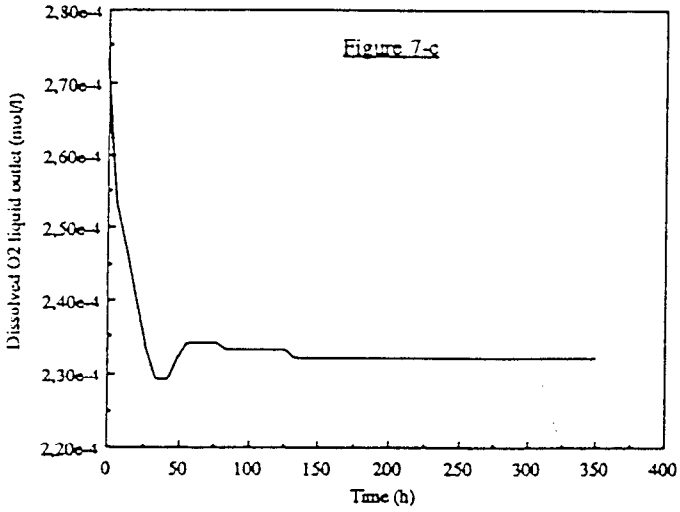

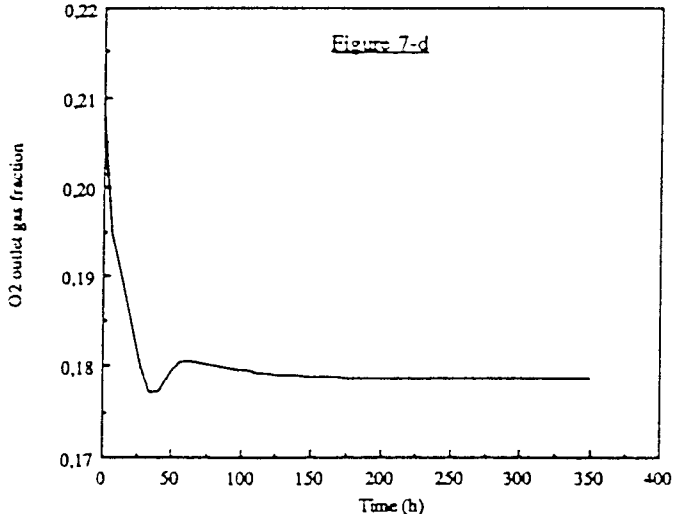

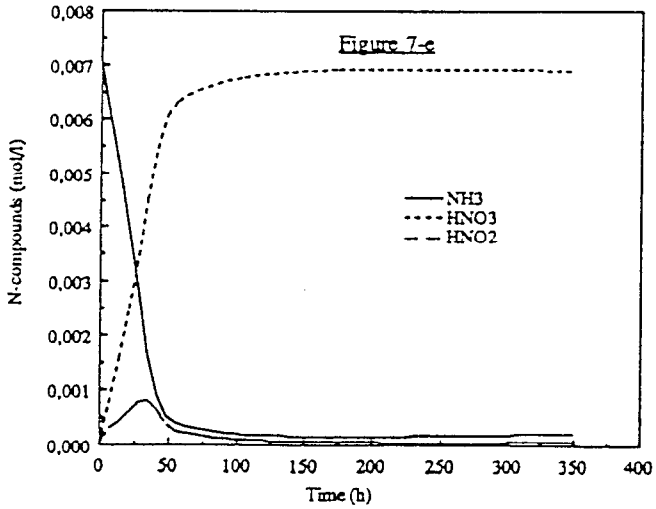

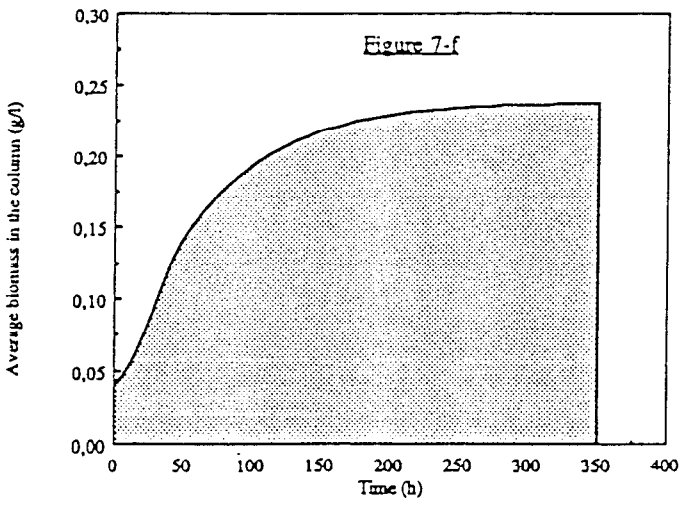

Figures 8 a-f: Results of a simulation for a standard configuration modified with an initial biomass concentration of 2 mg/l for each microorganism (process of 350 h.) The curves (a-e) represent the composition in the gas or in the liquid outlet flows.

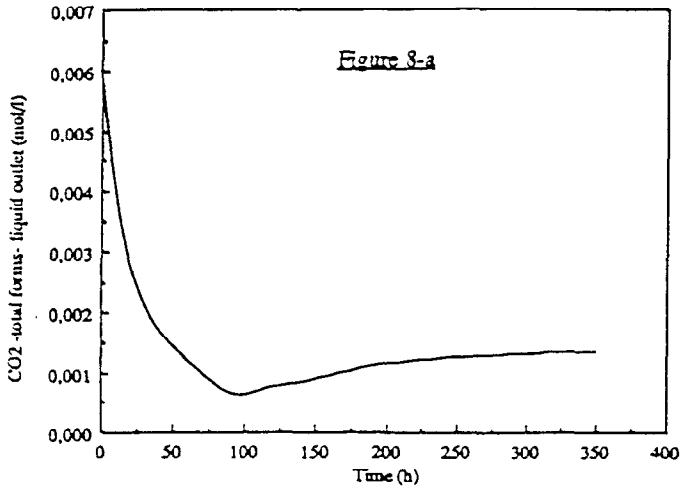

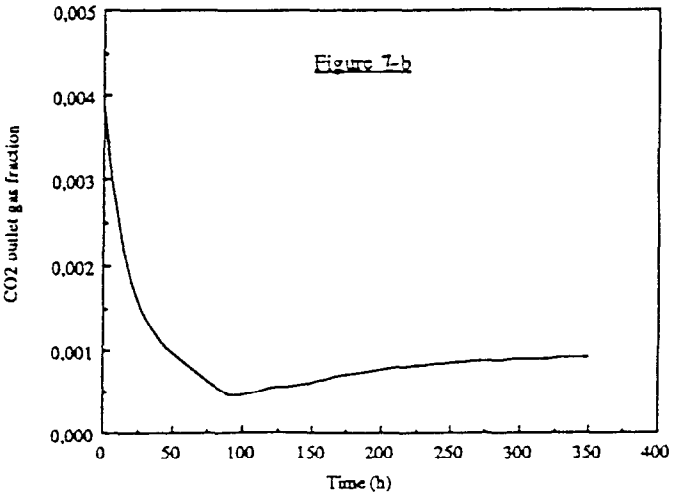

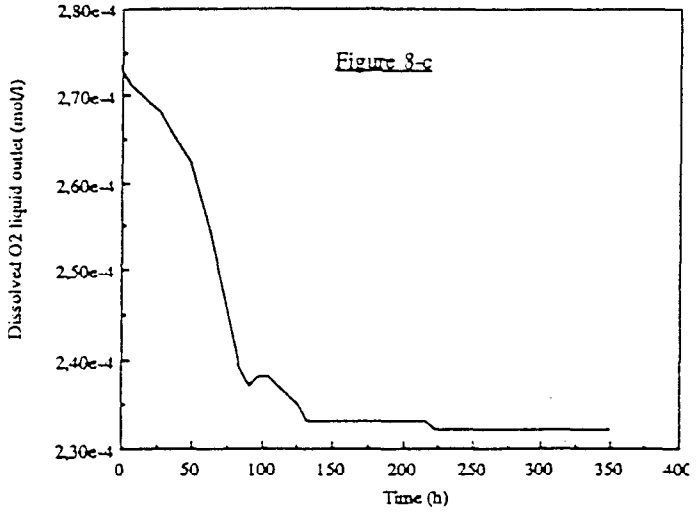

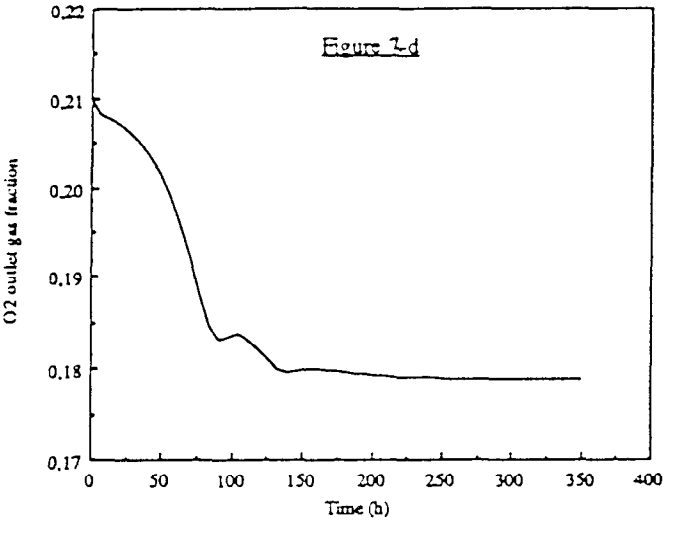

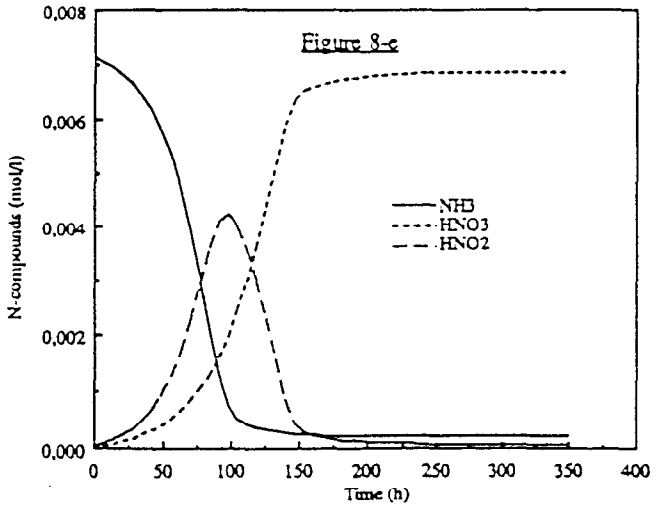

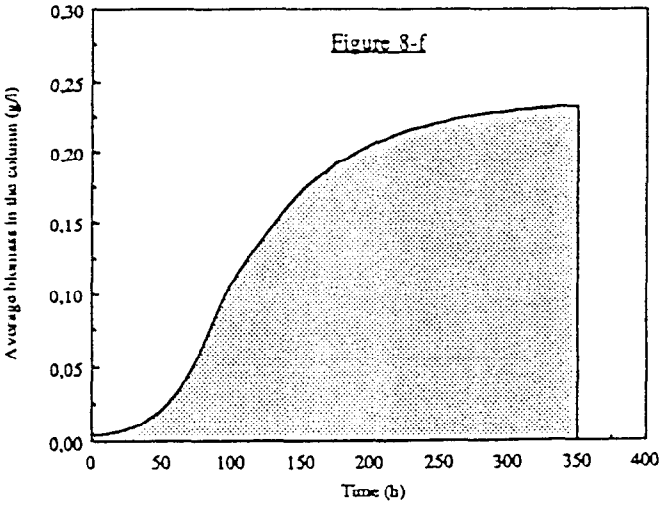

Figures 9 a-f: Results of a simulation for a standard configuration modified with an initial biomass concentration of 200 mg/l for each microorganism (process of 350 h.) The curves (a-e) represent the composition in the gas or in the liquid outlet flows.

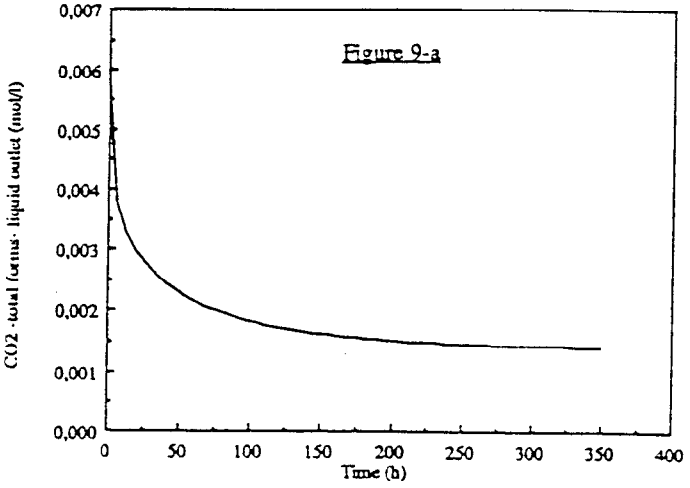

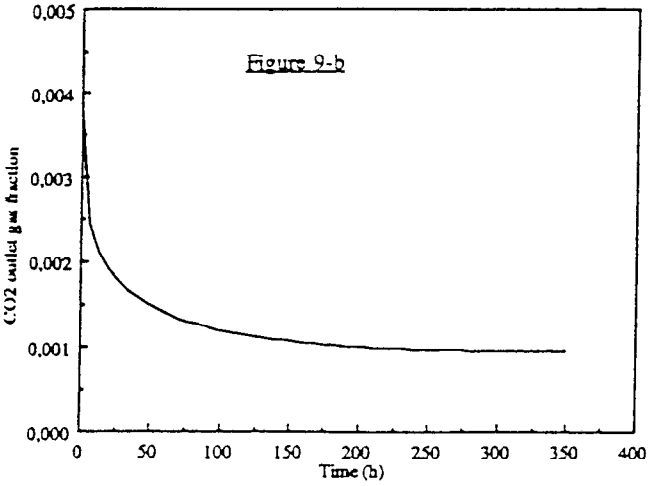

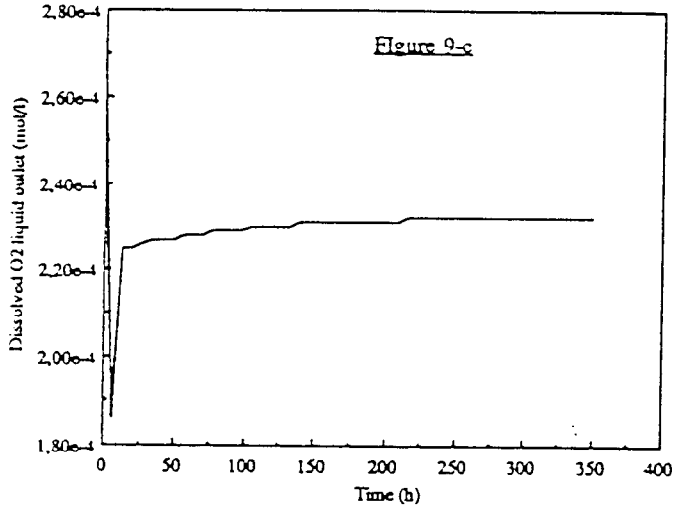

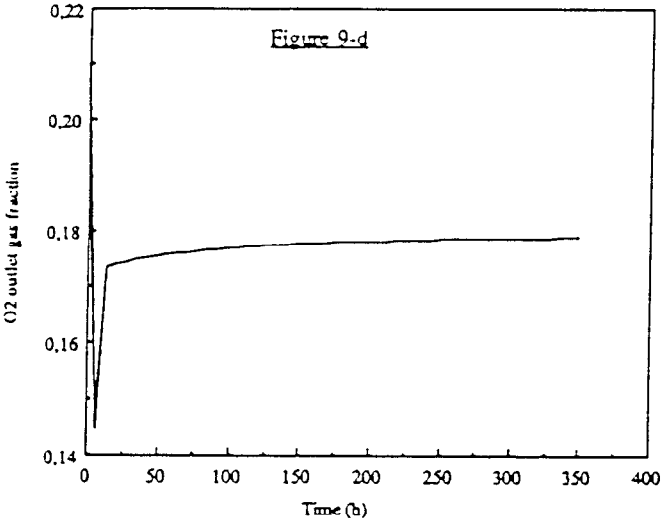

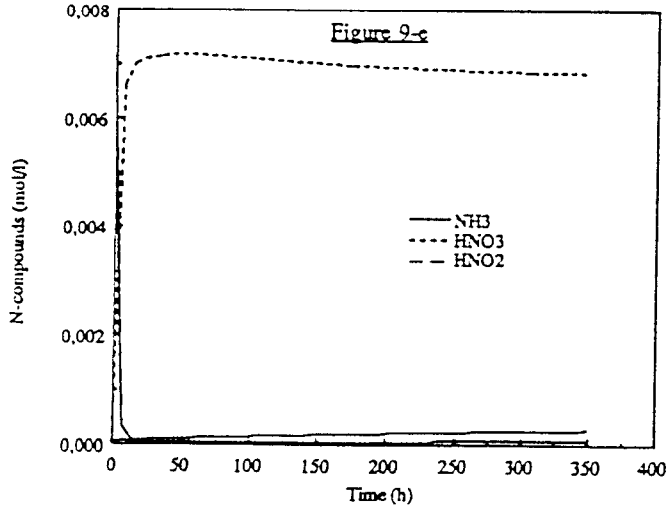

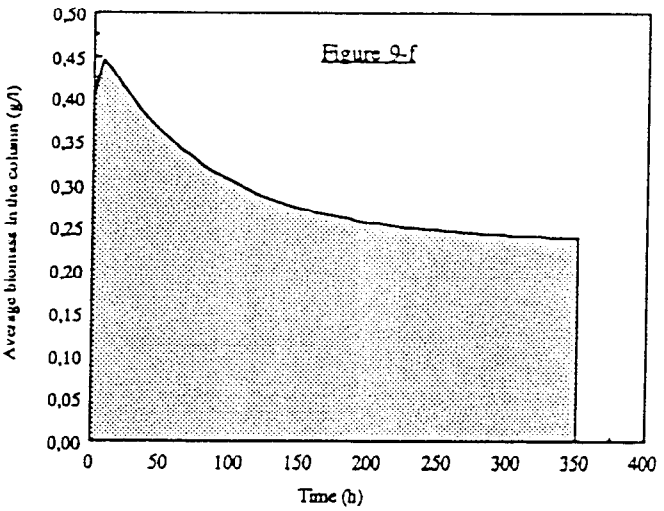

Figures 10 a-f: Results of a simulation for a standard configuration modified with a liquid recycling flow rate of 0 ml/min (process of 350 h.) The curves (a-e) represent the composition in the gas or in the liquid outlet flows.

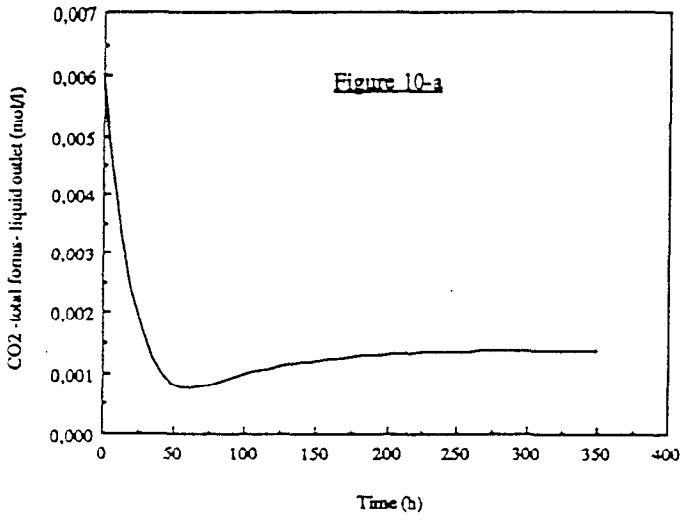

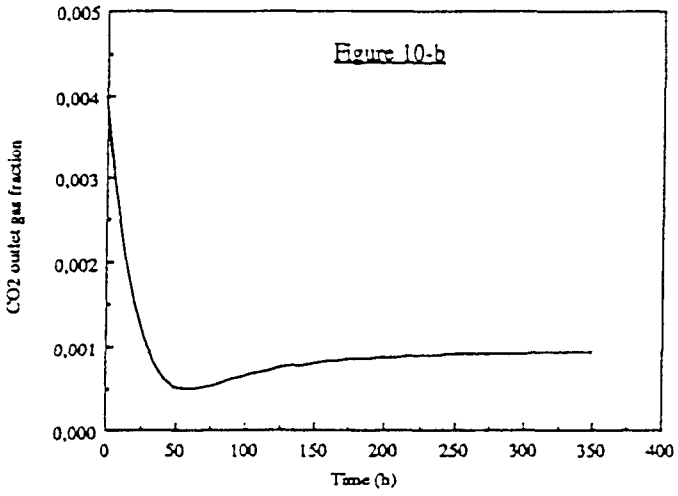

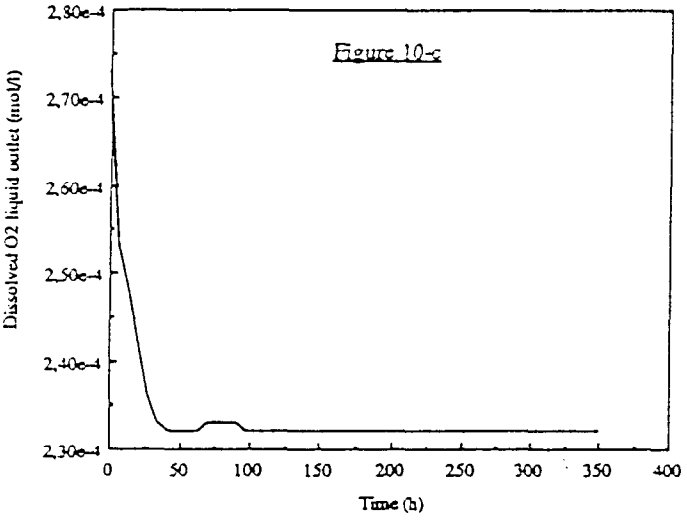

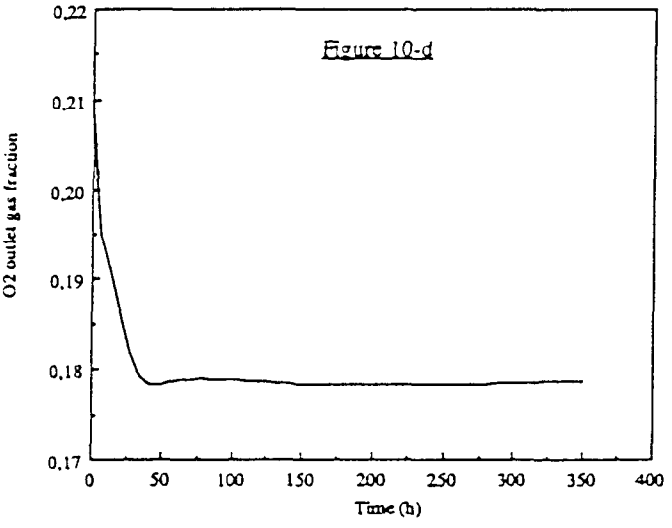

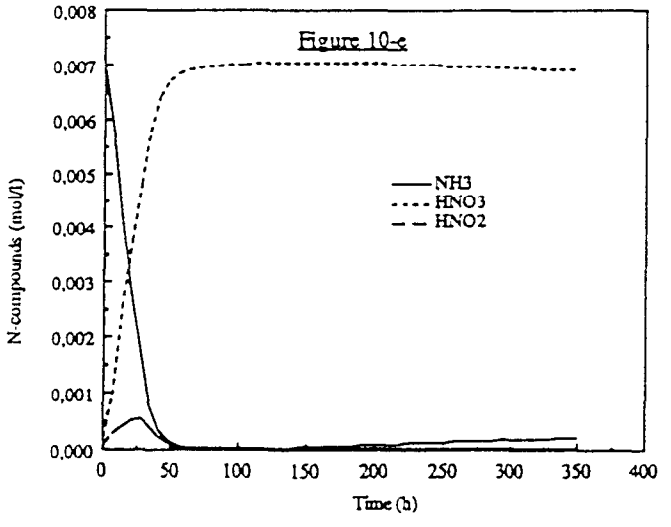

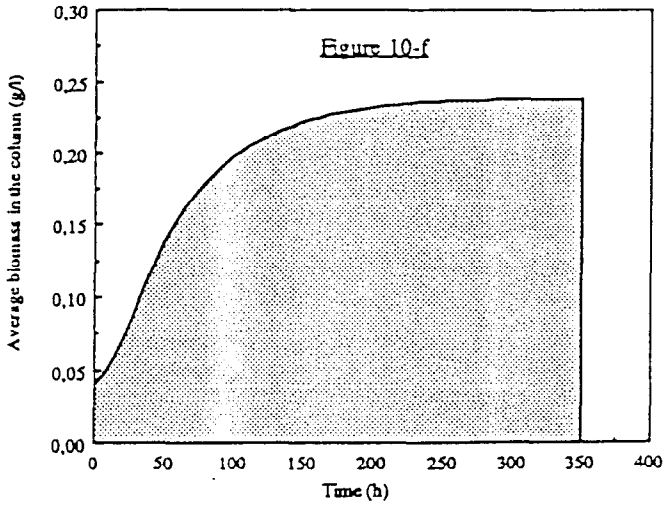

Figures 11 a-f: Results of a simulation for a standard configuration modified with a liquid recycling flow rate of 45 ml/min (process of 350 h.) The curves (a-e) represent the composition in the gas or in the liquid outlet flows.

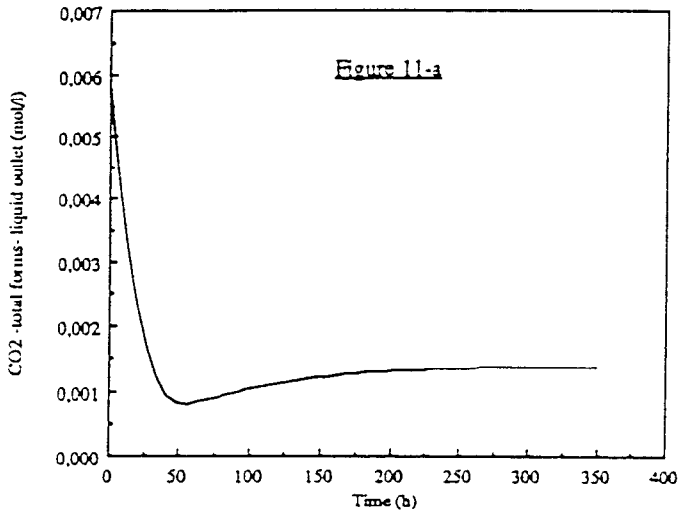

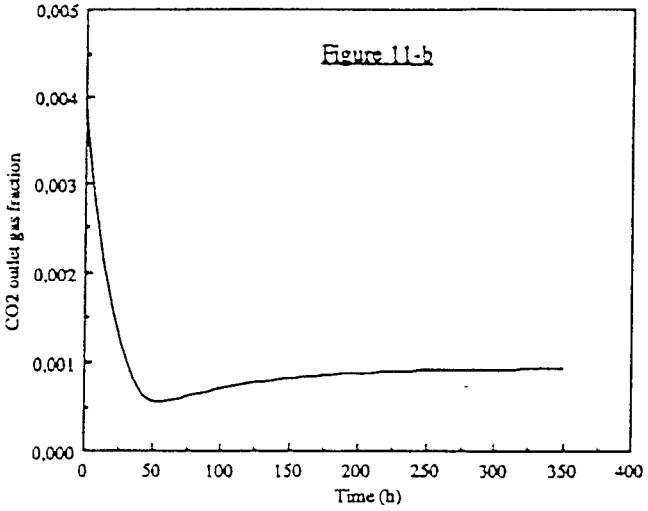

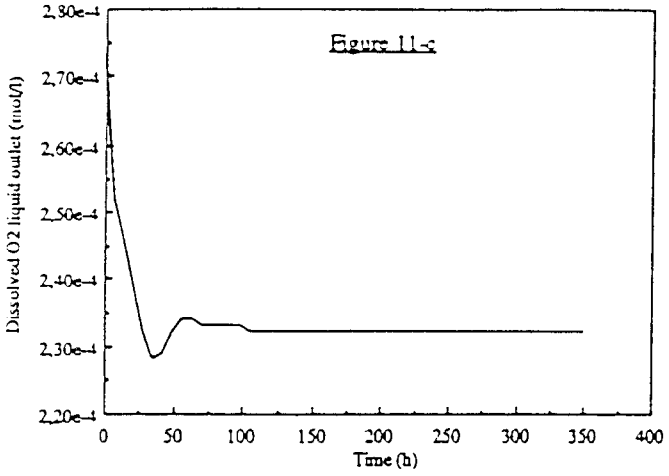

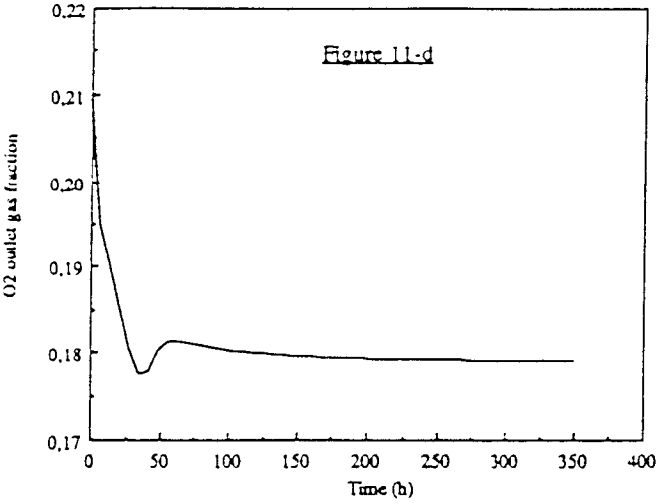

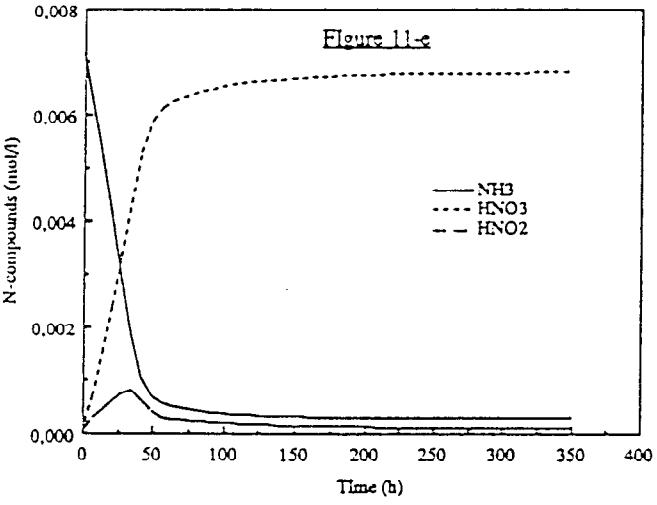

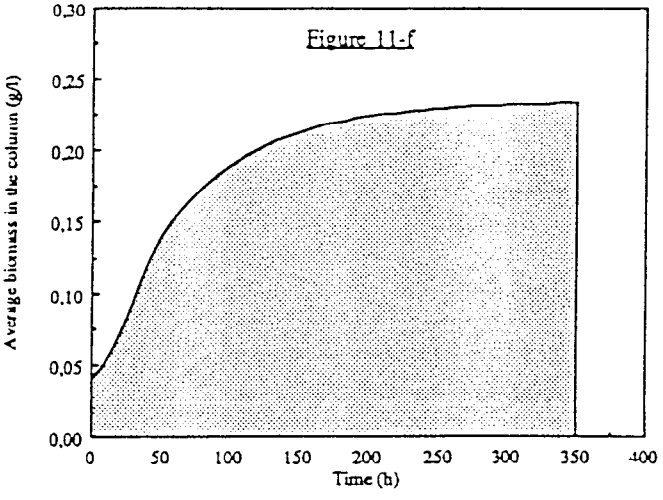

Figures 12 a-f: Results of a simulation for a standard configuaration modified with a gas total flow rate inside the column of 5 l/min (process of 350 h.) The curves (a-e) represent the composition in the gas or in the liquid outlet flows.

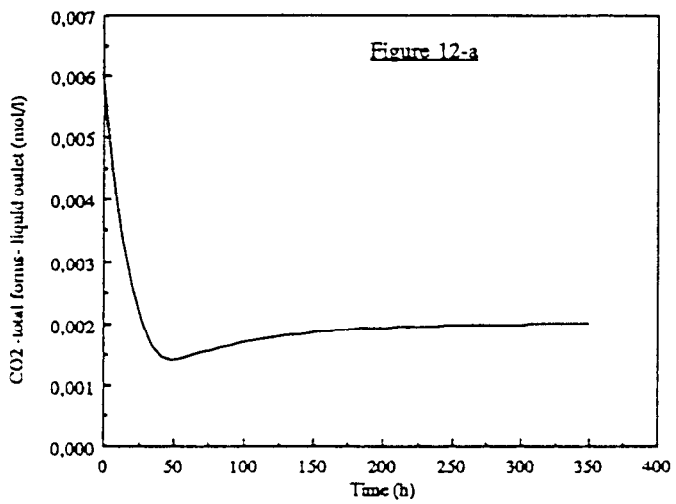

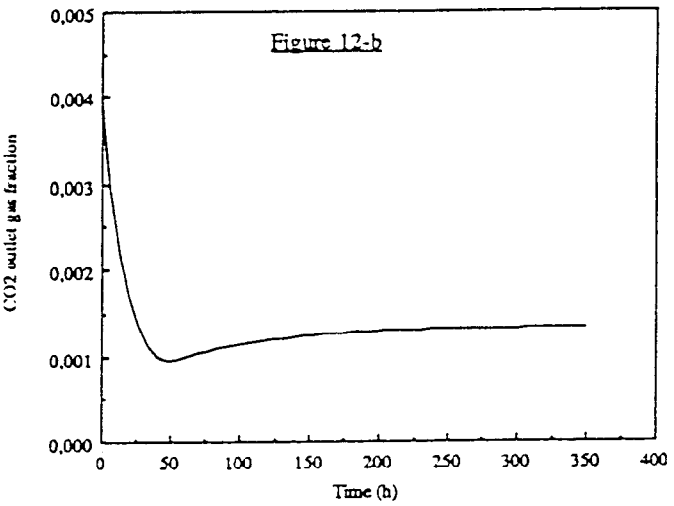

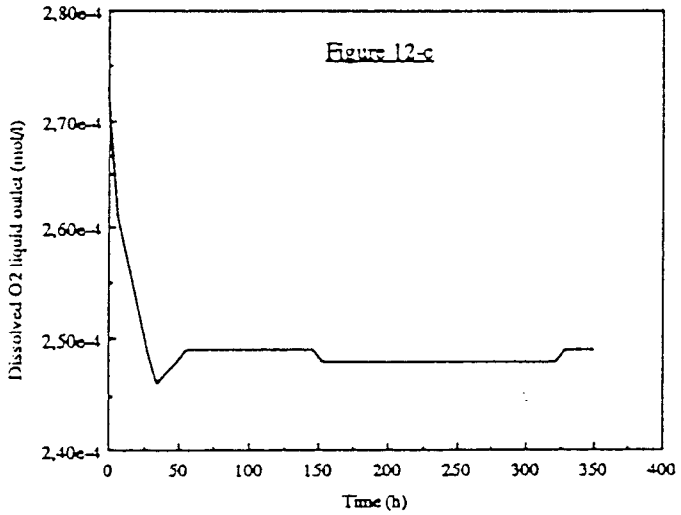

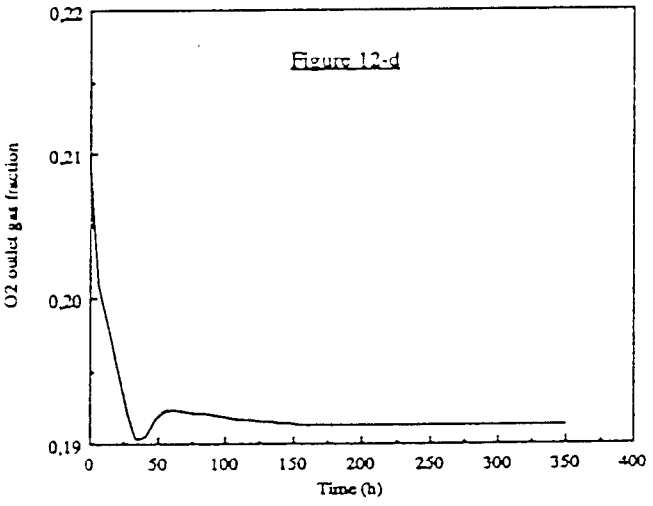

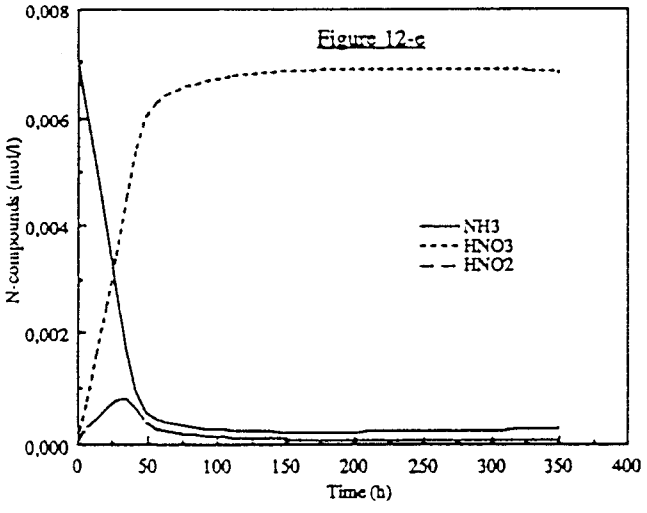

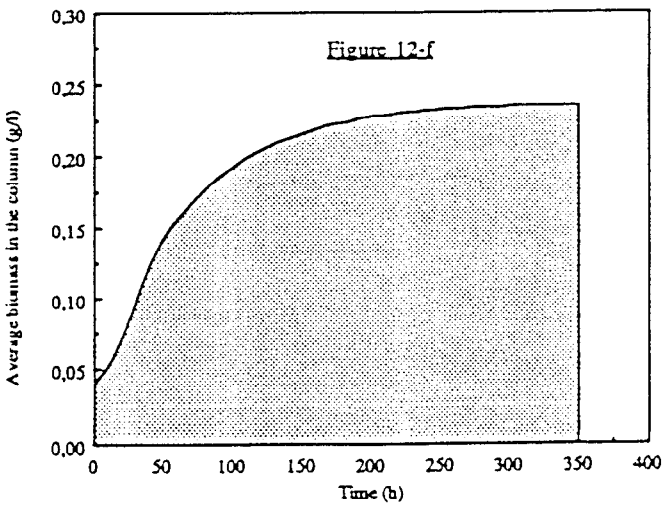

Figures 13 a-f: Results of a simulation for a standard configuration modified with a gas recycling ratio of 199 (process of 350 h.) The curves (a-e) represent the composition in the gas or in the liquid outlet flows.

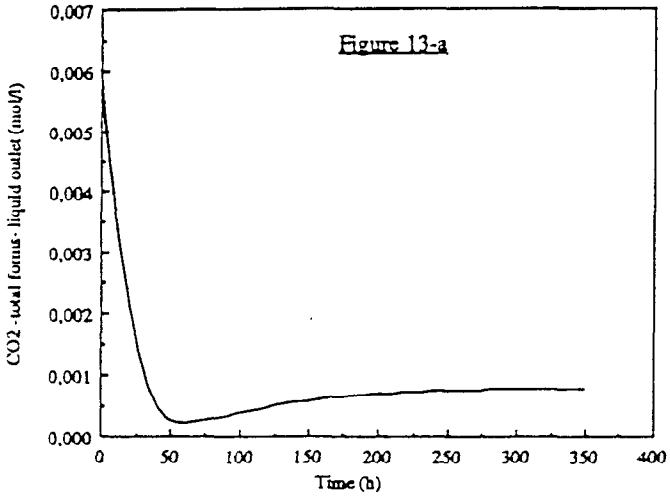

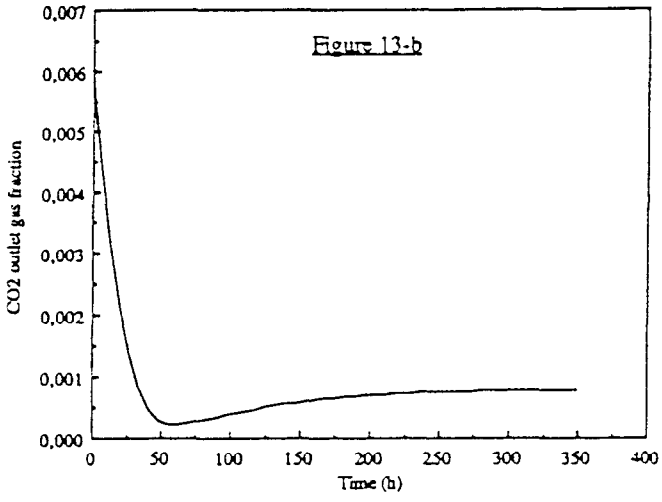

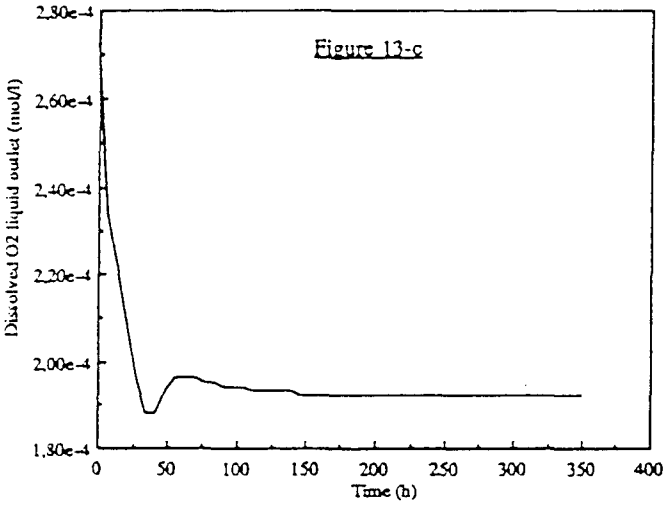

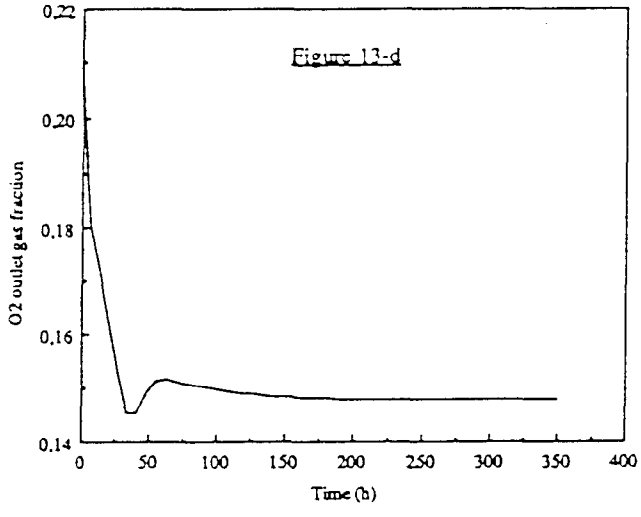

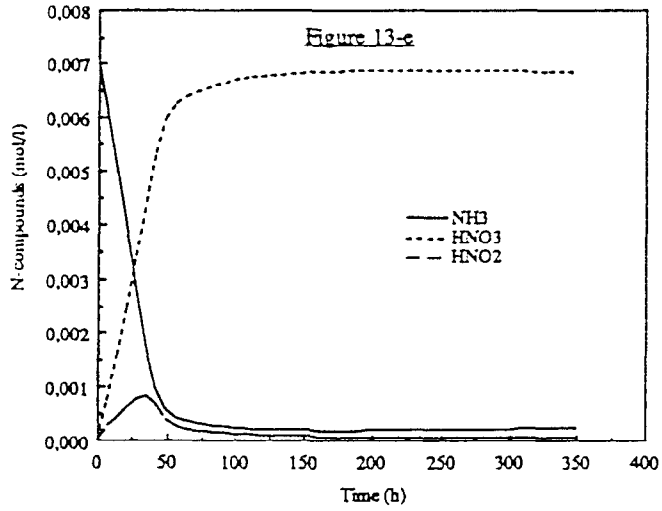

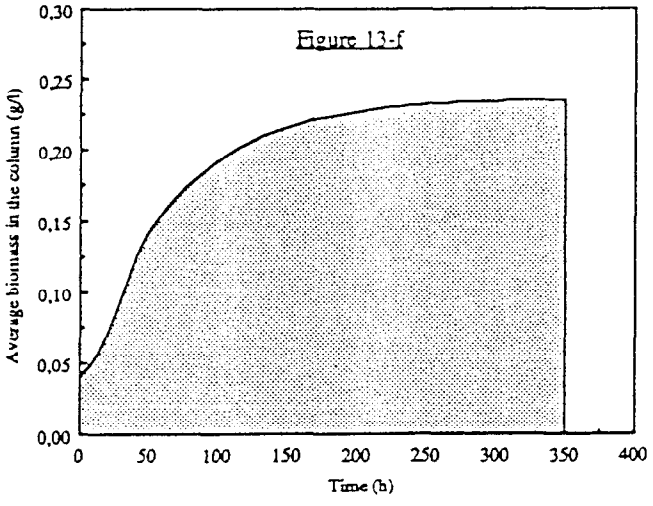

Figures 14 a-f: Results of a simulation for a standard configuration modified with back-mixing fraction of 75% both for gas and liquid (process of 350 h.) The curves (a-e) represent the composition in the gas or in the liquid outlet flows.

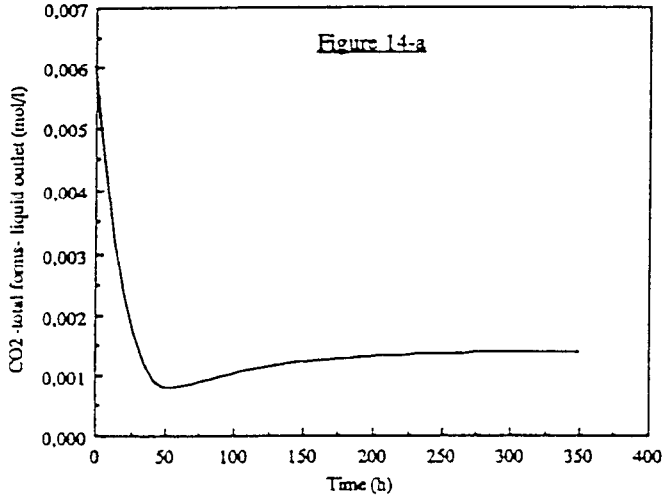

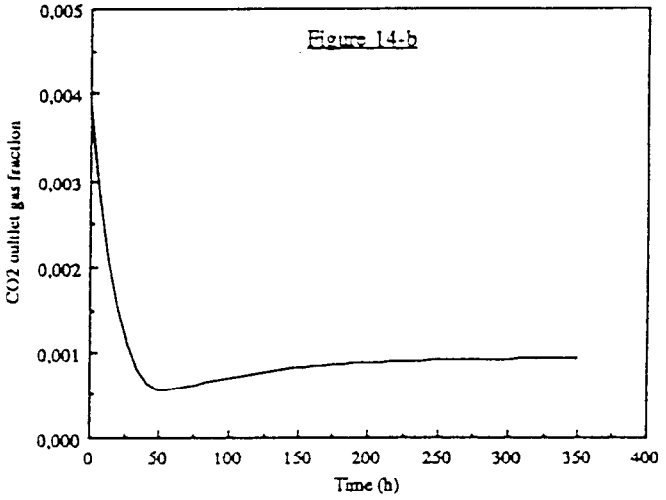

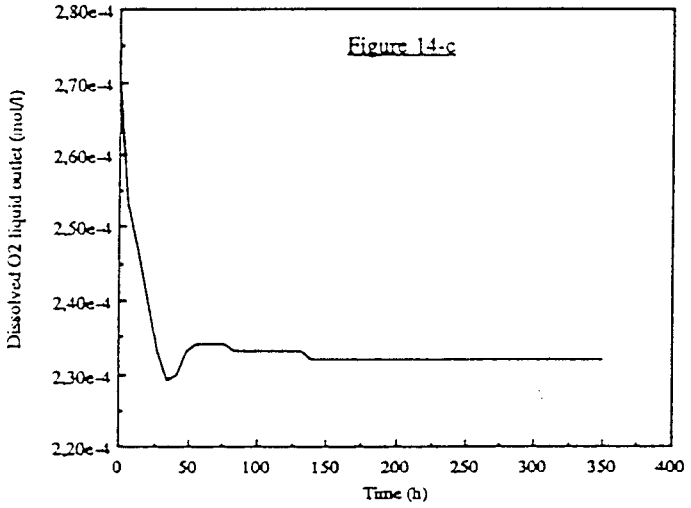

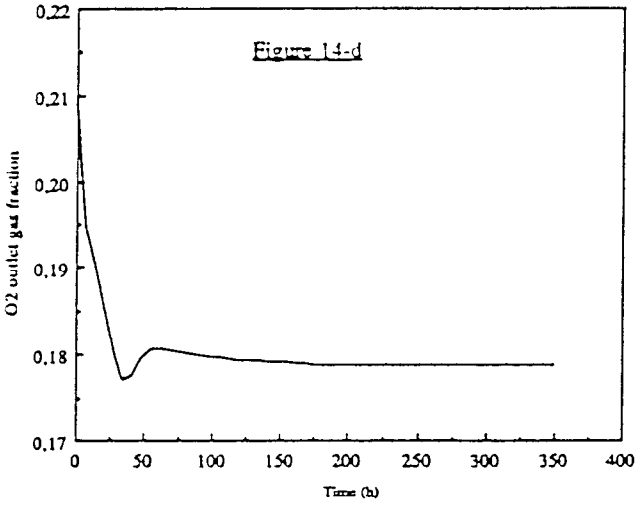

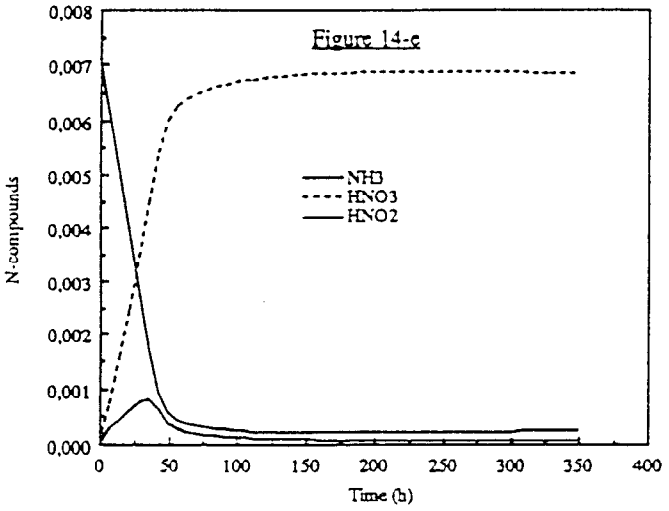

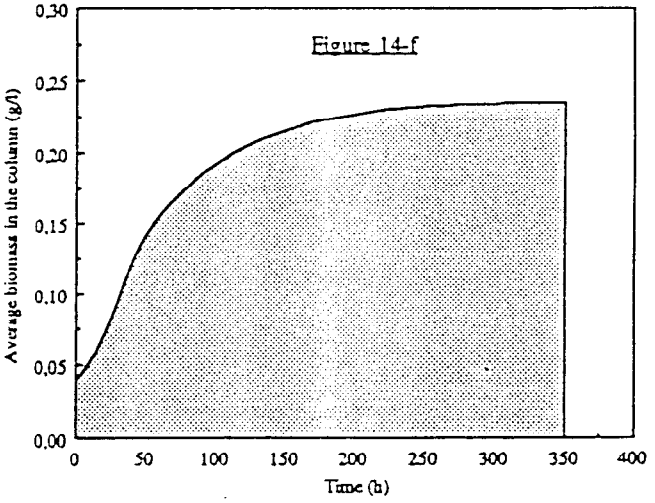

Conclusion

The RTD simulations show the importance of the hydrodynamics parameters f (liquid back-mixing fraction), f' (gas back-mixing fraction) and N (number of equivalent stirred tanks for the fixed bed). From the experimental RTD measurement leaded at UAB laboratory (TN 25.330), it seems that f have a high value (greater than 75%), what increase the perfectly mixed behaviour of the column. The simulations for different f and f' configuration show that f and f' have no influence on long dynamics, but are important for short dynamics (less than 8 hours). The influence of recycling and of the liquid back-mixing increase the difficulties to estimate the number of tanks equivalent (N) for the fixed bed.

The standard configuration is a reasonnable compromise for comparing the different simulations together. Three main results can be retained from the different simulations:

- the steady state behaviour, in outlet flow and inside the bed, is reached by the liquid and the gas phase more quickly than by the fixed biomass. The delay needed to reach the steady state depend on the flow rates inside the column and is shorter for high flow rates than for low flow rates;
- the biomass (*i.e.* the nitrification) is concentrated in the bottom of the bed. The distribution inside the bed depends on the flow rate, and is affected by the choice of the number of stirred tanks for the fixed bed. The steady state of the biomass distribution seem difficult to reach, even with a process of 1 month;
- in the standard configuration, as in the other simulations performed, the oxygen and the biofilm limitations are never reached, in any part of the column.

For the next technical note, shorter dynamics will be studied by simulating transient behaviours (changes in charge and in flow rates) during a long process. If possible, the hydrodynamic parameters f and N will be identified from experimental values.

References

Cox D. J., Bazin M. J. and Gull K. (1980)"Distribution of bacteria in a continuous-flow nitrification column" Soil Biol. Biochem. Vol.12. pp 241-246.

Hunik J. H., Bos C. G., den Hoogen M. P., De Gooijer C. D. and Tramper J. (1994)"Co-Immobilized *Nitrosomonas europea* and *Nitrobacter agilis* cells: validation of a dynamic model for simulataneous substrate conversion and growth in K-carrageenan gel beads". Biotech. Bioeng. Vol. 43. pp 1153-1163.

Forler C. (1994) "Development of a fixed bed pilot reactor for a continuous axenic coculture of *Nitrosomonas europea* and *Nitrobacter winogradsky*" YGT ESA/YCL. X-997.

Appendices

Concentrations profiles inside the column

Appendix A: standard configuration, process of 750 h

Appendix B: standard configuration, process of 350 h

Appendix C: 1-tank configuration, process of 350 h

Appendix D: 10-tanks configuration, process of 350 h

Appendix E: 2 mg initial biomass, process of 350 h

Appendix F: 200 mg initial biomass, process of 350 h

Appendix G: liquid recycling: 0 ml/min, process of 350 h

Appendix H: liquid recycling: 45 ml/min, process of 350 h

Appendix I: gas flow recycling ratio: 199, process of 350 h

Appendix J: gas flow rate in the column: 5 l/min, process of 350 h

Appendix K: back-mixing (f and f' parameters): 75%, process of 350 h

NH3 - [Standard configuration]

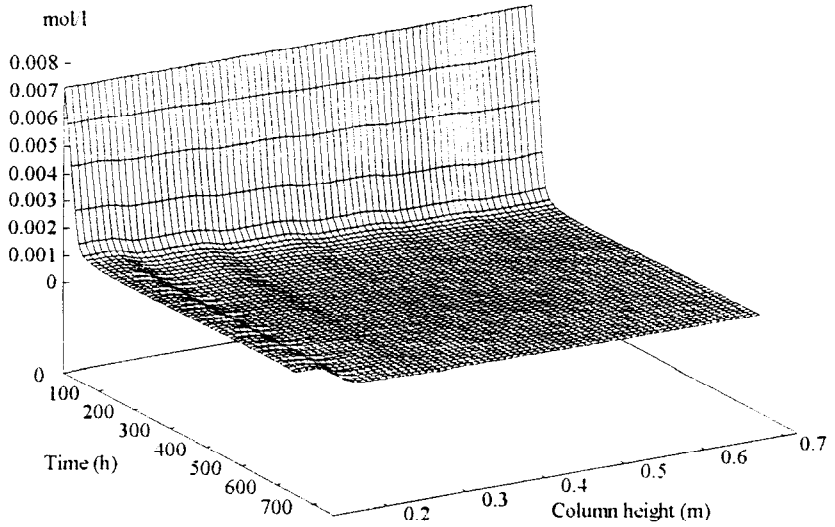

HNO3 - [Standard configuration]

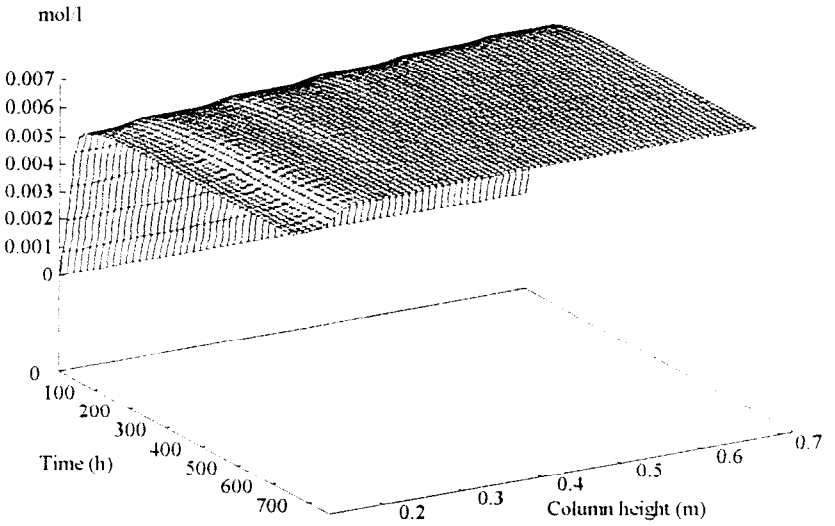

HNO2 - [Standard configuration]

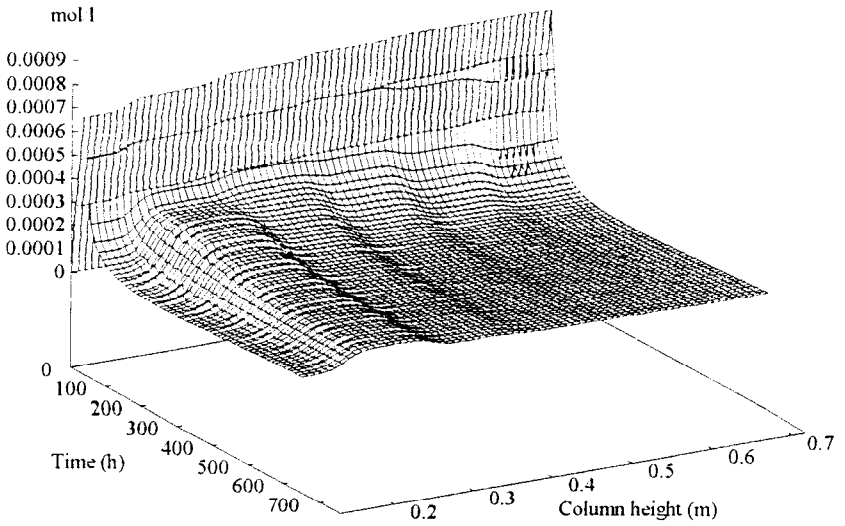

CO2 liquid - [Standard configuration]

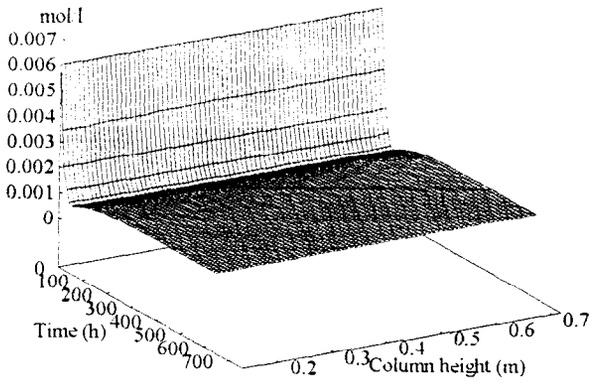

CO2 gas - [Standard configuration]

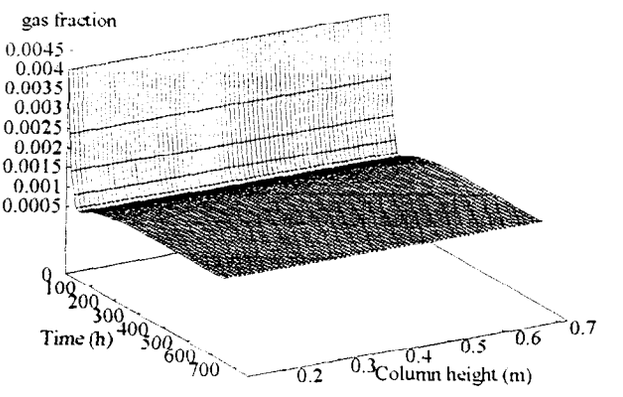

O2 liquid - [Standard configuration]

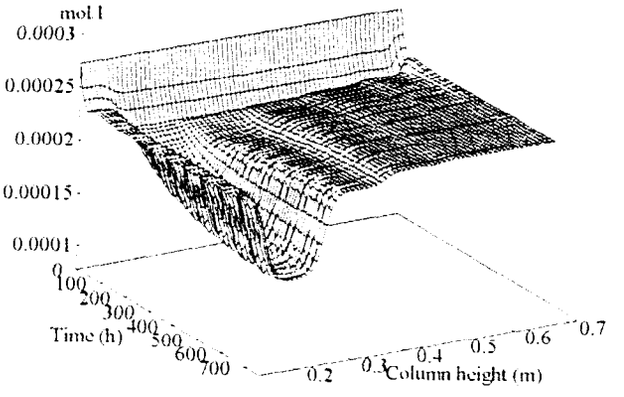

O2 gas - [Standard configuration]

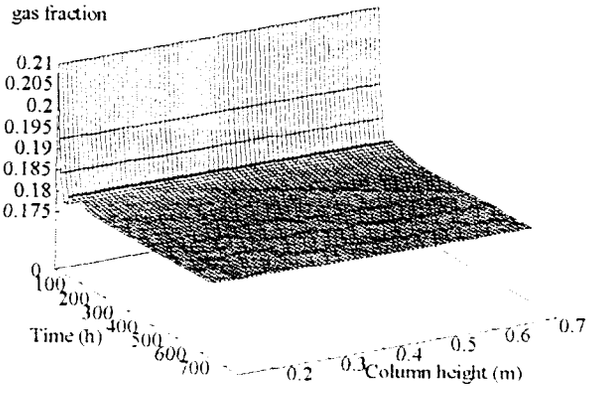

Nitrosomonas - [Standard configuration]

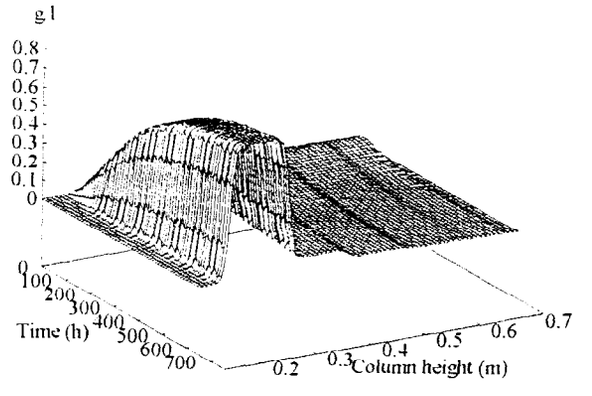

Nitrobacter - [Standard configuration]

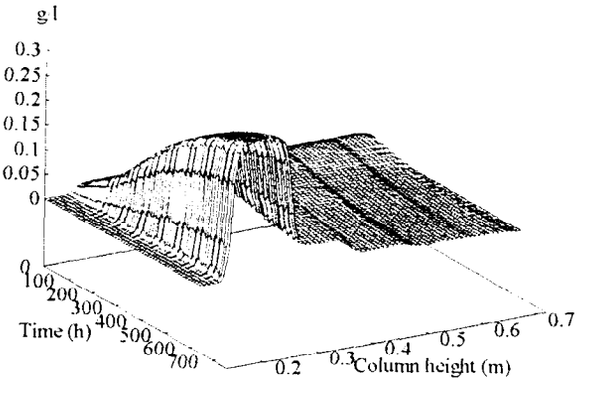

NH3 - [Standard configuration]

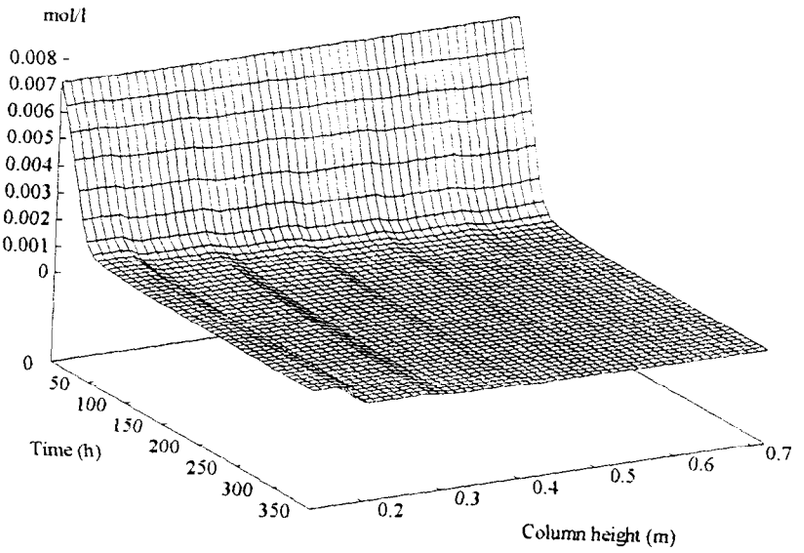

HNO3 - [Standard configuration]

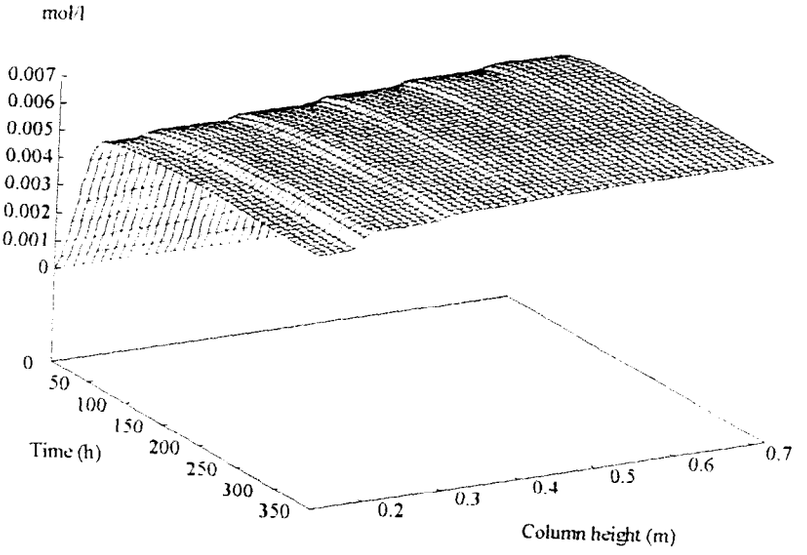

HNO2 - [Standard configuration]

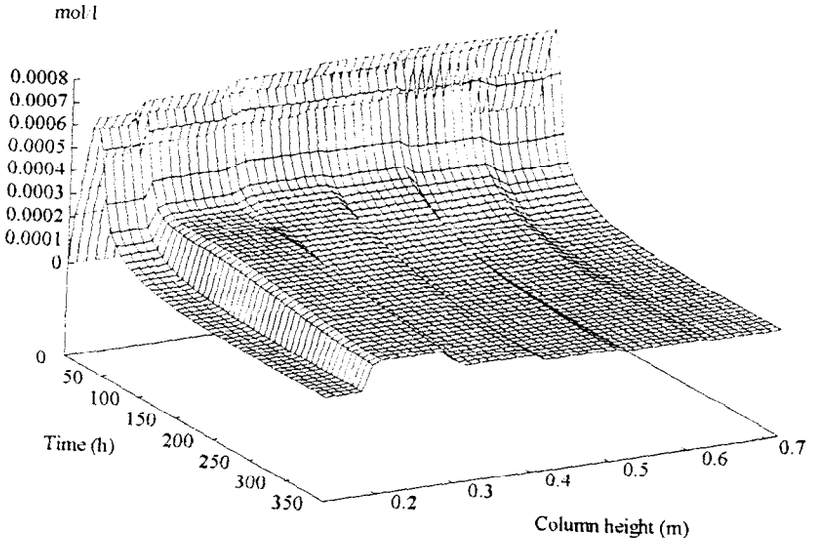

CO2 liquid - [Standard configuration]

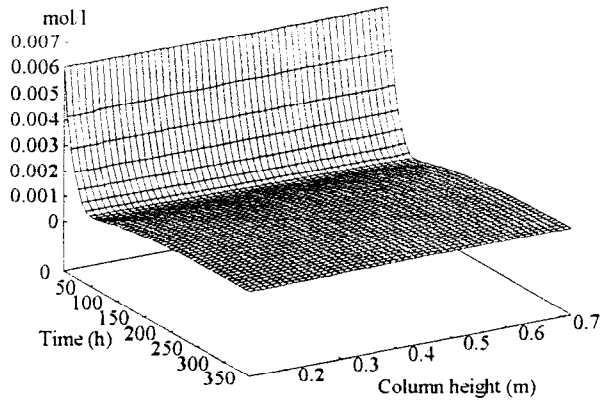

CO2 gas - [Standard configuration]

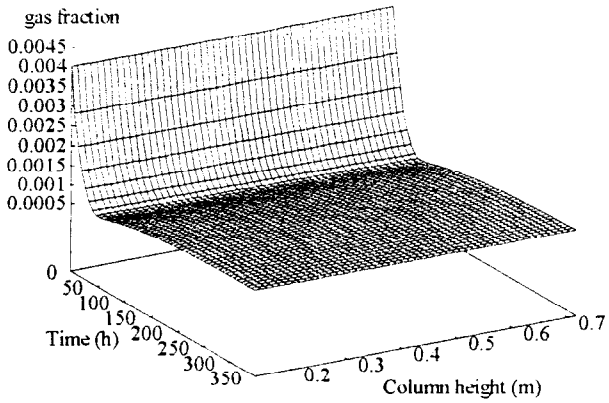

O2 liquid - [Standard configuration]

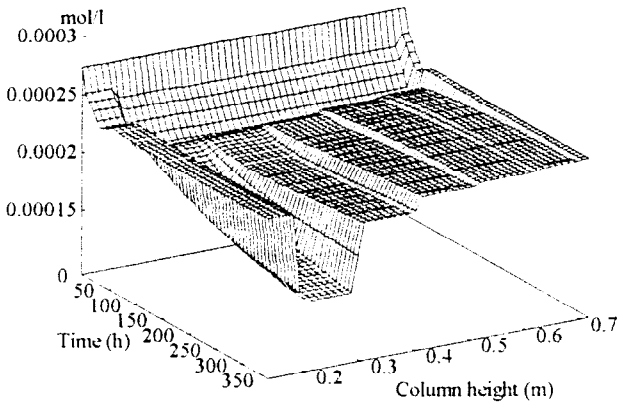

O2 gas - [Standard configuration]

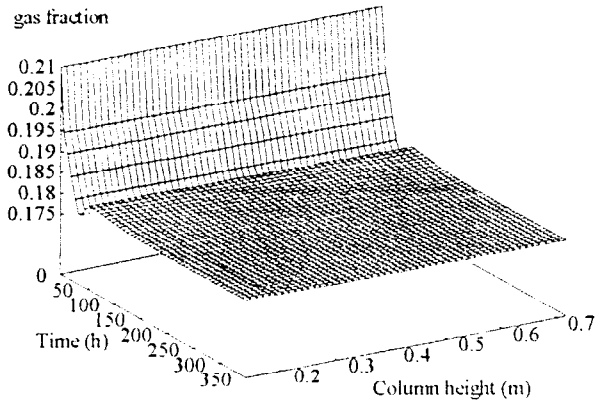

Nitrosomonas - [Standard configuration]

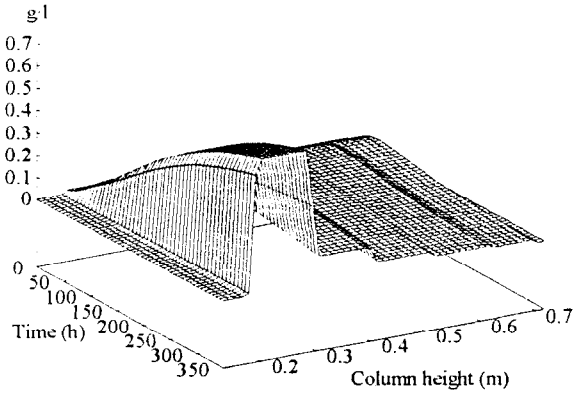

Nitrobacter - [Standard configuration]

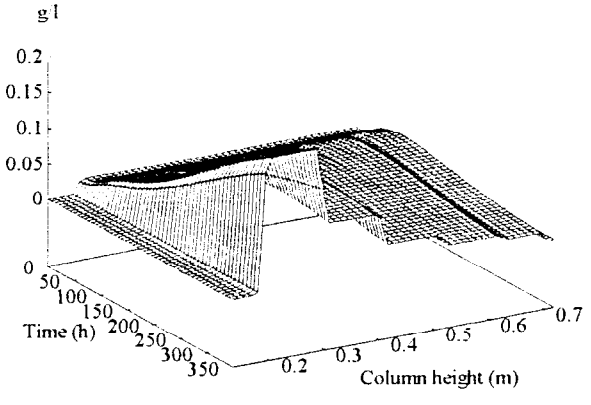

NH3 - [1-tank configuration]

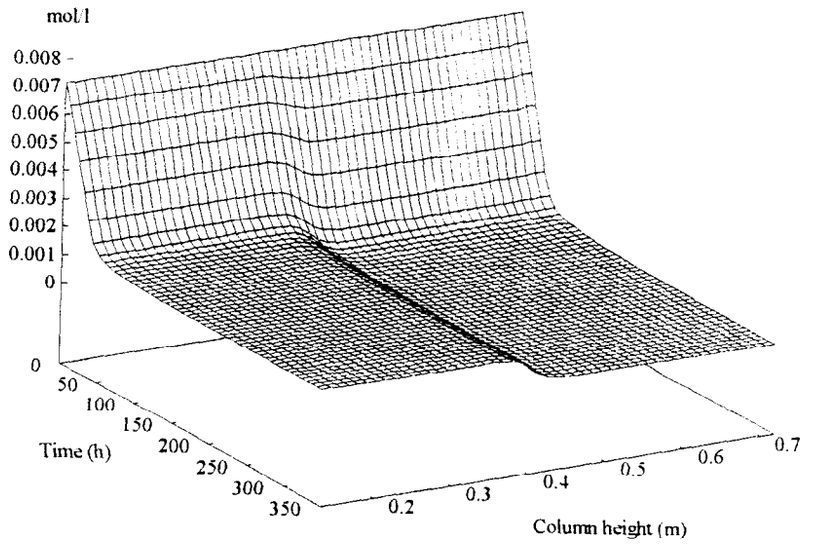

HNO3 - [1-tank configuration]

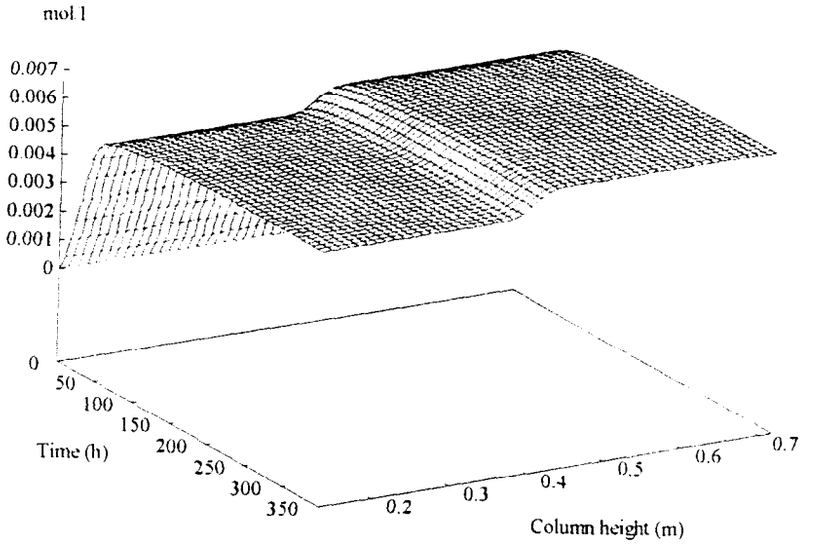

HNO2 - [1-tank configuration]

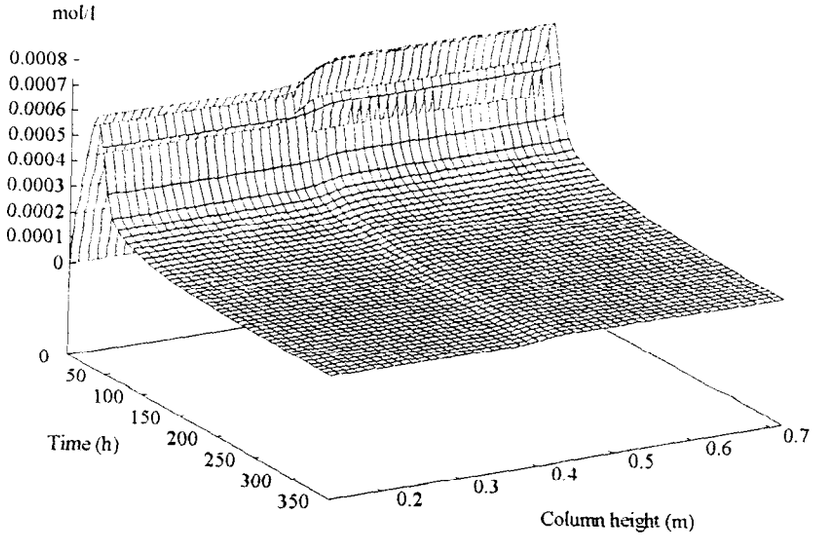

Appendix C: 1-tank configuration, process of 350 h [section 2.3]

CO2 liquid - [1-tank configuration]

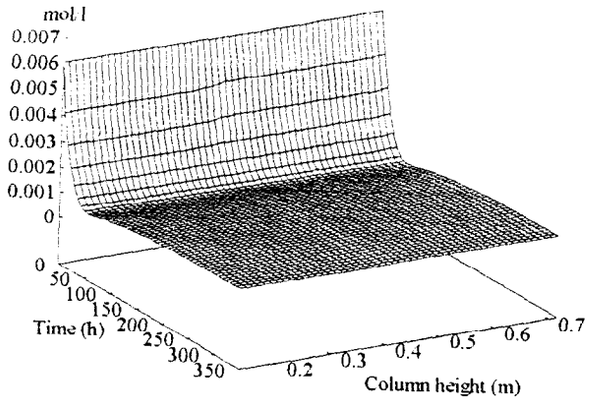

CO2 gas - [1-tank configuration]

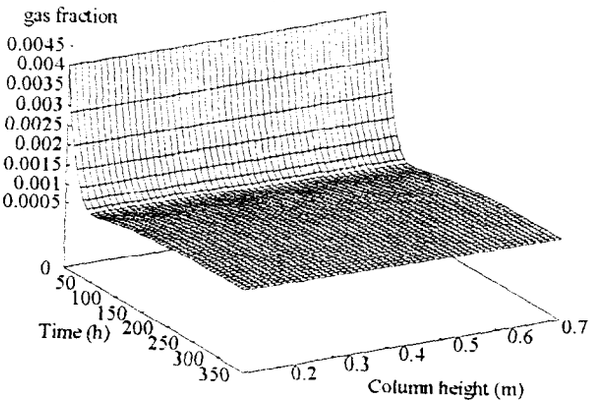

O2 liquid - [1-tank configuration]

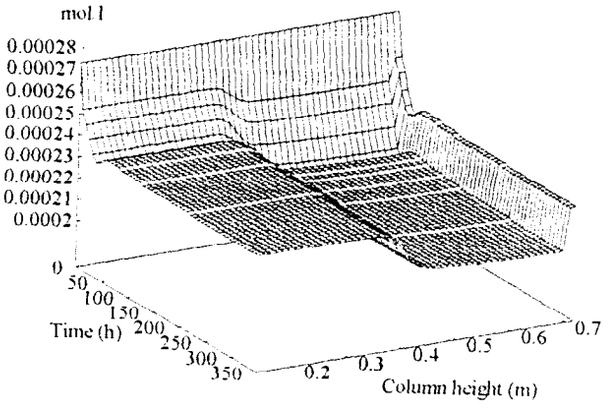

O2 gas - [1-tank configuration]

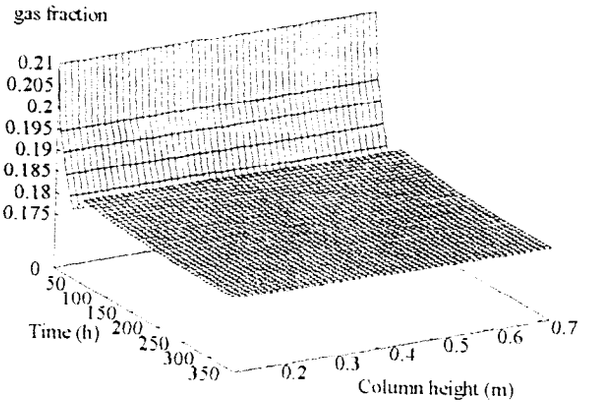

Nitrosomonas - [1-tank configuration]

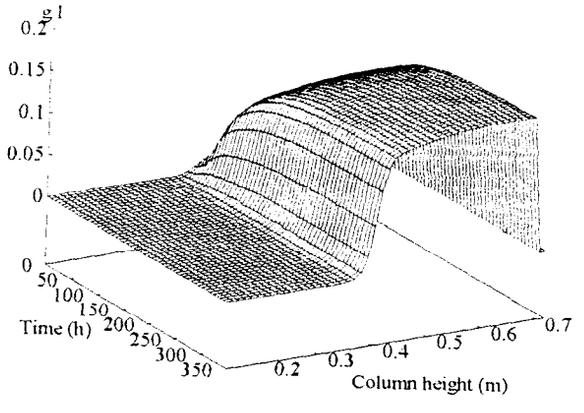

Nitrobacter - [1-tank configuration]

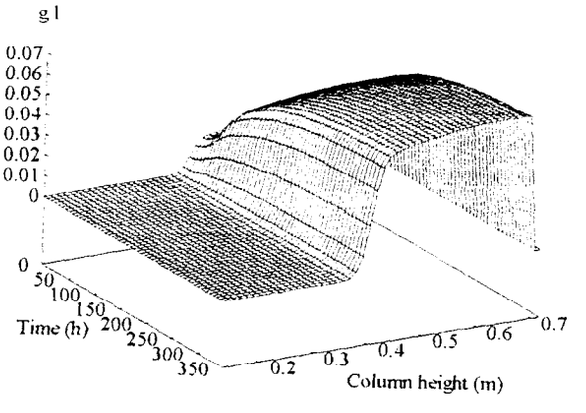

NH3 - [10-tank configuration]

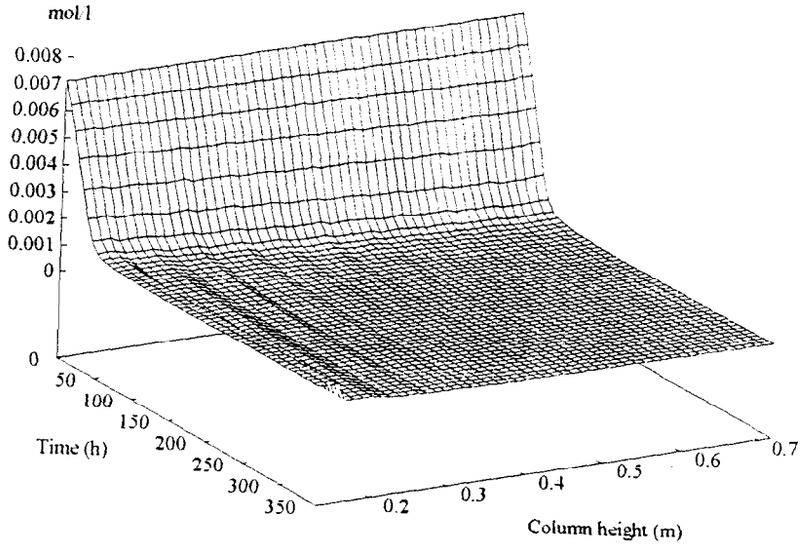

HNO3 - [10-tank configuration]

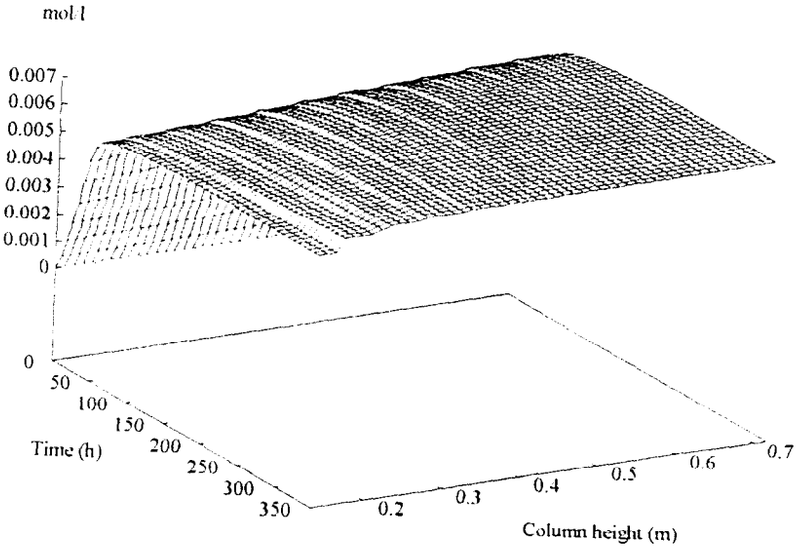

HNO2 - [10-tank configuration]

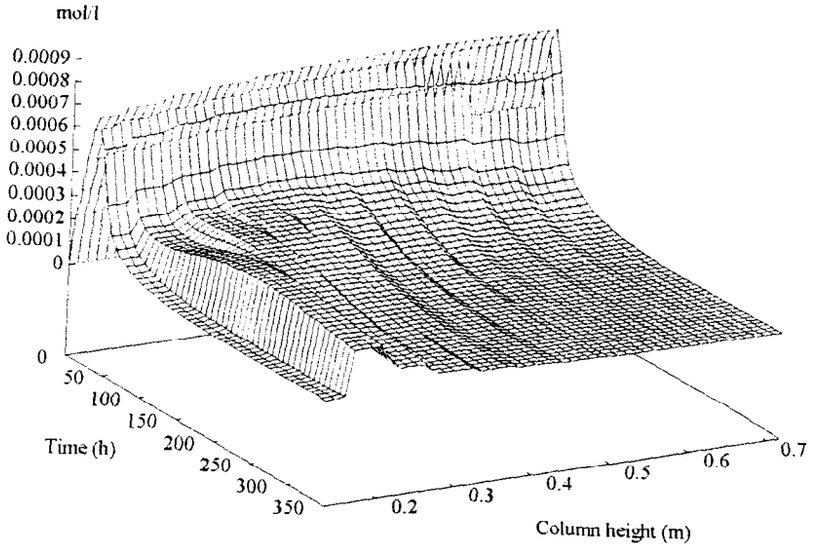

Appendix D: 10-tanks configuration, process of 350 h [section 2.3]

CO2 liquid - [10-tank configuration]

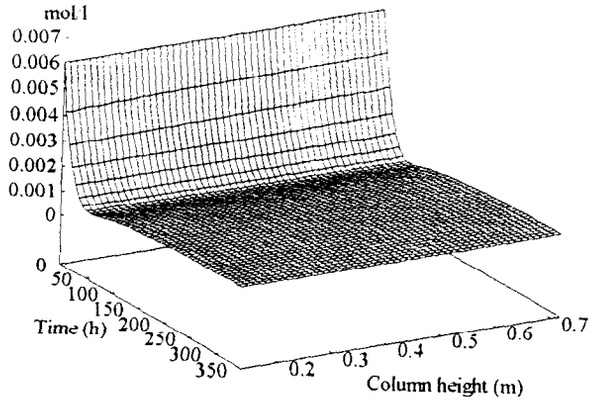

CO2 gas - [10-tank configuration]

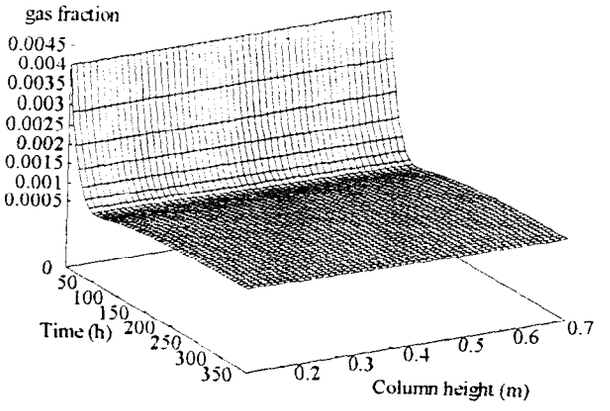

O2 liquid - [10-tank configuration]

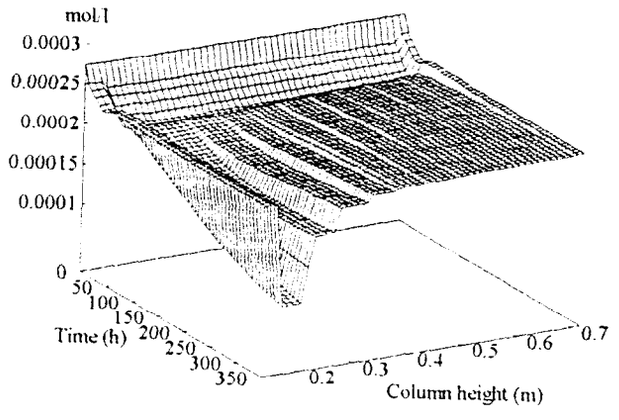

O2 gas - [10-tank configuration]

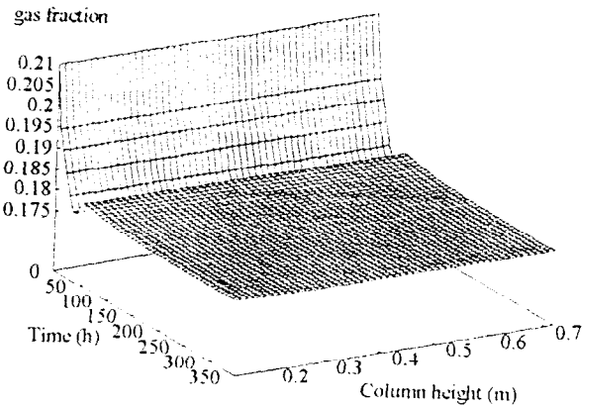

Nitrosomonas - [10-tank configuration]

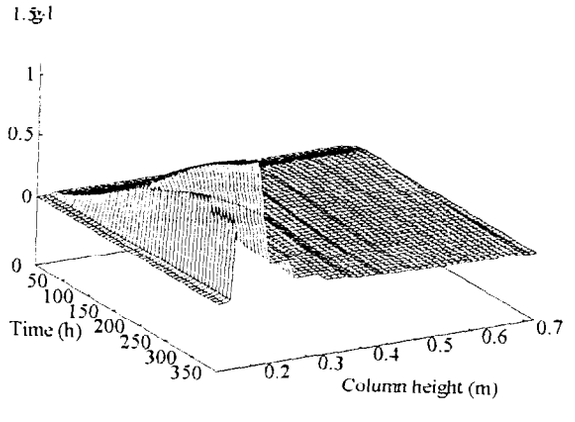

Nitrobacter - [10-tank configuration]

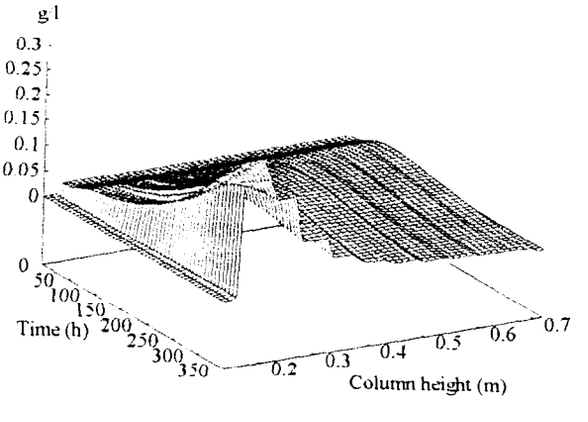

Appendix E: 2 mg initial biomass, process of 350 h [section 2.4]

NH3 - [2mg initial biomass]

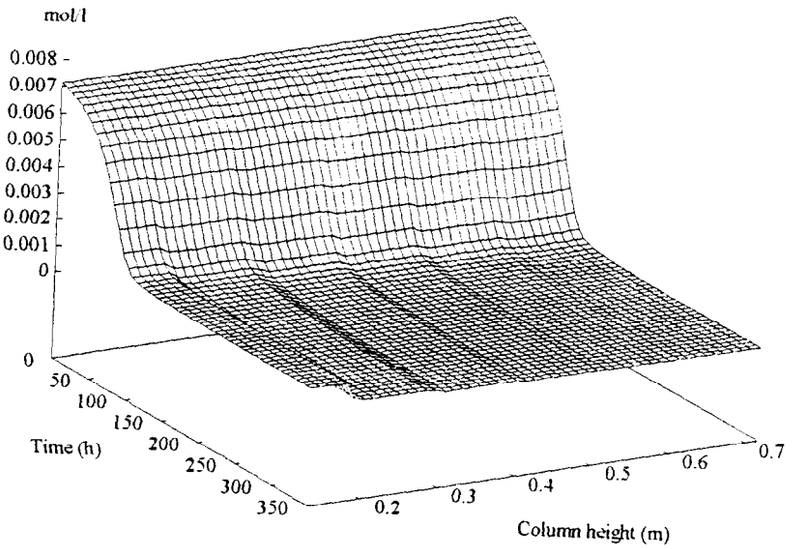

HNO3 - [2mg initial biomass]

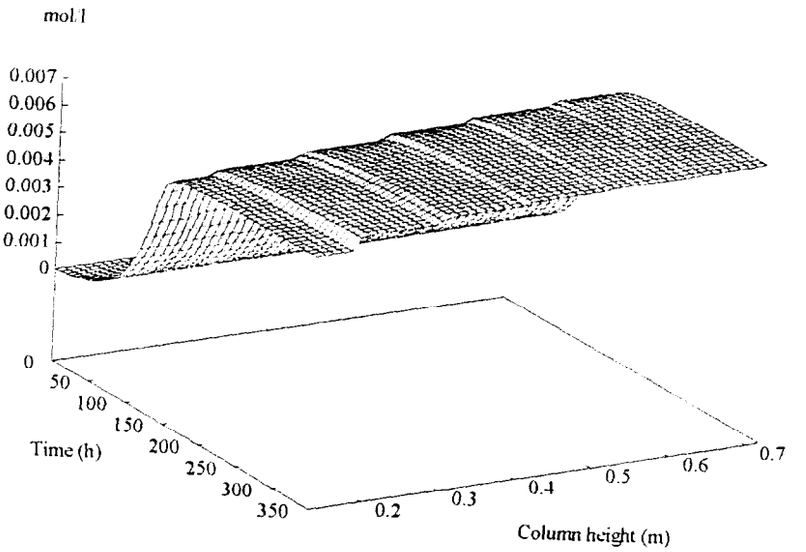

HNO2 - [2mg initial biomass]

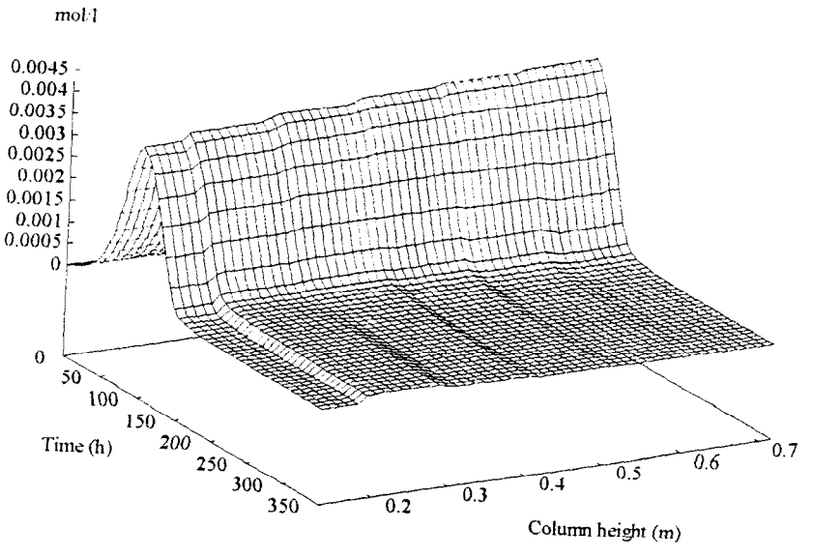

Appendix E: 2 mg initial biomass, process of 350 h [section 2.4]

CO2 liquid - [2mg initial biomass]

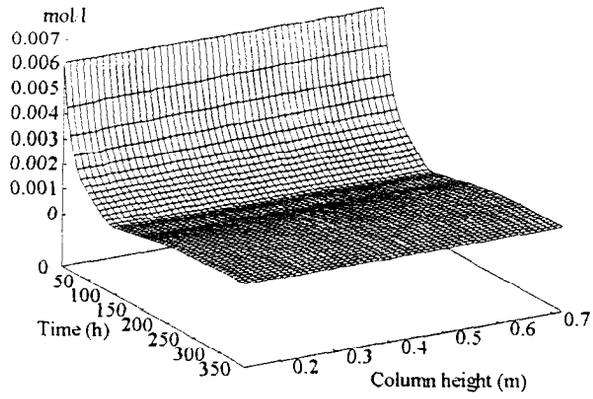

CO2 gas - [2mg initial biomass]

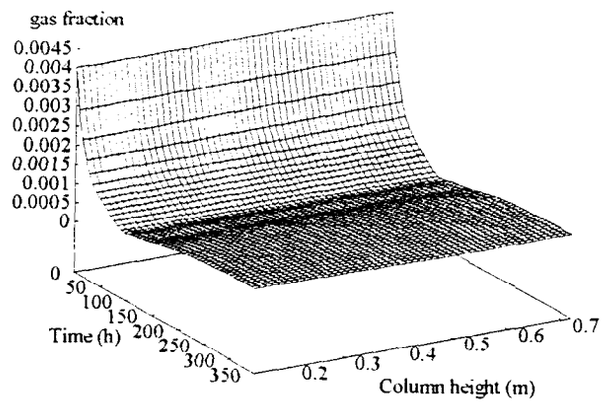

O2 liquid - [2mg initial biomass]

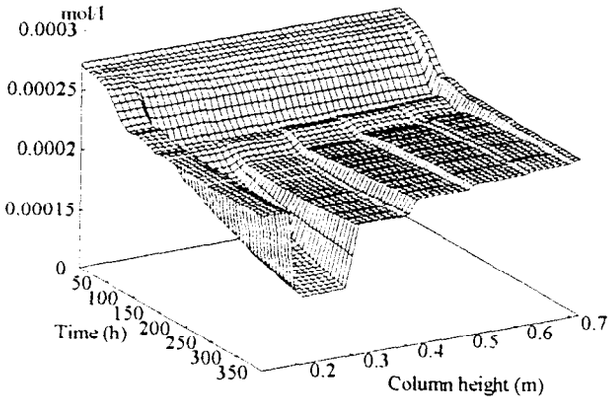

O2 gas - [2mg initial biomass]

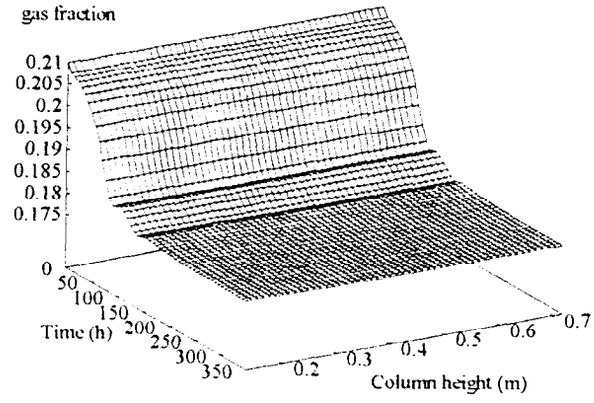

Nitrosomonas - [2mg initial biomass]

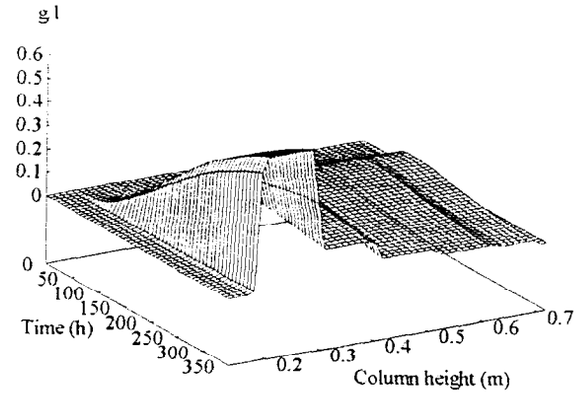

Nitrobacter - [2mg initial biomass]

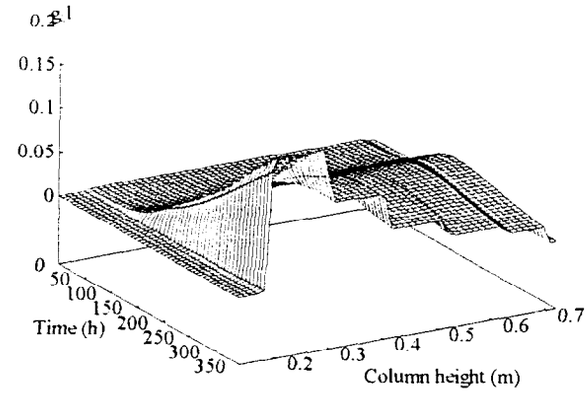

NH3 - [200mg initial biomass]

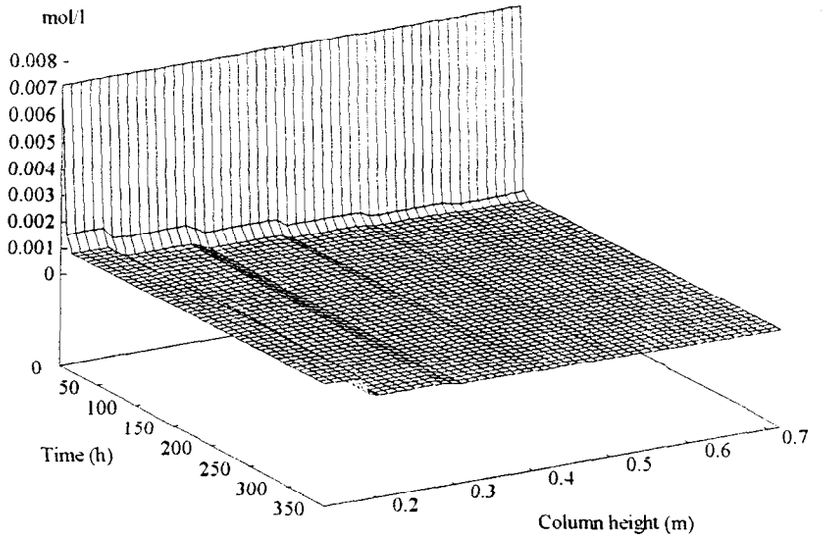

HNO3 - [200mg initial biomass]

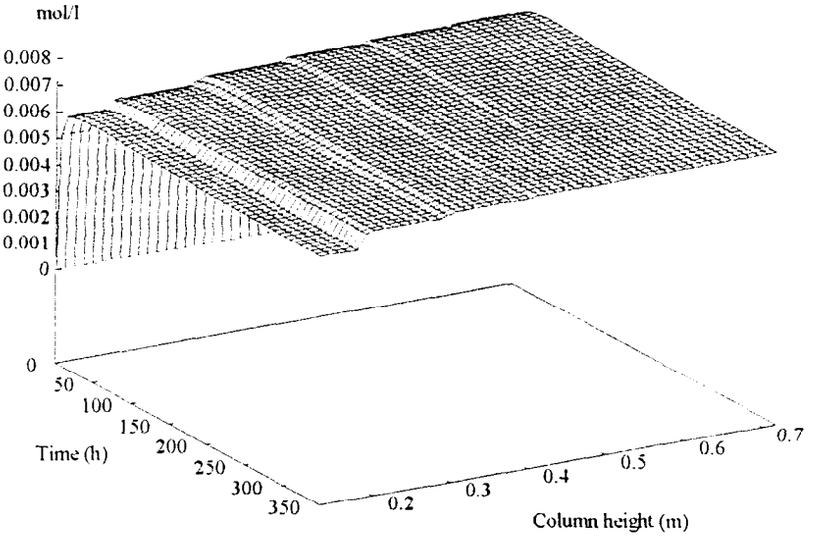

HNO2 - [200mg initial biomass]

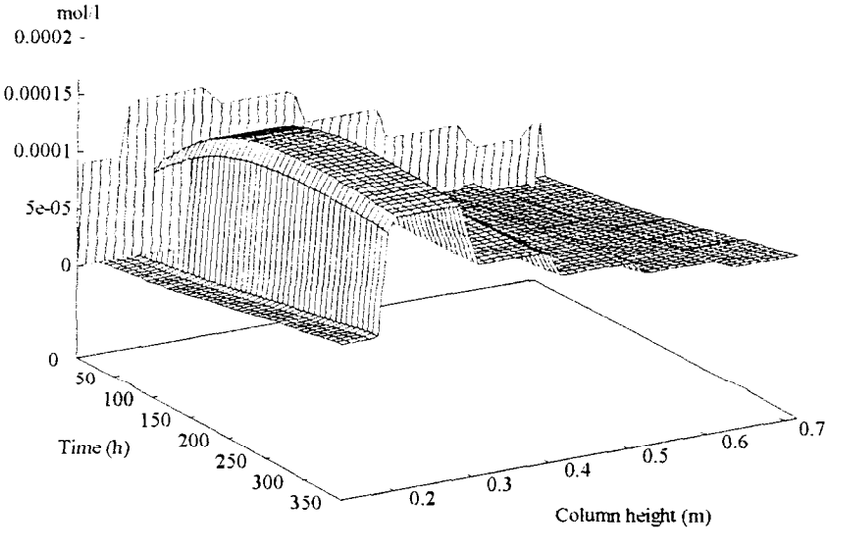

Appendix F: 200 mg initial biomass, process of 350 h [section 2.4]

CO2 liquid - [200mg initial biomass]

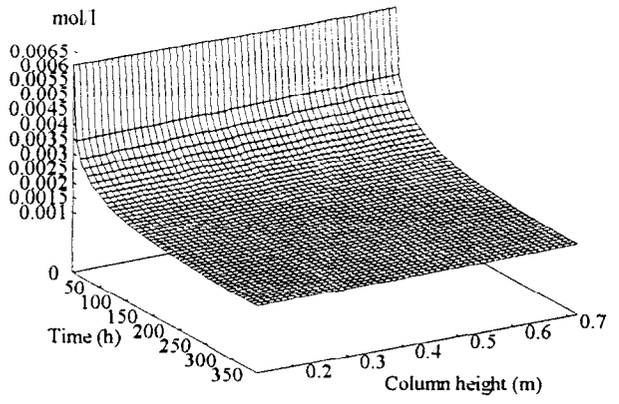

O2 gas - [200mg initial biomass]

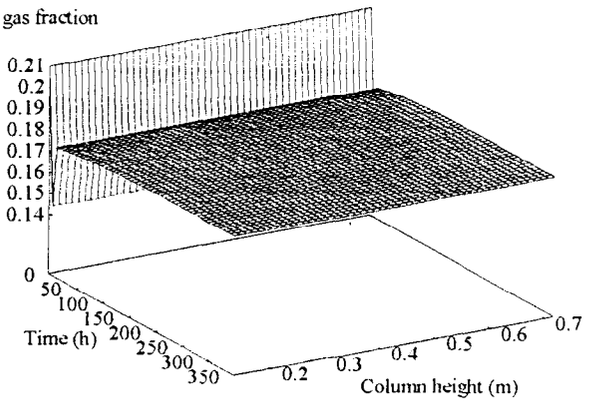

O2 liquid - [200mg initial biomass]

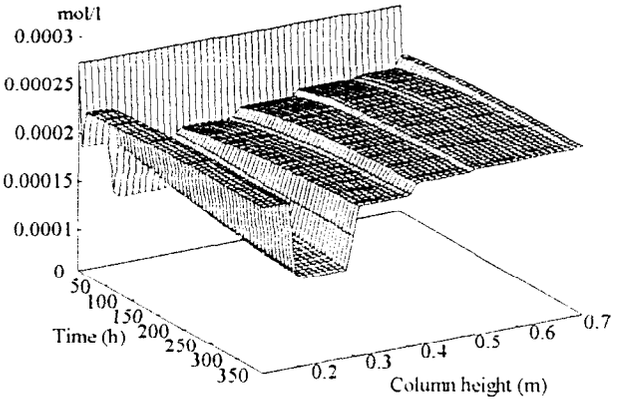

CO2 gas - [200mg initial biomass]

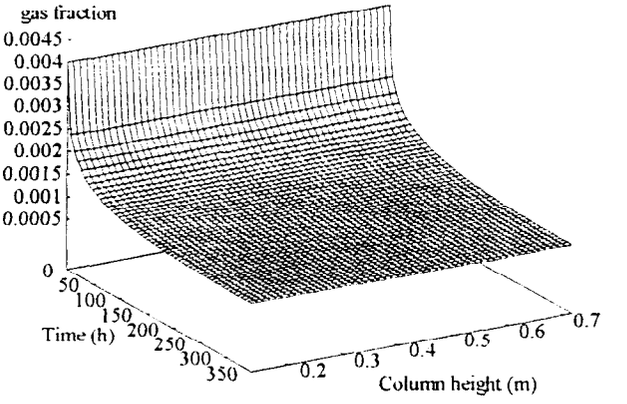

Nitrosomonas - [200mg initial biomass]

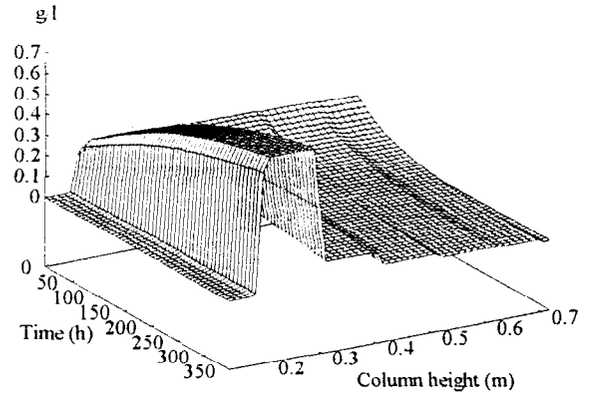

Nitrobacter - [200mg initial biomass]

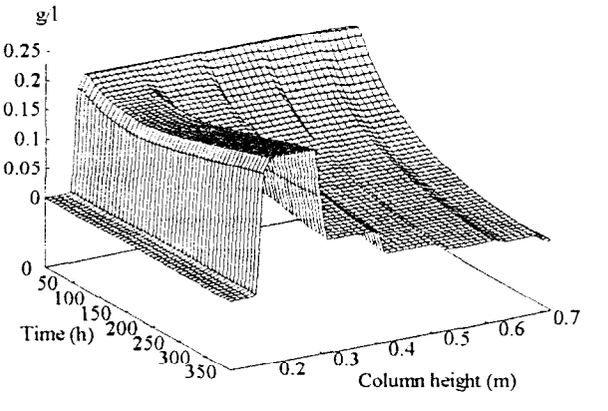

Appendix G: Liquid recycling of 0 ml/min, process of 350 h [section 2.5]

NH3 - [Liquid recycling: 0 ml/min]

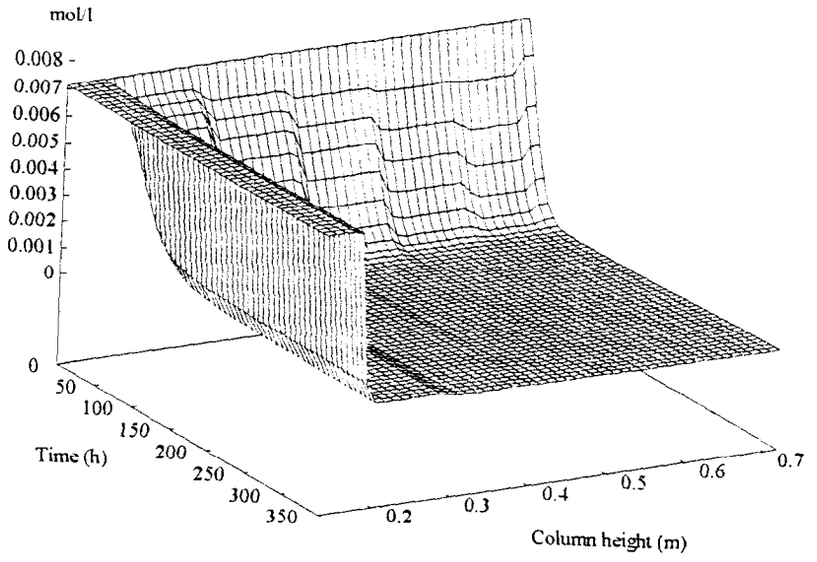

HNO3 - [Liquid recycling: 0 ml/min]

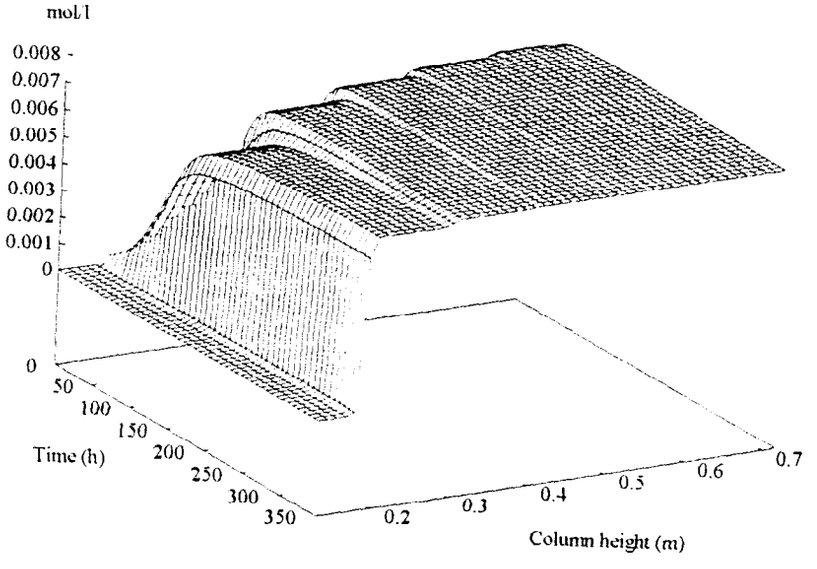

HNO2 - [Liquid recycling: 0 ml/min]

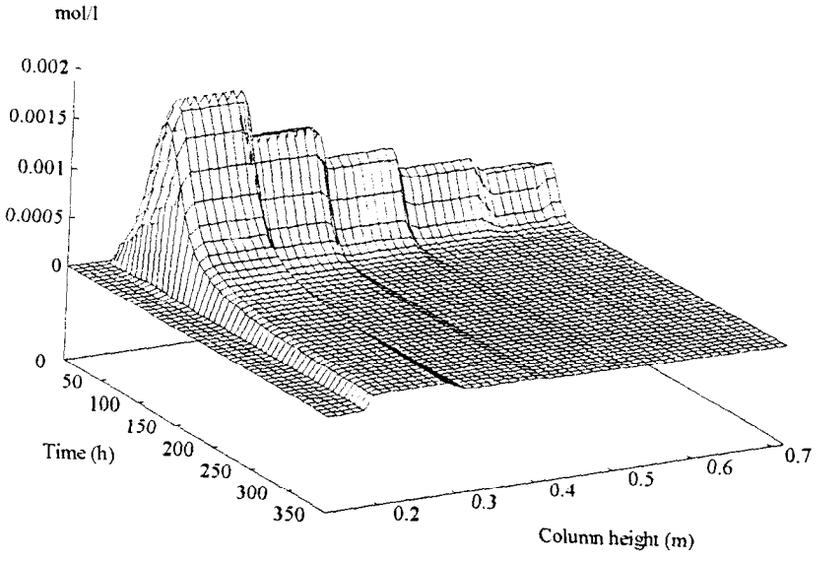

Appendix G: Liquid recycling of 0 ml/min, process of 350 h [section 2.5]

CO2 liquid - [Liquid recycling: 0 ml/min]

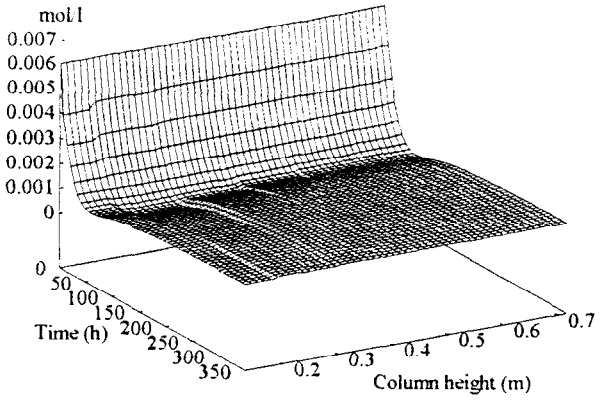

CO2 gas - [Liquid recycling: 0 ml/min]

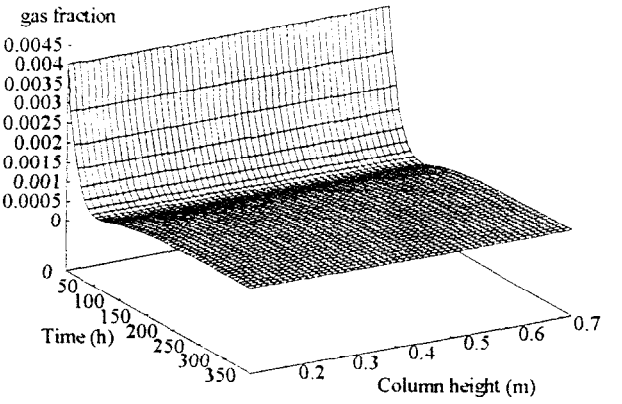

O2 liquid - [Liquid recycling: 0 ml/min]

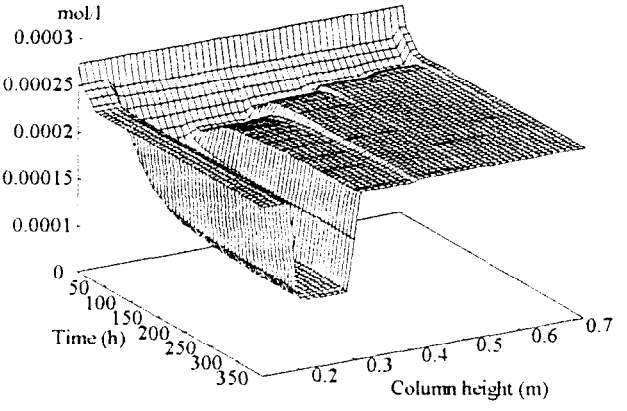

O2 gas - [Liquid recycling: 0 ml/min]

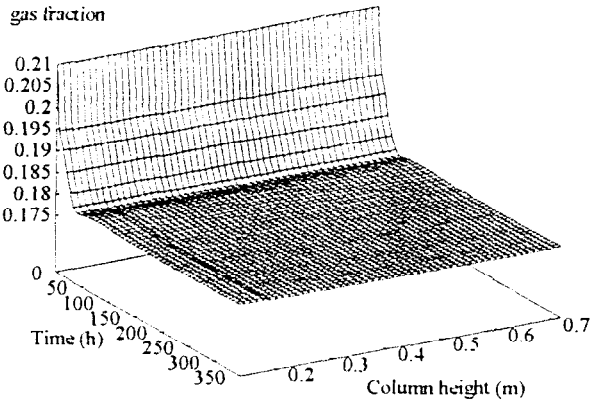

Nitrosomonas - [Liquid recycling: 0 ml/min]

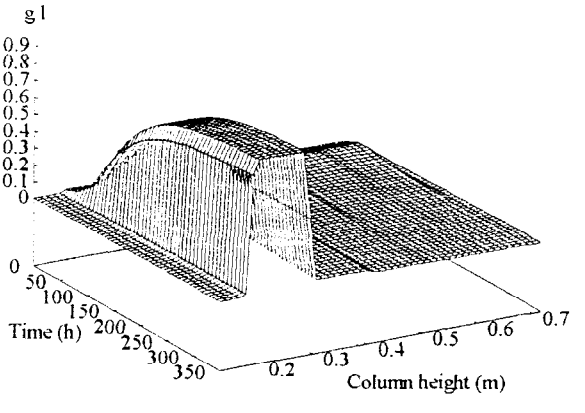

Nitrobacter - [Liquid recycling: 0 ml/min]

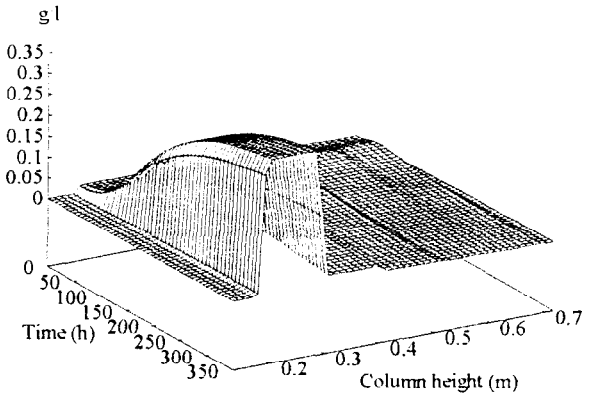

Appendix H: Liquid recycling of 45 ml/min, process of 350 h [section 2.5]

NH3 - [Liquid recycling: 45 ml/min]

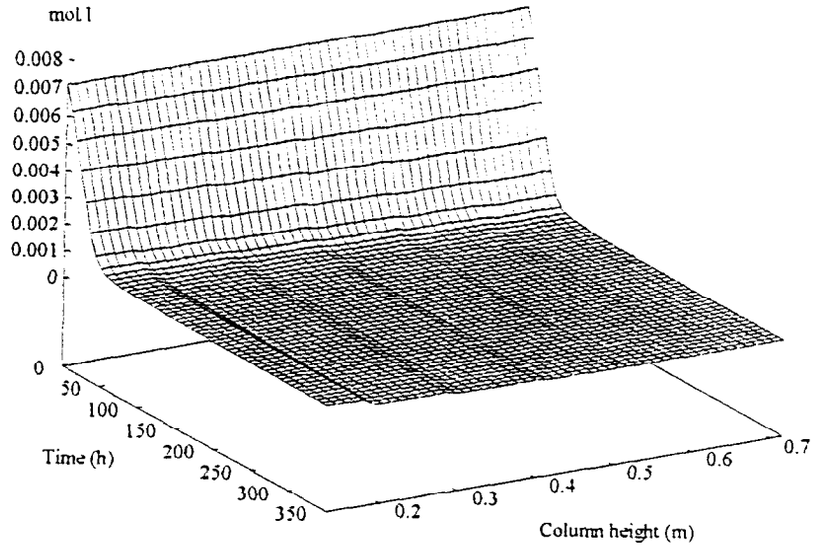

HNO3 - [Liquid recycling: 45 ml/min]

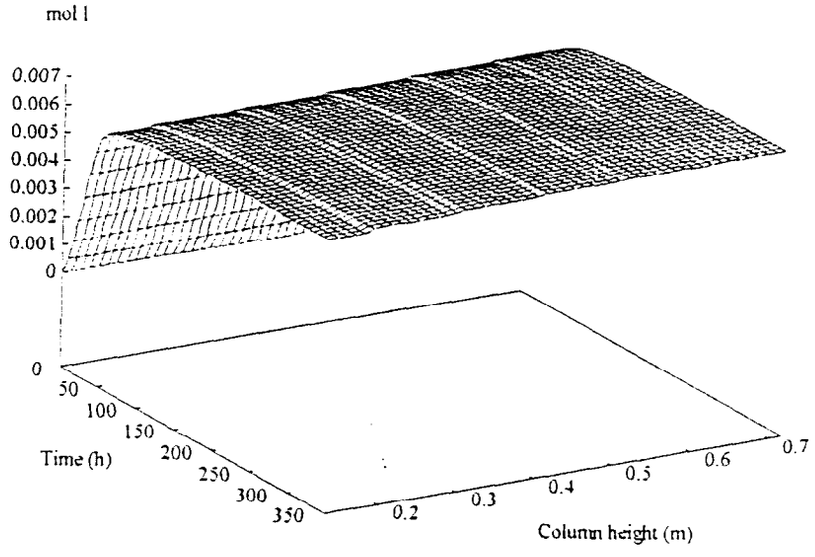

HNO2 - [Liquid recycling: 45 ml/min]

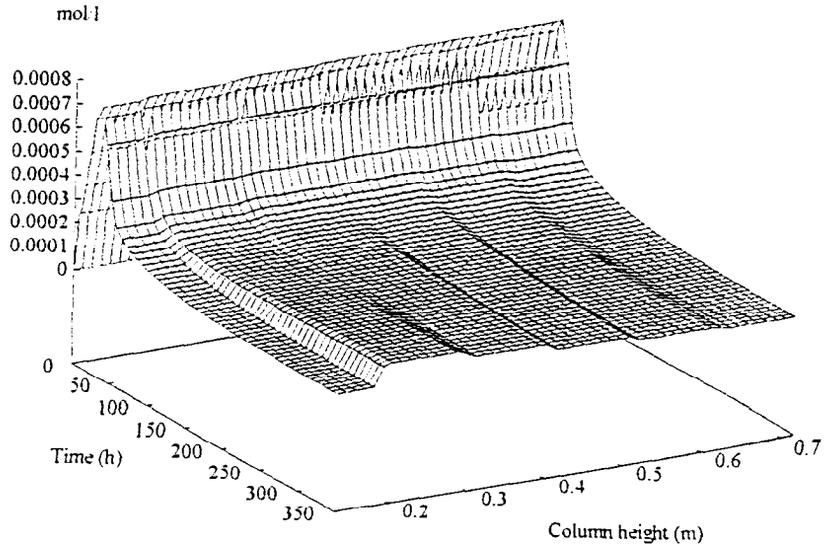

CO2 liquid - [Liquid recycling: 45 ml/min]

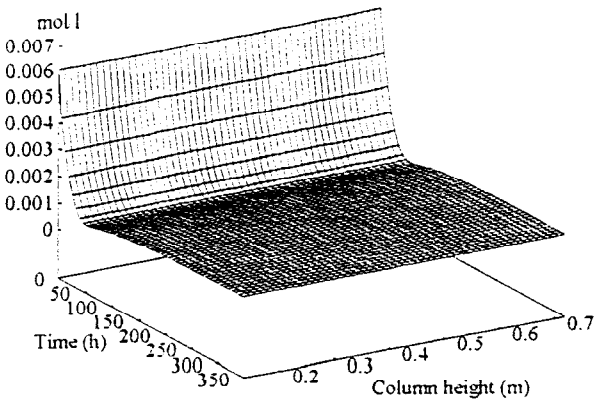

CO2 gas - [Liquid recycling: 45 ml/min]

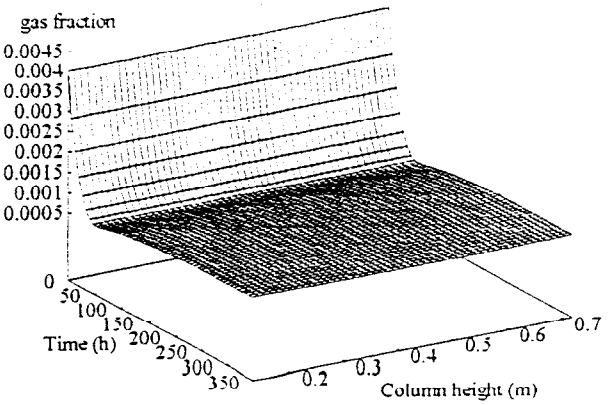

O2 liquid - [Liquid recycling: 45 ml/min]

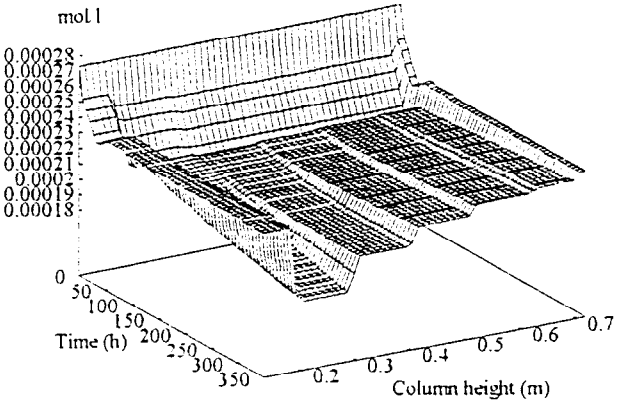

O2 gas - [Liquid recycling: 45 ml/min]

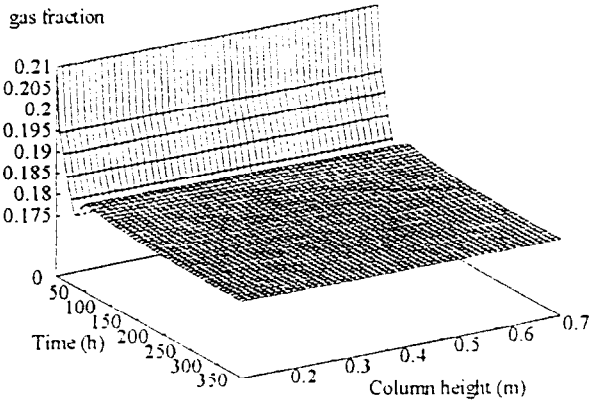

Nitrosomonas - [Liquid recycling: 45 ml/min]

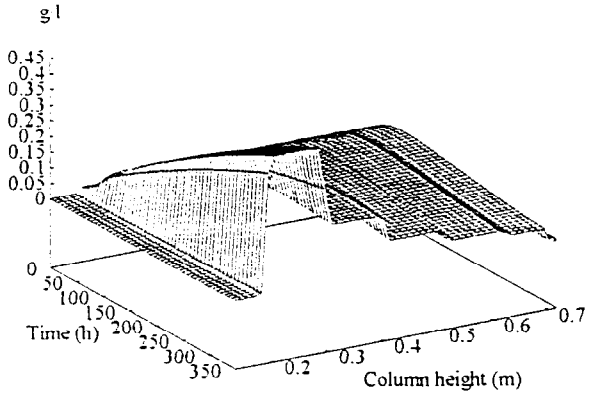

Nitrobacter - [Liquid recycling: 45 ml/min]

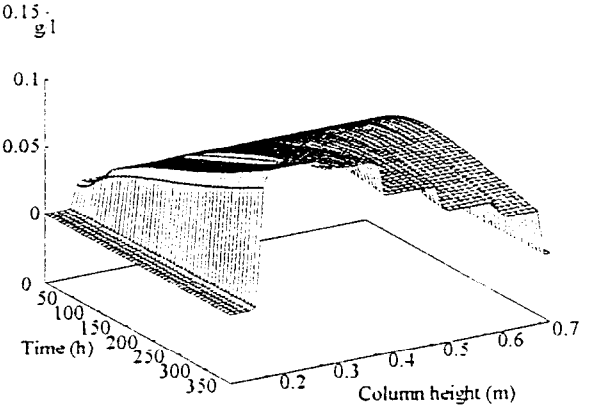

NH3 - [Gas flow recycling ratio: 199]

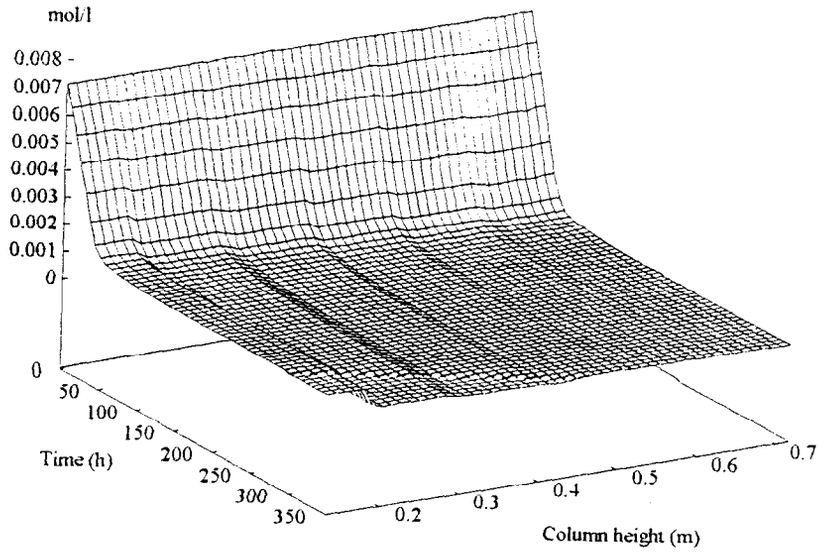

HNO3 - [Gas flow recycling ratio: 199]

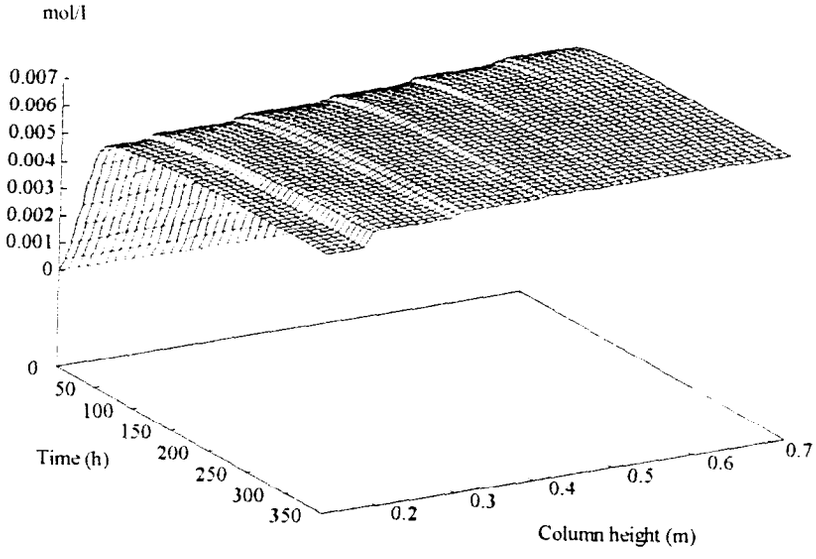

HNO2 - [Gas flow recycling ratio: 199]

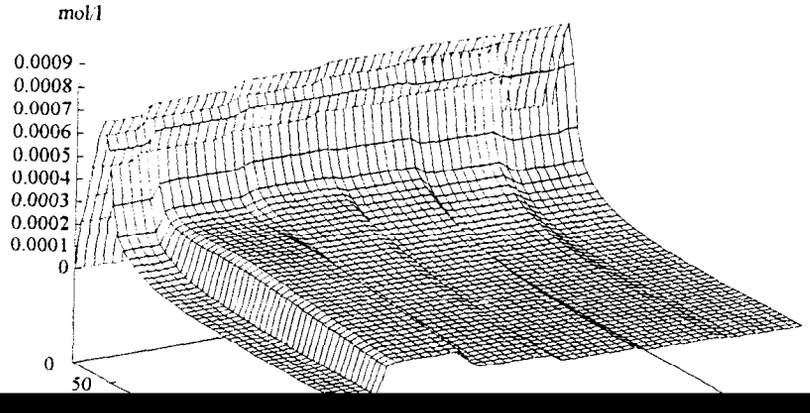

Appendix I: Gas flow recycling ratio of 199, process of 350 h [section 2.6]

CO2 liquid - [Gas flow recycling ratio: 199]

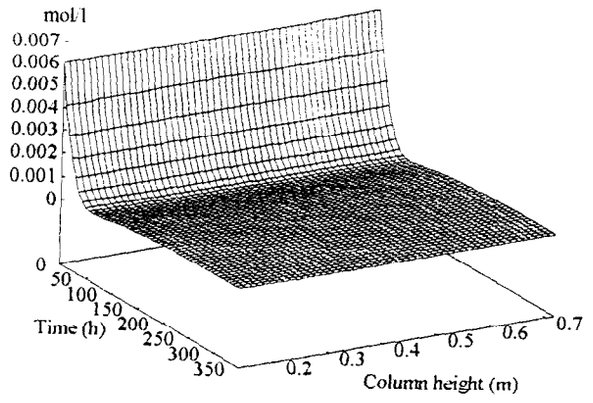

CO2 gas - [Gas flow recycling ratio: 199]

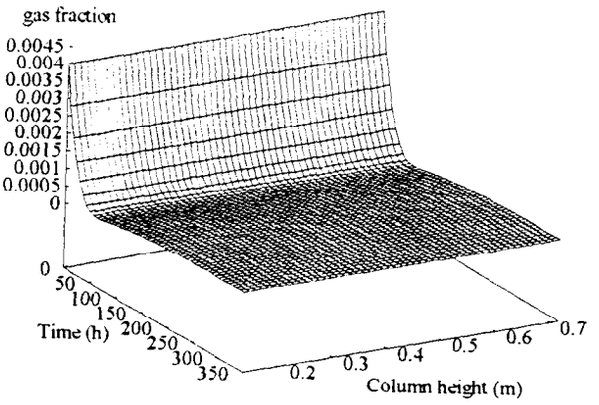

O2 liquid - [Gas flow recycling ratio: 199]

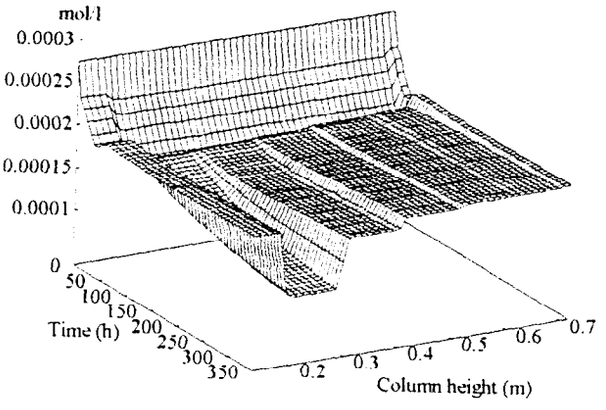

O2 gas - [Gas flow recycling ratio: 199]

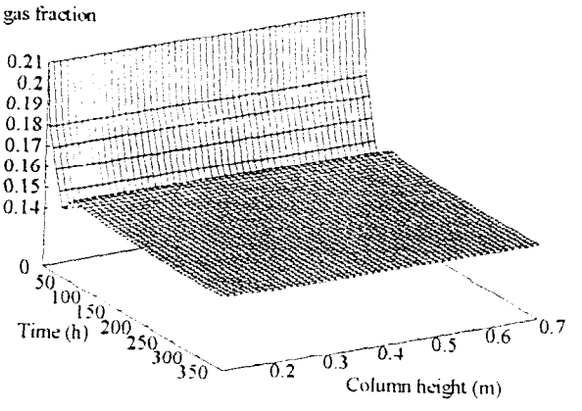

Nitrosomonas - [Gas flow recycling ratio: 199]

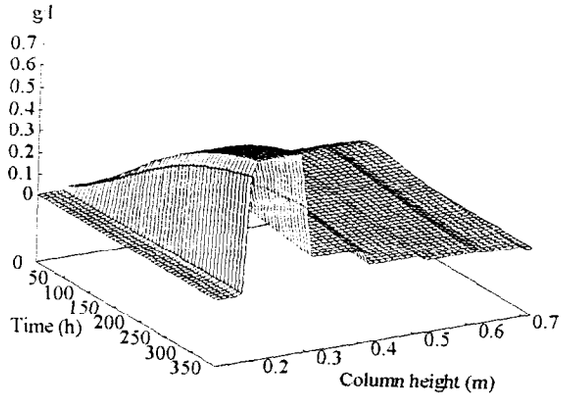

Nitrobacter - [Gas flow recycling ratio: 199]

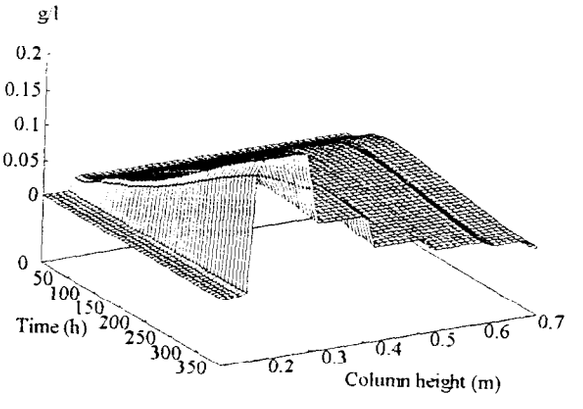

Appendix J: Gas flow rate in the column of 5 l/min, process of 350 h [section 2.6]

NH3 - [Gas flow rate in the column: 5 l/min]

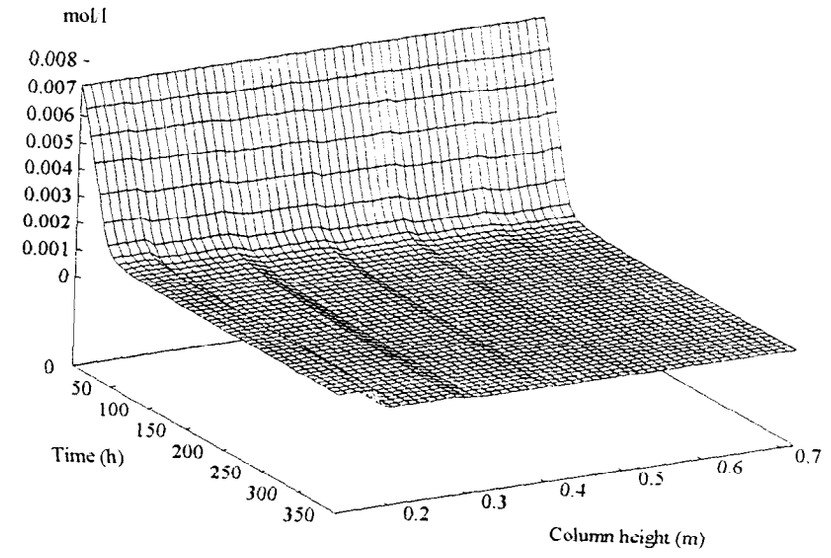

HNO3 - [Gas flow rate in the column: 5 l/min]

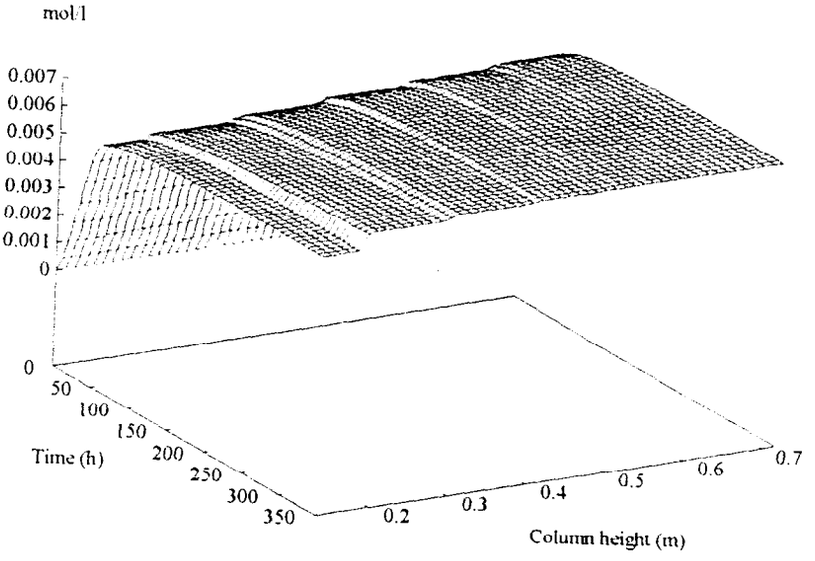

HNO2 - [Gas flow rate in the column: 5 l/min]

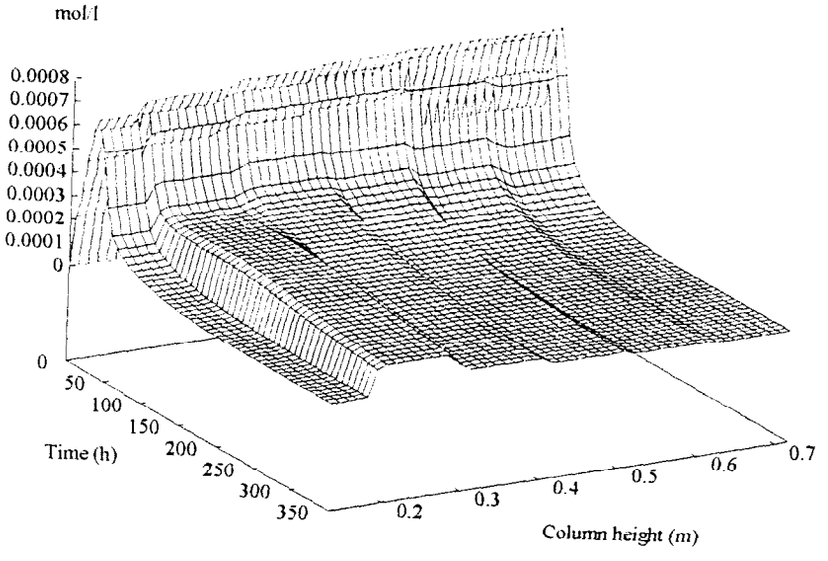

Appendix J: Gas flow rate in the column of 5 l/min, process of 350 h [section 2.6]

CO2 liquid - [Gas flow rate in the column: 5 l/min]

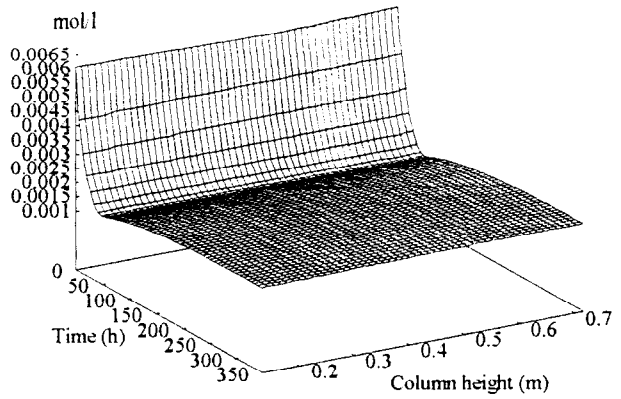

CO2 gas - [Gas flow rate in the column: 5 l/min]

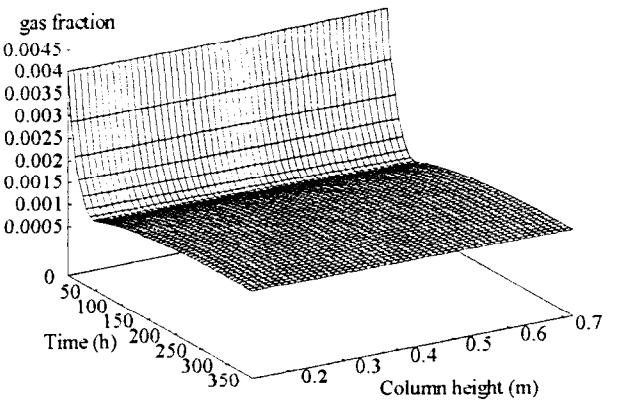

O2 liquid - [Gas flow rate in the column: 5 l/min]

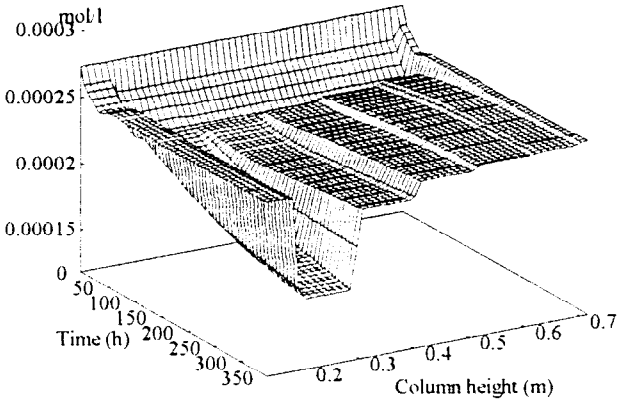

O2 gas - [Gas flow rate in the column: 5 l/min]

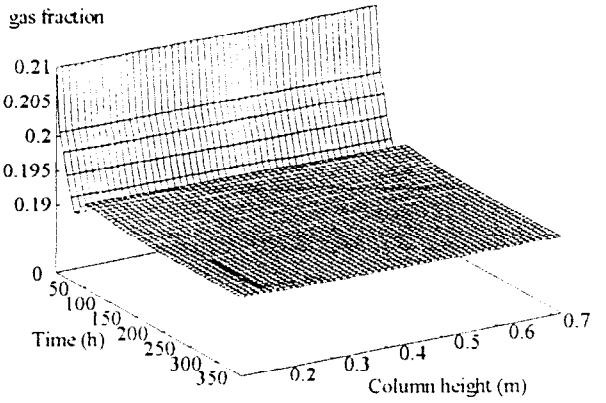

Nitrosomonas - [Gas flow rate in the column: 5 l/min]

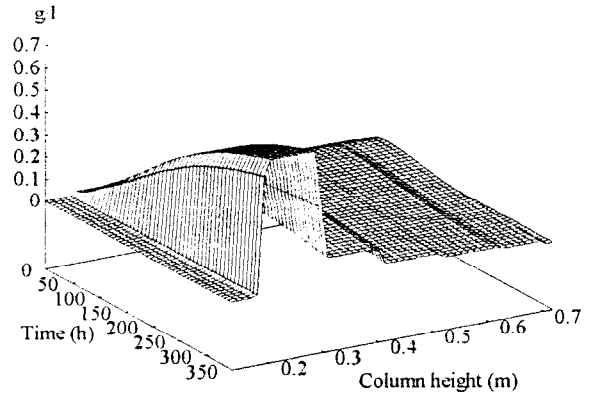

Nitrobacter - [Gas flow rate in the column: 5 l/min]

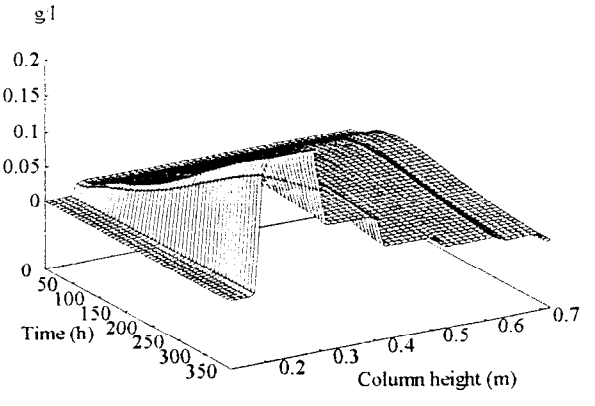

Appendix K: Back-mixing (f and f' parameters) of 75%, process of 350 h[section 2.7]

NH3 - [Back-mixing: 75%]

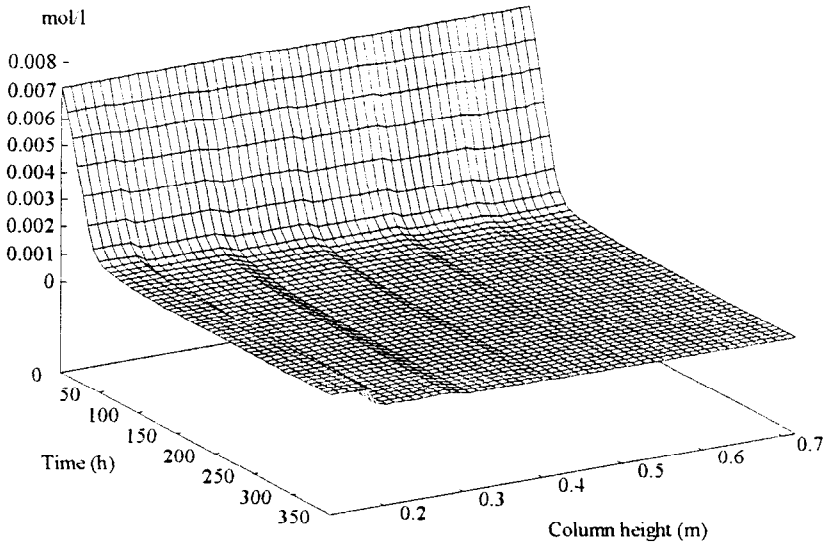

HNO3 - [Back-mixing: 75%]

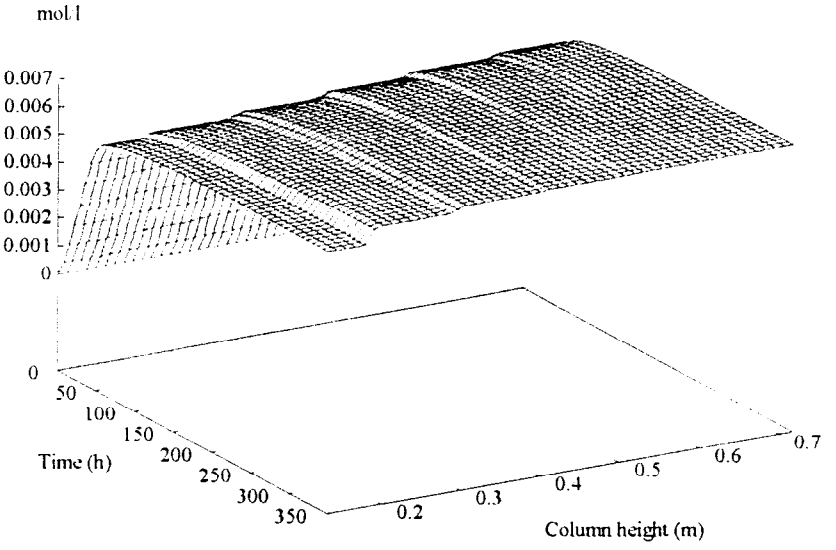

HNO2 - [Back-mixing: 75%]

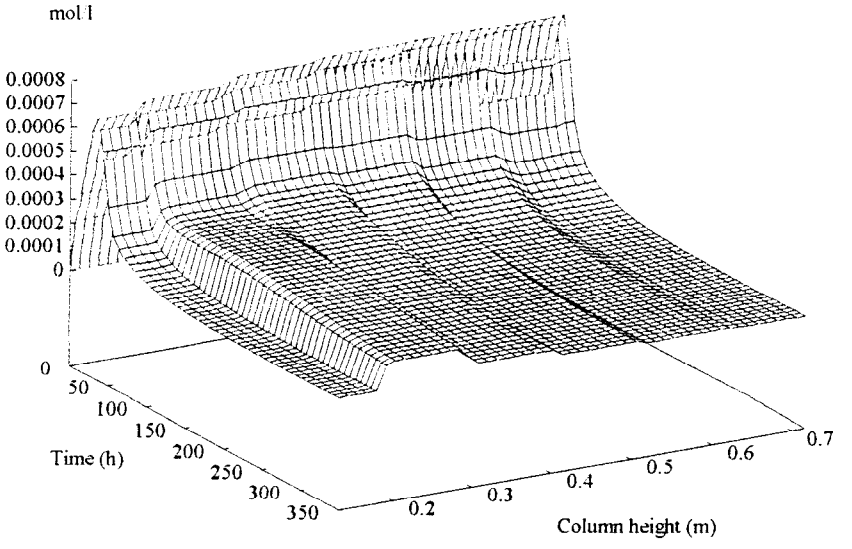

Appendix K: Back-mixing (f and f' parameters) of 75%, process of 350 h[section 2.7]

CO2 liquid - [Back-mixing: 75%]

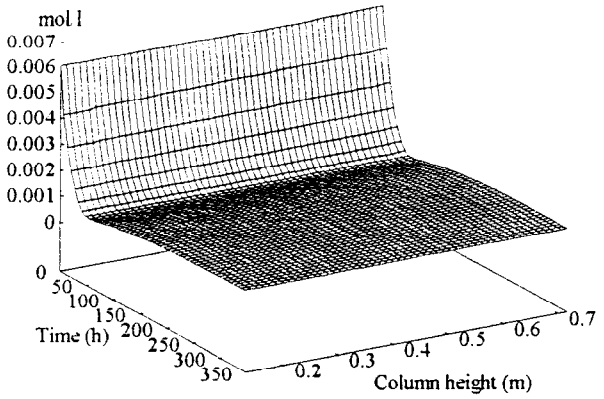

CO2 gas - [Back-mixing: 75%]

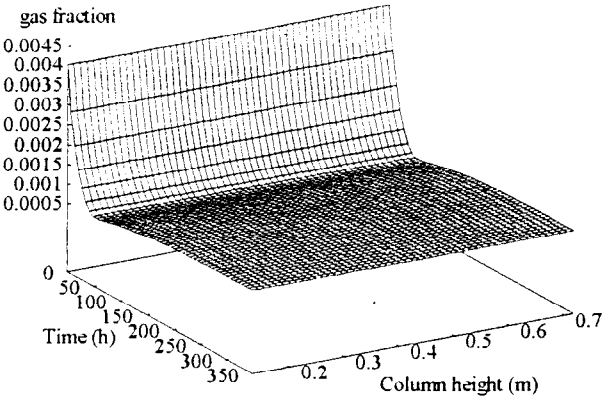

O2 liquid - [Back-mixing: 75%]

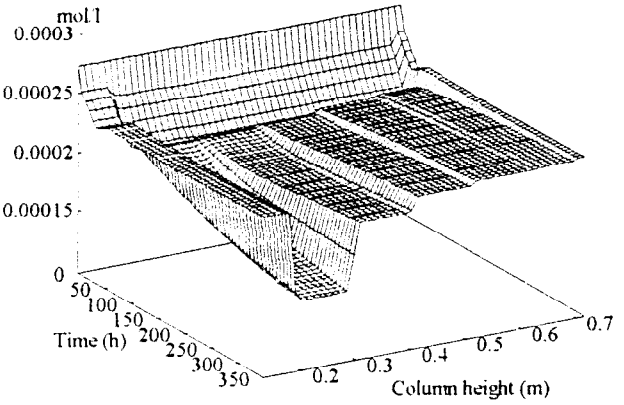

O2 gas - [Back-mixing: 75%]

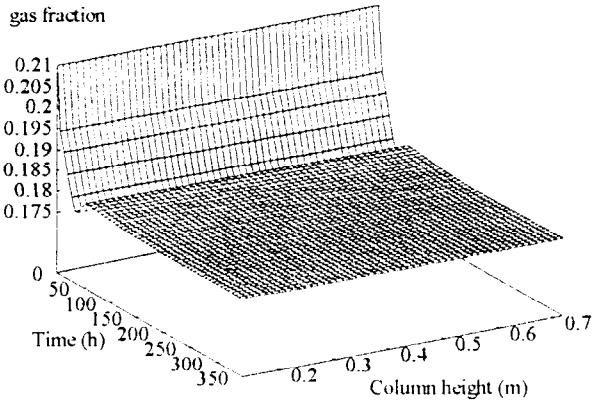

Nitrosomonas - [Back-mixing: 75%]

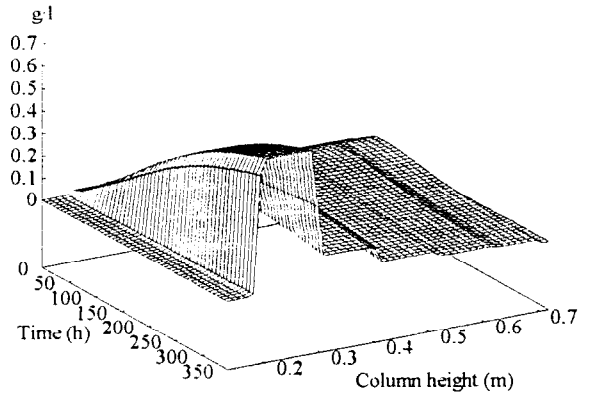

Nitrobacter - [Back-mixing: 75%]